TÉCNICO LISBOA

A comparison of internal grid topologies of offshore wind farms regarding reliability analysis

Tiago Alexandre Pais Pereira

Thesis to obtain the Master of Science Degree in

Electrical and Computer Engineering

Supervisor: Prof. Rui Manuel Gameiro de Castro

Examination Committee

Chairperson: Prof.ª Maria Eduarda de Sampaio Pinto de Almeida Pedro

Supervisor: Prof. Rui Manuel Gameiro de Castro

Members of the Committee: Doutora Ana Isabel Lopes Estanqueiro

July 2017

Acknowledgements

I would like to gratefully acknowledge various people who have journeyed with me during the period that I have worked on this thesis.

I would like to thank my Supervisor, Prof. Rui Castro, for his expertise, understanding, generous guidance, encouragement and support demonstrated along the development of this thesis.

I owe an enormous debt of gratitude to my family. I cannot thank you enough for all the support, love and education you have given me, I would not be the man I am today if it was not for you. You all keep me going, and this thesis would not have been possible without you. Special thanks to my mother for all the unconditional love and always believing in my abilities, you are my role model.

Most especially, I would like to thank my girlfriend, Mariana Santos, for her constant love, unconditional support and encouragement, for believing in my ability to finish this thesis, and for the sacrifices she has made to enable me to get the work done.

I am hugely indebted to my friend, Eng. Gaspar Cano, for finding out time to review, for being ever so kind to show interest in my research and for giving his precious advice. Thanks for your constant patience, encouragement and support.

I also like to thank all my friends for the good times, support, and comprehension along the development of this thesis.

Resumo

Na última década, os parques eólicos *offshore* surgiram como uma relevante fonte de energia renovável, que comparativamente aos parques eólicos *onshore*, se caracterizam por maior intensidade de vento, mas maior investimento e custos de operação e manutenção. Isto realça a importância do aumento de fiabilidade, pois a ocorrência de uma falha pode resultar em elevados tempos de indisponibilidade, pela inacessibilidade do parque durante condições climatéricas adversas.

Neste trabalho é realizada uma análise de fiabilidade da rede interna do parque eólico *offshore*, comparando diferentes topologias e os seus benefícios económicos. Como as interrupções na produção de energia levam a uma perda na receita, o objetivo é determinar a topologia que encontra o equilíbrio entre uma boa fiabilidade e um custo aceitável. De forma a aumentar a fiabilidade de uma topologia, são usadas redundâncias entre cada dois conjuntos de geradores ou entre dois conjuntos de pares já redundantes. Também são consideradas duas abordagens para o dimensionamento dos cabos.

Os resultados demonstram que a utilização de uma redundância apresenta um Valor Atual Líquido positivo e uma Taxa Interna de Retorno interessante, aos olhos de um investidor. É mais lucrativo dimensionar os cabos de forma a suportar o cenário de operação nominal em vez de lidar com todos os cenários de falhas. A topologia que apresenta os melhores resultados económicos e um bom resultado de fiabilidade é a topologia onde os cabos são dimensionados para suportar o cenário de operação nominal, com uma redundância, no meio, entre cada dois conjuntos de geradores.

Palavras-Chave: Parque Eólico *Offshore*, Topologia da Rede Interna, Analise de Fiabilidade, Avaliação Económica, Redundância, Dimensionamento do Cabo

Abstract

In the last decade, offshore wind farms emerged as an important renewable energy solution, characterized by higher winds, higher investment and higher operation and maintenance costs compared to onshore solutions. This highlights the importance of an increased reliability on offshore wind farms, because the occurrence of a failure can result in higher downtimes due to inaccessibility of the site during harsh weather conditions.

This study performs a reliability analysis of the internal grid of an offshore wind farm, comparing different topologies and their economic benefits. Since interruptions in power production lead to income losses, the challenge is to find which topology has the right balance between high reliability and acceptable costs. To increase the topology reliability, this study uses a redundancy between each pair of two strings or a redundancy between already redundantly paired sets of strings. It also considers two different approaches for the cable rating selection.

The results show that the use of a redundancy can lead to a positive Net Present Value and an interesting Internal Rate of Return, which can be an appealing investment. Moreover, it is more profitable to simply rate the cables to support a normal operation scenario for rated power rather than increasing the cable ratings to support all failure scenarios. Overall, the topology that presents the best economic results combined with a good reliability result is the topology with cable ratings based on regular conditions with a redundancy in the middle of the string between each pair of two strings.

Keywords: Offshore Wind Farm, Internal Grid Topology, Reliability Analysis, Economic Evaluation, Redundancy, Cable Rating

Contents

List of Tables

List of Figures

Abbreviations

CAIDI – Customer Average Interruption Index

CAPEX – Capital Expenditures

cdf – cumulative distribution function

ENS – Total Load Energy Not Supplied

HVAC – High Voltage AC

HVDC LCC – High Voltage DC Line Commutated Converter

HVDC VSC – High Voltage DC Voltage Source Converter

IRR – Internal Rate of Return

MVAC – Medium Voltage AC

NPV – Net Present Value

NRD – New Redundancy Design

OPEX – Operational Expenditures

pdf – probability distribution function

SAIDI – System Average Interruption Index

SAIFI – System Average Interruption Frequency Index

TRU – Topology with Rating Upgrades

TRRC – Topology with Rating for Regular Conditions

Chapter 1

Introduction

This chapter gives a brief overview of the work done for this thesis. Before establishing the work's targets and original contributions, its scope and motivations are brought up. At the end of this chapter, the work's structure is provided.

1.1 Overview

The utilization of wind resources to produce energy has been present in human civilization for the last 3000 years. First reliable sources dated from 200 B.C. show windmills being utilized for agriculture, milling and pumping in Persia (one of them is presented in Figure 1). This utilization has been under constant development over the past centuries and in 1887 the first wind generator was built. This happened in Scotland and its goal was to light James Blyth's (its creator) home holiday. Nowadays, wind energy is one of the most promising renewable energy sources to produce electricity, mostly because it provides safety, environmental sustainability and economic reliability [1].

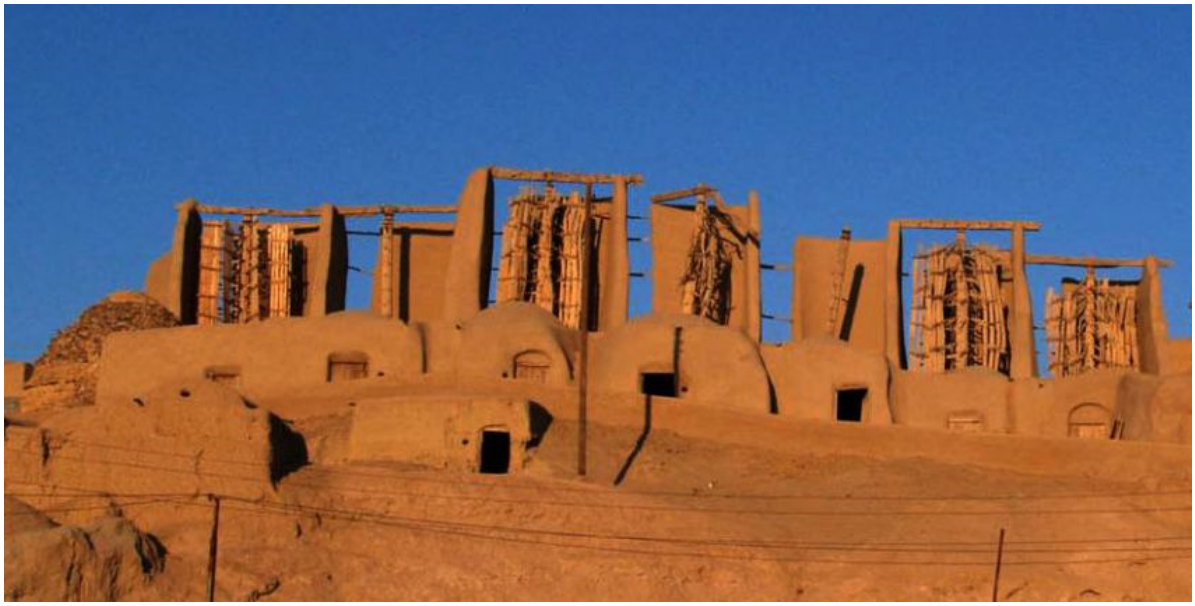

Figure 1. Persian windmill [2].

Until recently, records of the wind potential for energy conversion were based on meteorology stations. These measures were used to make meteorological predictions but were not suitable for the right evaluation of wind potential. To overcome this situation, in 1989 the European Wind Atlas was published (Figure 2), which gives the average wind speed and the power density for a height of 50 meters. Another important publication was the European Wind Atlas Offshore (Figure 3), which shows that offshore sites have more wind potential when compared to onshore sites [1].

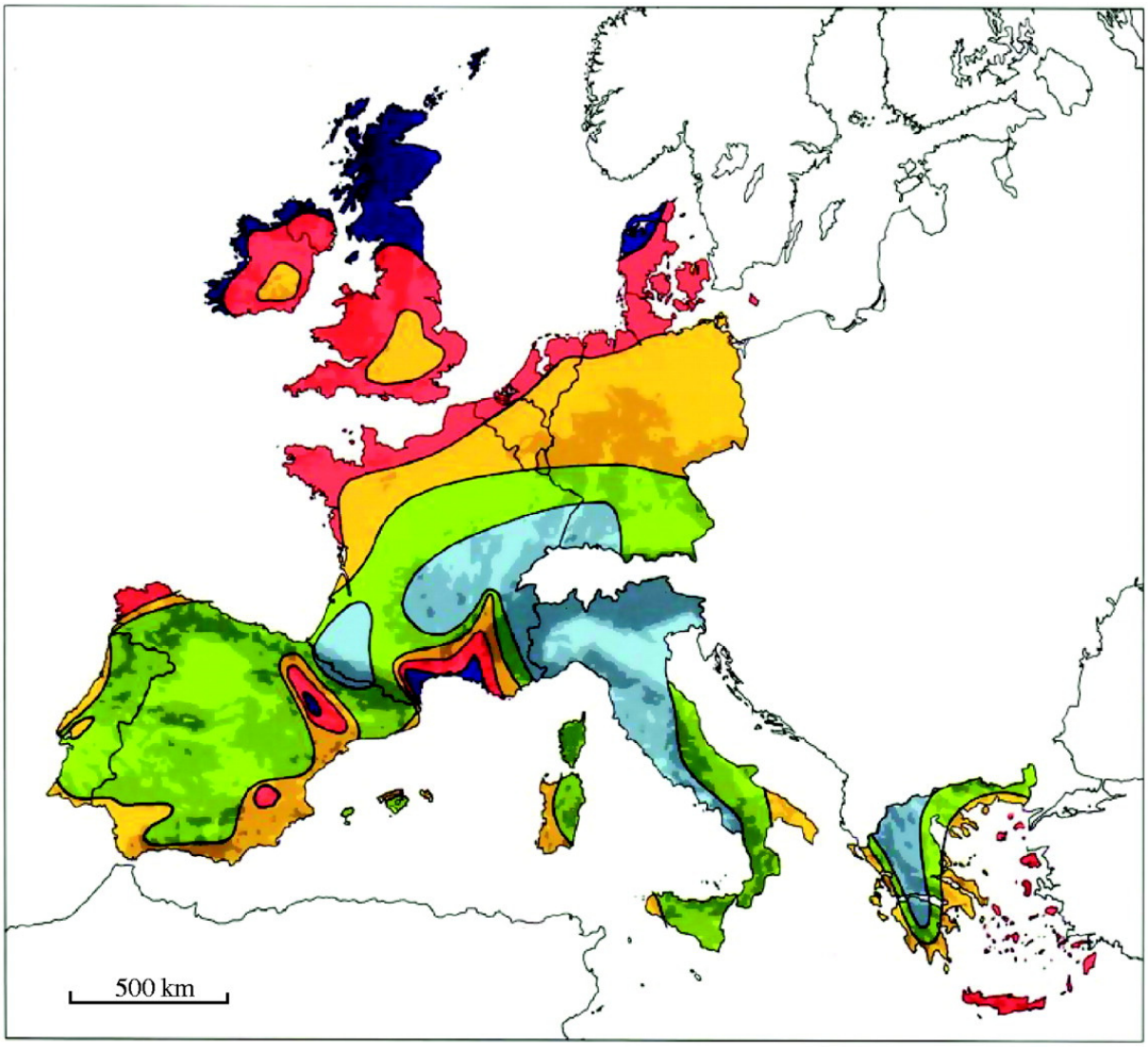

wind resources at 50 m above ground level for five different topographic conditions

	sheltered terrain		open plain		at a sea coast		open sea		hills and ridges	
	$m s^{-1}$	$W m^{-2}$	$m s^{-1}$	$W m^{-2}$	$m s^{-1}$	$W m^{-2}$	$m s^{-1}$	$W m^{-2}$	$m s^{-1}$	$W m^{-2}$
	>6.0	>250	>7.5	>500	>8.5	>700	>9.0	>800	>11.5	>1800
	5.0–6.0	150–250	6.5–7.5	300–500	7.0–8.5	400–700	8.0–9.0	600–800	10.0–11.5	1200–1800
	4.5–5.0	100–150	5.5–6.5	200–300	6.0–7.0	250–400	7.0–8.0	400–600	8.5–10.0	700–1200
	3.5–4.5	50–100	4.5–5.5	100–200	5.0–6.0	150–250	5.5–7.0	200–400	7.0 – 8.5	400 – 700
	<3.5	<50	<4.5	<100	<5.0	<150	<5.5	<200	<7.0	<400

Figure 2. European Wind Atlas [3].

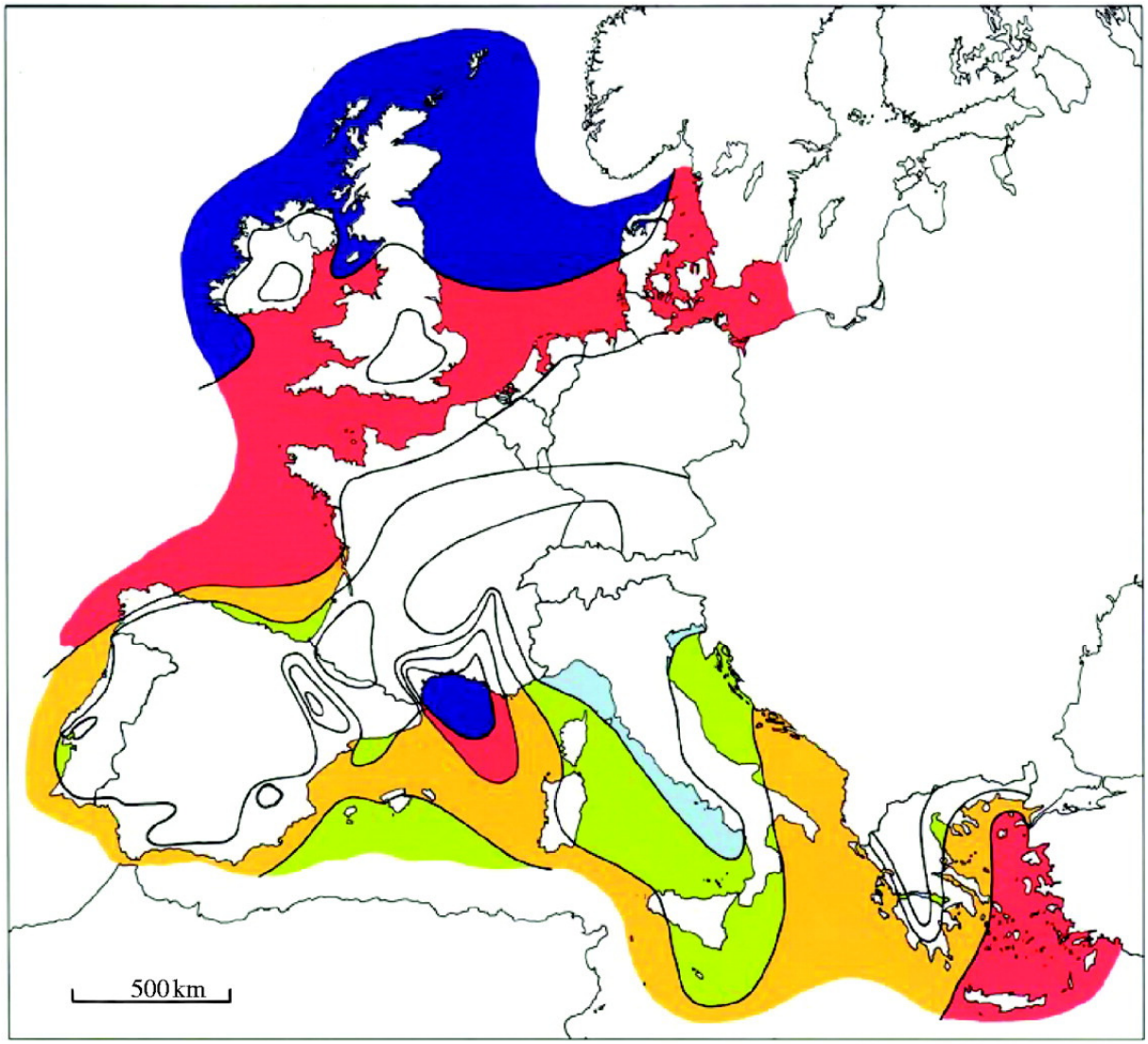

wind resources over open sea (more than 10 km offshore) for five standard heights										
	10 m		25 m		50 m		100 m		200 m	
	$m s^{-1}$	$W m^{-2}$	$m s^{-1}$	$W m^{-2}$	$m s^{-1}$	$W m^{-2}$	$m s^{-1}$	$W m^{-2}$	$m s^{-1}$	$W m^{-2}$
	>8.0	>600	>8.5	>700	>9.0	>800	>10.0	>1100	>11.0	>1500
	7.0–8.0	350–600	7.5–8.5	450–700	8.0–9.0	600–800	8.5–10.0	650–1100	9.5–11.0	900–1500
	6.0–7.0	250–300	6.5–7.5	300–450	7.0–8.0	400–600	7.5 – 8.5	450 – 650	8.0 – 9.5	600 – 900
	4.5–6.0	100–250	5.0–6.5	150–300	5.5–7.0	200–400	6.0 – 7.5	250 – 450	6.5 – 8.0	300 – 600
	<4.5	<100	<5.0	<150	<5.5	<200	<6.0	<250	<6.5	<300

Figure 3. European Wind Atlas Offshore [4]**.**

The main difference between onshore and offshore sites lies in the fact that, due to the lack of surrounding obstacles, wind is much less turbulent in the sea, which does not happen in onshore sites [1]. It was only in 1990 that the first offshore wind farm appeared off the coast of Sweden, with a rated power of 220kW. The first commercial offshore wind farm was installed a year later in Denmark, with a rated power of 450kW [5].

From then onwards, the size of the wind turbines, the distance to shore and the water depth where the turbines are installed kept increasing, as well as the size of the offshore wind farms. Among all of the operational offshore wind farms, one that is worth mentioning is the London Array (630 MW) in the

United Kingdom [6]. This is the largest offshore wind farm in the world and is composed of 175 wind turbines - a photography is presented in Figure 4. Currently in its construction stage, there is one large offshore site that is also worth mentioning - the Gemini (600 MW), in the Netherlands, which is expected to become operational in 2017 [7].

Figure 4. London Array offshore wind farm, in the United Kingdom [6]**.**

1.2 Motivations and Objectives

Offshore wind farms experience higher winds resulting in higher production, but investment costs and operation and maintenance costs are also higher. This highlights the importance of increased reliability on offshore wind farms, because a single failure may result in a long downtime period, due to the inaccessibility of the site during harsh weather conditions. The topology of the internal collection system is a key issue, as it determines the redundancy levels (alternative paths to drain the electrical energy) of the offshore wind farms. Since interruptions in power production from an offshore wind farm lead to income losses, the challenge in designing offshore wind farms is to find the right balance between high reliability and acceptable costs.

The objective of this thesis is to perform a reliability performance analysis of the internal grid of an offshore wind power system, comparing different topologies and their economic benefits. By comparing different topologies, it is possible to determine and evaluate which is the most reliable installation. To perform a reliability assessment, it is required to simulate the reliability for each component in the system, determine the impact of each contingency on each load point, determine the frequency of

production interruption and sum up the impact of all contingencies. Overall, this study addresses the reliability impact of different topological solutions while maintaining an economic rationale between the layout design and the energy production output.

1.3 Outline of the Thesis

In order to achieve the objectives proposed, this work is organized in the following order:

Chapter 2 provides some fundamental knowledge about all covered topics, such as wind resources, wind energy, some conceptions and design specifications about wind farms, and some economic aspects and basic concepts in evaluating the reliability of power systems.

Chapter 3 presents a brief explanation of the software piece that was developed to accomplished the reliability and economic evaluation of the proposed topologies and all the assumptions and scenarios that were made so that trustworthy results could be obtained through the simulations. These include power and fault scenarios, cable ratings, equipment cost and reliability data. It also presents a validation of the software developed.

Chapter 4 presents all the proposed topologies analysed by the developed software.

Chapter 5 presents the results obtained by the developed software for the different topologies.

Chapter 6 presents the conclusions of this work and discusses possible future work to be done in this field.

Chapter 2

Theory Framework

This chapter provides some fundamental knowledge about all of the topics covered in this work. It begins with an introduction about wind resources, followed by some information on wind energy. Some conceptions and design specifications about wind farms are also presented. Finally, it introduces some economic aspects and basic concepts in evaluating the reliability of power systems.

2.1 Wind Resource

Wind speed and direction are constantly changing. So, three distinct areas can be identified over a spectral analysis. The first one is macro-meteorology, characterized by low frequency (representing a few days in a time scale) and associated with the movement of a big mass of air. The second one is micro-meteorology, which is characterized by high frequency (a few seconds in time) and associated with atmosphere turbulence. Finally, there are the empty zone periods (representing a period between 10 minutes and 2 hours), associated with low energy events [1].

According with these three areas wind speed can be described in the following mathematical terms:

$$u(t) = \overline{u} + u'(t) \tag{1}$$

where:

$u(t)$ – wind speed [m/s],

$\overline{u}$ – average wind speed [m/s],

$u'(t)$ – turbulence [m/s].

The average wind speed is calculated based on a sampling from 10 minutes to 1 hour, relying on the empty zone periods. This value represents the steady state of energy available for wind turbines. For slow wind speed variations, the wind representation can be obtained from statistical distributions, more specifically through probability density functions [1].

2.1.1 Weibull Distribution

The records of probability density have greater importance if they can be described by an analytical expression. One of the most suitable probability distribution functions is the Weibull Distribution.

$$f(u) = \frac{k}{c}\left(\frac{u}{c}\right)^{k-1} exp\left\{-\left[\left(\frac{u}{c}\right)^{k}\right]\right\} \tag{2}$$

where:

$f(u)$ – probability distribution function (pdf) of wind speed,

u – wind speed [m/s],

c – scale parameter,

k – form parameter.

Integrating the probability distribution, the cumulative probability can be represented as:

$$F(u) = exp\left\{-\left[\left(\frac{u}{c}\right)^{k}\right]\right\} \tag{3}$$

where $F(u)$ is the cumulative distribution function (cdf) of wind speed u. This cumulative probability is the probability of the wind speed being equal or higher than u. This definition only takes place in wind energy studies.

One important parameter of the Weibull distribution is the average annual wind speed [m/s]:

$$u_{avg\_annual} = c\Gamma\left(1 + \frac{1}{k}\right) \tag{4}$$

where Γ is the gamma function.

2.1.2 Rayleigh Distribution

If the form parameter in the Weibull distribution is equal to 2, the Rayleigh Distribution is obtained. The biggest advantage of this distribution is that it only has one parameter. This is very useful if no records are available, except for an estimate of the annual average wind speed.

$$f(u) = \frac{\pi}{2}\frac{u}{u_{avg\_annual}^2} exp\left[-\frac{\pi}{4}\left(\frac{u}{u_{avg\_annual}}\right)^2\right] \tag{5}$$

where:

$f(u)$ – pdf of wind speed,

u_{avg_annual} – annual average wind speed [m/s].

In a similar way, the cumulative probability can be represented as:

$$F(u) = exp\left[-\frac{\pi}{4}\left(\frac{u}{u_{avg\_annual}}\right)^2\right] \quad (6)$$

where $F(u)$ is the cdf of wind speed.

2.1.3 Prandtl Law

An important aspect to consider is the friction between the earth surface and the wind, which contributes negatively to the wind speed. The air layer called the superficial layer is the one which has most interest to wind generation. However, it is where most friction is present. Terrain topology and surface roughness conditions strongly affect the wind speed profile in this layer. This can be described by the Prandtl Law:

$$u(z) = \frac{u_*}{k} ln\left(\frac{z}{z_0}\right) \quad (7)$$

where:

k – Von Karman constant,

u_* – friction speed [m/s],

z_0 – surface roughness [m].

Normally, to analyse this location, measuring devices are installed at a lower height than the wind generator hub. So, using the Prandtl Law to extrapolate the measurings to the height of the wind generator hub, the following expression can be obtained:

$$\frac{u(z)}{u(z_{measure})} = \frac{ln\left(\frac{z}{z_0}\right)}{ln\left(\frac{z_{measure}}{z_0}\right)} \quad (8)$$

where:

$u(z_{measure})$ – wind speed at height $z_{measure}$ [m/s],

$z_{measure}$ – height [m].

Surface roughness (z_0) can be obtained from table values that are available for the analysis of wind potential, such as the ones presented in Table 1.

Table 1. Typical values of Surface Roughness [1].

Terrain Description	Surface Roughness, z_0(m)
Very smooth, ice or mud	0.00001
Calm open sea	0.0002
Blown sea	0.0005
Snow surface	0.003
Lawn grass	0.008
Rough pasture	0.01
Fallow field	0.03
Crops	0.05
Few trees	0.1
Many trees, hedges, few buildings	0.25
Forest and woodlands	0.5
Suburbs	1.5
Centres of cities with tall buildings	3.0

2.2 Wind Energy

One requirement for energy production by wind generators is the existence of a permanent wind source above some threshold of density (volumetric mass). Most wind generators are projected to produce the rating power for wind speeds around 13 to 16 m/s [1].

2.2.1 Wind Power

Energy can neither be created nor destroyed so, according to the first law of thermodynamics, it can only can be transformed from one state to another. The expression below contains the conversion of the kinetic energy that flows across the area swept by the rotating blades into electrical energy. Wind power can be calculated as:

$$P_{Wind} = \frac{1}{2}\rho A u^3 \tag{9}$$

where:

P_{Wind} – wind power [W],

ρ – air density [kg/m^3],

A – swept area [m^2].

Due to the Betz law, aerodynamics and drive train losses, the power converted into electricity is lower and can be given by:

$$P_{WTG}(u) = \frac{1}{2} C_p(u) \rho A u^3 \tag{10}$$

where $C_p(u)$ is the power coefficient.

The application of fluid mechanics theory allows for the demonstration of the existence of a theoretical limit around 59.3% for the power coefficient. If an ideal turbine existed, it would be able to convert 59.3% of the wind power. In reality that never happens due to mechanical imperfections. Nowadays, a modern wind generator can extract around 50% of the wind power available [1].

2.2.2 Power Curve

For each wind generator, the $C_p(u)$ is different and varies according to the wind speed. The power curve derives directly from $C_p(u)$ so it is unique for each wind turbine and is provided by each manufacturer. This curve specifies the electrical power output of the wind turbine, over a range of wind speeds. An example of this is presented in Figure 5.

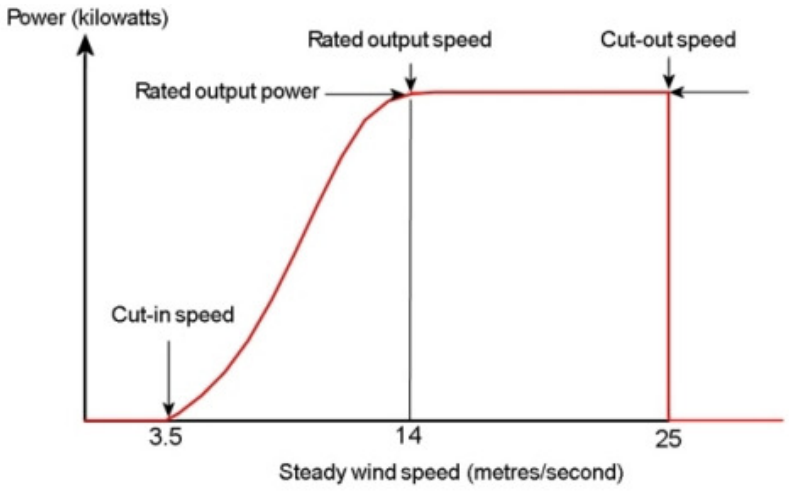

Figure 5. Typical wind turbine power output with steady wind speed [8]**.**

From the cut-in speed to the rated output speed, the power output is approximately proportional to the cube of the wind speed, as expected. For wind speeds higher than the rated speed, the output of wind turbines is the rated power. This is achieved by controlling the angle of the blade and the power electronics.

Wind turbines do not operate at all wind speeds - neither for wind speeds below the cut-in speed nor for wind speeds above the cut-out speed. The former because the energy that can be obtained from the wind is not enough to counterbalance the cost of having the wind turbine connected; the latter due to safety reasons.

2.2.3 Energy Calculation

The power production of a wind generator depends on the wind speed, which in turn depends on the weather. Wind speed fluctuates over time so, if there is a large amount of wind speed samples over a long time for a specific site it is possible, using the Raleigh distribution or the Weibull distribution, to represent the probability density function of the wind speed. Combining that with the power curve from a wind turbine, the expected annual energy production can be obtained:

$$E_{WTG} = 8760 \int_{u_0}^{u_{max}} f(u) \times P_{WTG}(u) du \quad (11)$$

Where E_{WTG} is the annual energy production [MWh].

2.2.4 Construction Technology

A wind turbine can be divided in three main parts: the rotor, the nacelle and the tower [5]. The rotor captures the wind energy due to its rotation. It is the combination of the blades (usually three) and the rotor hub (where the blades meet the turbine shaft) that allows for the conversion of wind energy into mechanical energy. The nacelle is composed by many important elements like the gearbox, the generator and the breaks. Finally, there is the tower, which acts as a support for the whole structure.

It has been common practice to adapt onshore designs to offshore designs, the main difference being in the materials that are used. Since offshore wind sites are more susceptible to hostile environments, the materials used have to be appropriate for these conditions [5].

2.3 Wind Farm Conception and Design

An offshore wind farm is composed by many elements aside from wind generators. To deliver the power produced by the wind generator to shore, the offshore wind farm needs to meet some requirements, such as having foundations, a collector system, a substation and a transmission system. The function of the foundations is to support the wind generators; the collector system connects all the wind turbines to the substation; and, finally, the substation connects the wind farm to the onshore grid through the transmission system and adapts the voltage between the two.

2.3.1 Layout

Nowadays, most offshore wind farms installed worldwide have a relatively small power capacity and the topologies of the electrical systems used have been as simple as possible. Offshore wind farms copy the practices of onshore sites. However, as the power capacity of offshore wind farms increases and the knowledge about the impact of the hostile environment they are susceptible to grows, the adequacy of the wind farm's electrical system design starts to become critical. A good electrical system design relies on good efficiency, good costs, good reliability and a good overall performance [9].

Another factor that affects wind farm performance is the wind turbine arrangement. This arrangement is usually disposed to minimize the wake effect. The wake effect is a wind flow disturbance created by the wind turbine in the upwind direction [5]. Thus, the space between the turbines is usually from 5 to 9 rotor diameters in the prevailing wind direction and from 3 to 5 rotor diameters in the perpendicular direction [1]. These spacing rules are shown in Figure 6. However, for the analysis conducted in this work, the wake effect has been neglected.

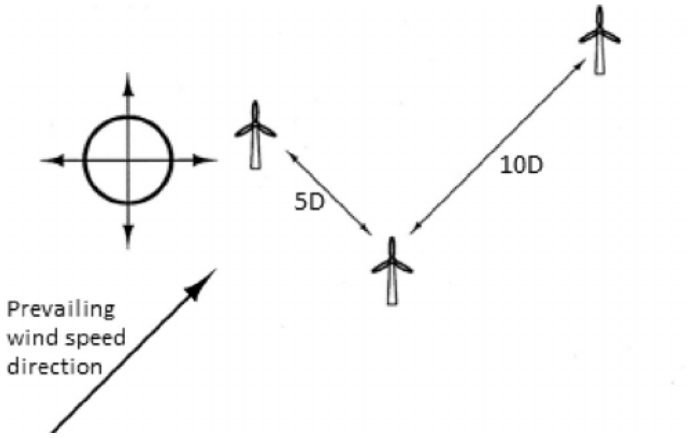

Figure 6. Wind turbine spacing rules [10]**.**

Depending on the wind farm's size and the desired level of reliability, the wind farm layout can be different. A typical configuration of the grid can be placing all the wind generators on a single series circuit (mostly used in small offshore wind farms). Another one can be distributing the wind turbines over several strings, which allows for low rated equipment and is used in large offshore wind farms. And, finally, a layout with a redundancy path can be obtained by allowing the establishment of a looped circuit between the wind turbines [9], [11].

2.3.2 Collector Systems

The function of the collector system is to connect all wind turbines, collect the energy produced by them and deliver it to the offshore substation. Therefore, it is one of the components of offshore wind farms on which improvements can mostly increase reliability. Until nowadays, the collector system has only represented a minor part of the total investment. This is because most offshore wind farms are small and have radial collectors. However, future large offshore wind farms come to change that. The major concern is related to the additional costs of subsea cables, either with extra length or higher ratings [9].

The purpose of using redundancy in a wind farm collector system is to keep as many wind turbines as possible connected during an equipment fault. Over the years, offshore wind farms have demonstrated that the required repair times are higher than on onshore sites. A cable fault has estimated repair times between 720h (during summer) to 2160h (during winter) [12]. So, the existence of redundancies in offshore wind farms is important and needs to be economically evaluated. If the cost of the redundancy is less than the amount of power that is not transmitted due to the fault, it is demonstrated that the redundancy is profitable [13].

Comparing the different layouts existing in offshore wind farms and other conceptual designs proposed by the offshore wind community ([14], [15]), four basic designs can be identified: radial design, single-sided ring design, double-sided ring design and star design [9]. Additionally, there are two other designs (represented in [9] and [16]) that are the most economically appealing and reliability increasing: the single return design and the double-sided half ring design, respectively.

2.3.2.1 Radial Design

The most common and straightforward arrangement is that in which several wind turbines are connected to a single cable feeder within a string, as seen in Figure 7. The number of wind turbines connected to each string feeder is dependent on the rating of the sea cables and the capacity of the wind generators. The biggest advantage of this design is the low cost and how simple it is to control. Its low cost is caused by the low total length necessary and the possibility of tapering the ratings of the cables away from the hub. The major disadvantage is its poor reliability, since even if a cable fault occurs at the end of the string it will prevent all the wind turbines in that string from producing power. A single fault occurring in any element of the string prevents all the other generators in that same string from generating power.

The 160 MW Horns Rev offshore wind farm in Denmark has adopted this design [17]. The 640 MW Krieger's Flak offshore wind farm [18] and the 420 MW Cape Wind offshore wind farm [19], which are in their planning stage, have proposed this as one of their designs.

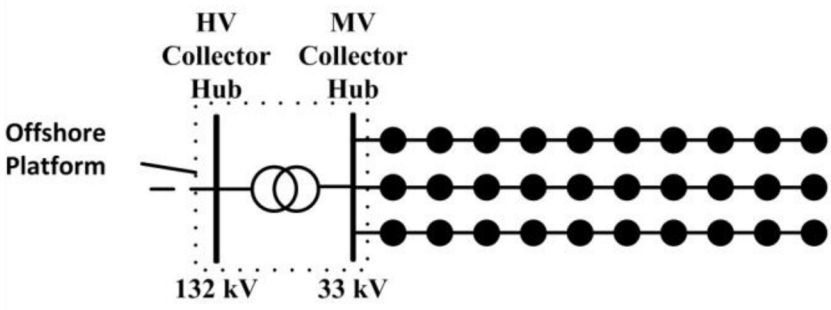

Figure 7. Wind farm radial design [16]**.**

2.3.2.2 Single-Sided Ring Design

To increase the reliability of the radial design, one connects the last turbine of the string to the hub with a long cable. So, the single-sided ring design requires an additional cable which needs to handle the full power flow of the string, as seen in Figure 8. This additional security comes with an additional cost due to the new longer cable and the higher cable rating requirements throughout the string circuit [9].

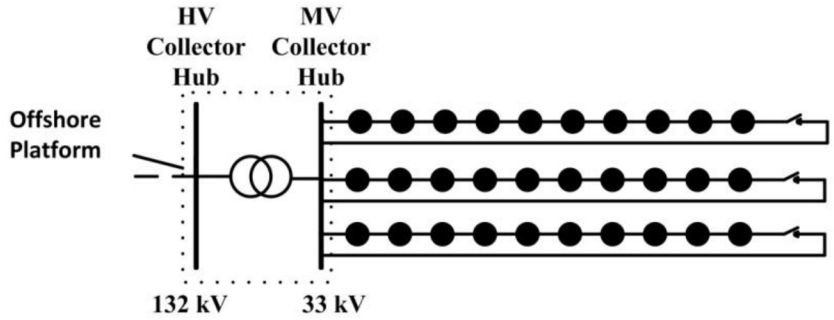

Figure 8. Wind farm single-sided ring design [16]**.**

2.3.2.3 Double-Sided Ring Design

To get the same reliability as in the single-sided ring design but decrease its cost, the last turbine of one string is connected to the last turbine of another string [13]–[15]. The downside of this design, presented in Figure 9, is that the connection between the hub and the first turbine of the string needs to handle the output of twice as many wind turbines as those on its string (all the turbines in the two connected strings) [9].

Regardless of the increase in reliability of the single-sided ring design and the double-sided ring design, most of the offshore wind farms do not use them at all. In fact, most of them do not have any redundancies [17]. Most offshore wind farms are small (less than 100 MW), where the fault probability is lower and the cost associated with having additional equipment is higher, so in these cases the redundancy is not economically profitable. In contrast, for large offshore wind farms (higher than 100 MW) the situation changes, mostly because repair downtimes are significant longer and the redundancy becomes economically profitable.

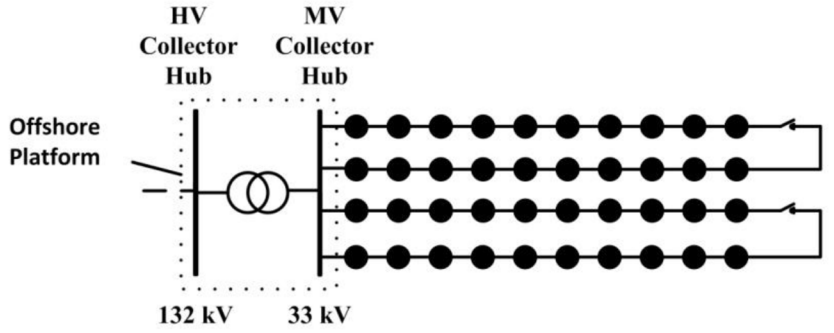

Figure 9. Wind farm double-sided ring design [16]**.**

2.3.2.4 Star Design

To reduce cable ratings and to provide a high level of reliability, one possible solution is the star design, since one cable outage only affects one turbine, except for the cable from the central turbine to the hub [13]–[15]. This design, presented in Figure 10, has as another advantage the reduction of cable ratings. Only the cable from the centre turbine to the hub needs to handle all power from all turbines in the string.

However, this design has its disadvantages too, like the additional expense needed for longer diagonal cables and the arrangement of the more complex switchgear required at the wind turbine at the centre of the star [9].

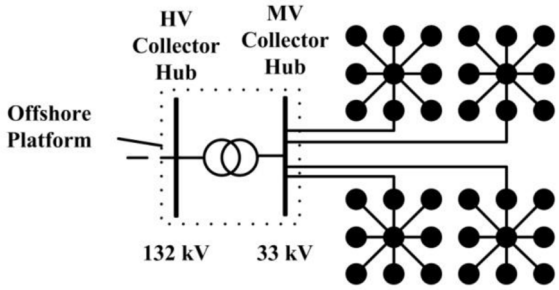

Figure 10. Wind farm star design [16]**.**

2.3.2.5 Single Return Design

An alternative design with the objective of minimizing the overall cost of the ringed collector and maintaining a good steady state performance has been derived from the single-sided and doubled-sided ring designs. It consists in having all the end turbines of all strings connected between them and one redundancy cable returning from one of the end turbines of one string to the main hub, as seen in Figure 11. The redundancy circuit is designed to support the full output power of a string when a fault happens in that string. The ratings in the redundancy do not support the failure of two string simultaneously, since the probability of that occurring is so small that it does not make it a profitable investment. This design has a significantly lower cost than the single-sided ring design and a competitive one compared to the radial design [9].

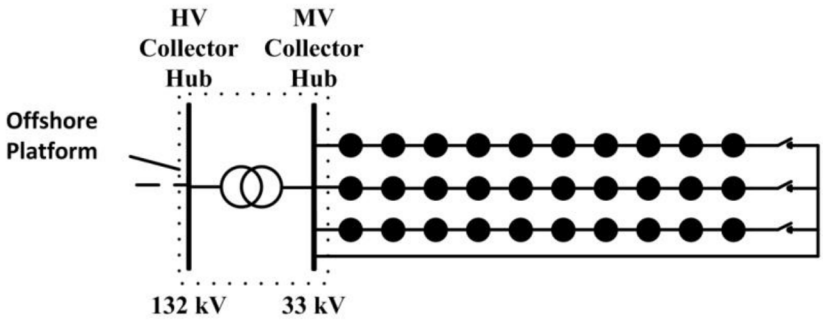

Figure 11. Wind farm single return design [16]**.**

2.3.2.6 Double-Sided Half Ring Design

This is a variant of the double-sided ring design that, instead of having the last turbine of one string connected to the last turbine of another, has its redundancy in the connection between the middle turbine of one string to the middle turbine of another, as seen in Figure 12. This layout only shuts down half of the turbines in the string in case of a cable fault. For that reason, this layout should include a remote controlled load switch in each string and in the redundancy [16].

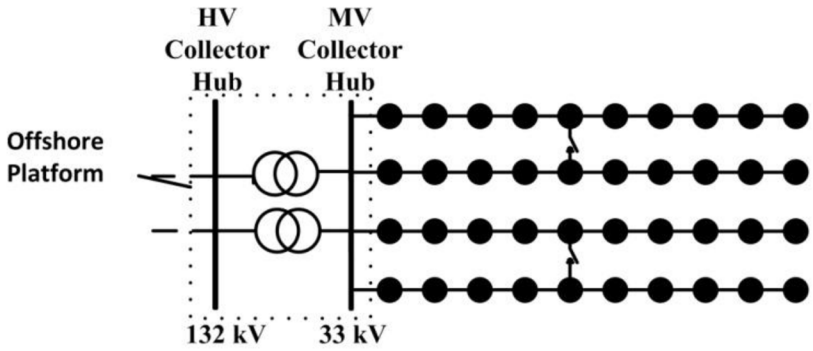

Figure 12. Wind farm double-sided half ring design [16]**.**

This interesting design only adds little modifications to the radial design, having a competitive cost when compared to it, while having a significantly lower cost than the double-sided ring design.

2.3.3 Array Cables

All wind turbines in one string are connected by array cables, whose function is to transmit all the energy produced in the turbines to the substation (an example of a submarine cable is presented in Figure 13). Since most of the wind turbines are AC powered, so are the array cables. When choosing the best type of submarine cable one must pay attention to the current capacity, conductor cores per cable and type of isolation [20].

Figure 13. 3-Core XPLE AC cable [21]**.**

A submarine cable is composed of several layers. From the inside to the outside, the cable has a conductor core, isolation, shield, sheath, armature, optic fibre and protecting sheath. The conduction core carries the power produced by the turbines and is formed by threaded wires joined together in a circular section. The isolation retains the propagation of the electrical current and isolates the conduction core. To smooth out the electrical field and avoid field concentration zones, the cables have the shield. The sheath is made from metallic materials and is connected to the earth, it also serves as a barrier for water. To provide mechanical strength and anti-corrosion protection, the cable has one layer called armature. The optical fibre is used to communicate and monitor cable purposes. And, finally, there is the protecting sheath, which is the final outer protection layer.

2.3.4 Transmission System

When all the energy produced by the wind turbines is collected in the substation, it must be transported to the shore. This is where the transmission system enters. There are four types of transmission systems available: Medium Voltage AC (MVAC), High Voltage AC (HVAC), High Voltage DC Line Commutated Converter (HVDC LCC) and High Voltage DC Voltage Source Converter (HVDC VSC). When choosing the more adequate transmission system, the factors that must be taken into account are the amount of power to be transmitted, the distance to shore and the economics aspects [22]. However, for the analysis conducted in this work, the transmission system was neglected.

2.4 Economic Aspects

The opportunities of using the sun, wind, water or wood to produce energy are countless. However, in each scenario it is necessary to evaluate economical aspects. If the energy cost is higher than the traditional sources of energy, the renewable project is not appealing for investors. So, to turn the situation around, governments need to give some economic incentives or subsidies for making the renewable project more profitable. The economic evaluation is an important step in selecting which of the possible scenarios is most profitable and to determine whether a renewable project is economically viable at all [1].

2.4.1 Indicators

To economically evaluate an offshore wind farm project, many indicators, which give a sort of measurement of the risk associated with the investment, can be taken into account. These indicators consist of costs, future income, equipment duration, operation and maintenance costs. Since the future is uncertain, these indicators give a prevision of the profitability of the project. The best-known indicators are the Net Present Value (NPV) and Internal Rate of Return (IRR).

The NPV is the difference between the present value of cash inflows and the present value of cash outflows. This indicator is used in capital budgeting to analyse the profitability of a project or investment. If the result of the NPV is positive the project is viable. That means the investment and the minimum return asked by the investor are covered, and a positive return is even possible. If the result of the NPV is null, that means the investment and the minimum return asked by the investor are covered, but nothing other than that. This means that the project is uncertain in terms of economic viability. A negative result of the NPV represents an economically unviable project.

$$NPV = \sum_{y=1}^{n} \frac{CF_y}{(1+r)^y} - \sum_{y=0}^{n-1} \frac{I_y}{(1+r)^y} \tag{12}$$

where:

CF_y – cash flow at year y [€],

I_y – investment at year y [€],

r – discount rate,

n – lifetime of the equipment [years].

The Internal Rate of Return (IRR) is the discount rate that turns the NPV null. This indicator has more value for the investor than the NPV, because it can give the maximum return that the investor can make with this investment. If the IRR is above the discount rate considered in the NPV, the project will have more value than the invested capital, which means it is economically viable. Otherwise, the minimum return asked by the investor is not accomplished, and the project is unviable.

$$0 = \sum_{y=1}^{n} \frac{CF_y}{(1+IRR)^y} - \sum_{y=0}^{n-1} \frac{I_y}{(1+IRR)^y} \tag{13}$$

The solution of the IRR is accomplished by iteration methods. In order to do a faster and easier calculation, one can go for an approximated calculation, given by a linear interpolation.

$$IRR \approx r_A + \frac{NPV_A}{NPV_A - NPV_B}(r_B - r_A) \tag{14}$$

where,

NPV_A – Net Present Value for a discount rate r_A [€],

NPV_B – Net Present Value for a discount rate r_B [€].

2.4.2 Wind Farm Cost

The cost assessment of an offshore wind farm must collect a very large amount of information regarding the cost associated with every aspect of the project. This information is owned by the manufacturers and is generally confidential [11], [16]. It is necessary to know the costs of components and foundations, the manpower, the installation vessels, the operation, maintenance and much more. Based on several studies [23]–[27], it is possible to estimate the costs associated with an offshore wind farm project.

2.4.2.1 Initial Costs (Investment Cost)

Until the offshore wind farm is ready to go online the investments made are referred to as initial costs, which are commonly known as CAPEX (Capital Expenditures). The range of costs for the CAPEX is shown in Table 2. The total investment cost will goes between 2350 k€/MW and 3600 k€/MW [28], [29].

Table 2. Range of costs for the CAPEX [30]**.**

Component	Range of Costs
Planning and Development	10 k€ – 80 k€
Offshore Wind Turbines	900 k€/MW – 1500 k€/MW
Collection and Transmission Cables	100 k€/MW
Switchgear	60 k€/Switchgear
Installation	450 k€/MW
Onshore Substation	30 k€/MW – 100 k€/MW
Foundations	350 k€/MW – 900 k€/MW

Comparing onshore with offshore wind farms, the investment costs and the final electricity costs are higher in offshore sites. This is due to the additional expenditure of subsea foundations, turbine installations, subsea plants, grid connections, and others. Just as an example, the turbine cost of an onshore site represents 75% of the total investment; meanwhile, the turbine cost of an offshore site represents only from 30% to 50% of the total investment [9].

2.4.2.2 Annual Costs

When the offshore wind farm is on-line all the costs are related with operation and maintenance. These costs are known as OPEX (Operational Expenditures). When analysing the operation and maintenance costs of an offshore wind farm it is obvious they are much higher than on onshore sites. This is caused by several factors like the distance to harbour, the exposure of the site, the accessibility conditions during bad weather, and the various equipments and vessels required. So, the annual costs are between 55 k€/MW and 93 k€/MW [23], [26], [31].

2.4.3 Wind Farm Feed-In Tariffs

Governments often adopt strategies to regulate the market and ensure that the goods or services are produced and distributed efficiently and the production occurs in socially and environmentally acceptable ways. Since renewable energies have a higher cost, it is necessary to have some type of regulation to make the renewable project attractive for investors. Two types of regulation are possible: price regulation and quantity regulation. The first is when the revenue is received under the form of a subsidy per kW of capacity installed or per kW produced. The second is when the income is determined through green certificates of renewable energy quotas. The most common strategies for applying this type of regulations are through investment subsidies, soft loans, tax credits, fixed regulated feed-in tariffs or fixed premiums additional to the electricity price. Examples of these mechanisms for several countries in 2010 are presented in Table 3.

Table 3. Offshore wind support mechanisms in several European countries in 2010 [32]**.**

Country	Current Support (ct €/kWh)	Term	Subsidies	Tax Incentives
Belgium	14.7 up to 216 MW 9.0 > 216 MW	20 years	Yes	No
Denmark	8.43 (Rodsand 2) Tender process	50.000 full load hours	No	No
Germany	15.0 (including sprinter bonus)	12 years plus possible extension	No	No
France	Initially 13.0 Then 3.0 to 13.0	Two ten year periods	No	Yes
United Kingdom	18.01	Certificates until 2037	Yes	Yes
Ireland	14.0	15 years	Yes	No
Netherland	Tender process	15 years	Yes	Yes
Sweden	6.76	15 years	Yes	Yes

2.5 Power Systems Reliability

For power systems, the reliability is the ability of the electrical system to satisfy the load demand. When analysing the reliability of a system, the assessment can be divided into two main aspects: system adequacy and system security. A schematic for system reliability is presented in Figure 14 [33].

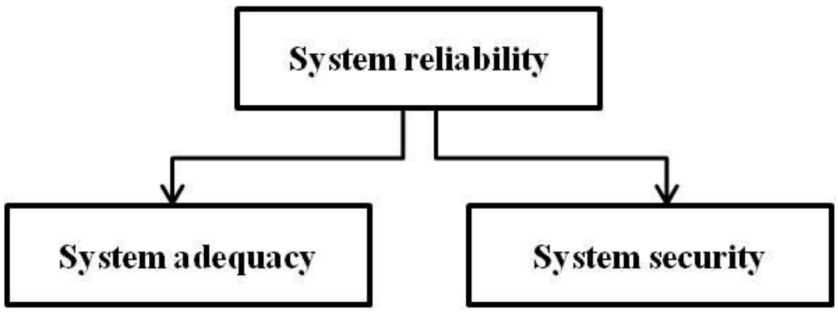

Figure 14. Division of system reliability [33]**.**

The system adequacy analyses whether all the facilities can fulfil all the load demands. The facilities considered in this analysis are everything in the power system, from the generators to the transmission system and the distribution system. This type of analysis is associated most of the time with static conditions [33], [34]. The system security analyses the system's ability to respond to dynamic and

transient disturbances that may happen. These disturbances are losses of generation or transmission facilities that are caused by local or widespread failures and can lead to dynamic, transient or voltage instability in the system. In this work, the focus lays on system adequacy for conducting reliability analysis in power systems.

2.5.1 System Analysis

Power systems are very complex and it is difficult to perform an analysis of system adequacy on the whole system. So, to perform an adequate analysis, the power system is divided in several segments which can be defined as functional zones of generation, transmission and distribution [33], [34]. The evaluation is made on each hierarchical level and combining all the results the evaluation of system adequacy for the whole power system is obtained. In this work, the focus lays on generation systems, which correspond to the HLI of the hierarchical level of Figure 15.

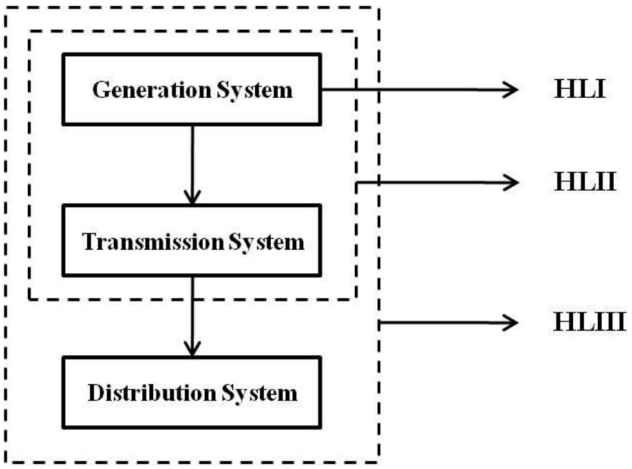

Figure 15. Hierarchical levels for system adequacy analysis [33], [34]**.**

2.5.2 Reliability Indices

One way to perform the reliability adequacy is using the stochastic and memoryless Markov process to transform the physical system to an appropriate and simple model, shown in Figure 16. This model only considers the present state and the precedent one, being independent of all other former states. The two-state model for a power system component can be either in-service or out-service. The process of changing the state of the system component is accomplished by two units. One is the failure rate and it is denoted by λ [1/year] and the other is the outage time and it is denoted by μ [hour/failure].

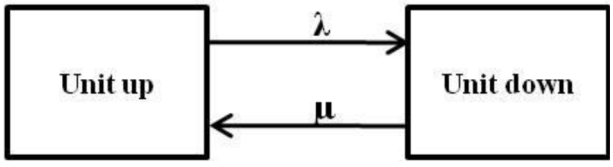

Figure 16. Markov two-state model for one unit [33]**.**

With the two units that characterize the Markov two-state model for one power component, the total unavailability per year in percentage per component can be calculated [33].

$$U = \frac{\lambda \times \mu}{8760} \times 100 \tag{15}$$

If the outages of two power components are independent (second order failure), this model can be expanded to include two independent components, as seen in Figure 17. The outage state can be forced or planned due to maintenance.

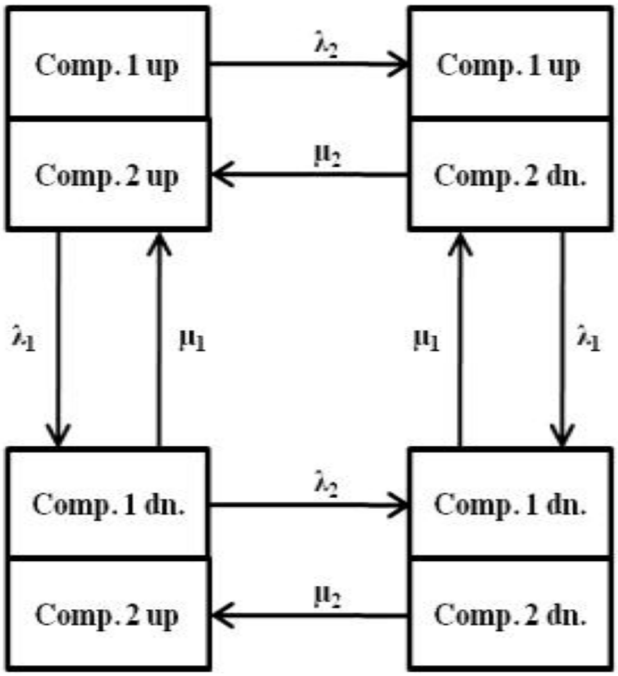

Figure 17. State space diagram of two independent components [16]**.**

The failure rate, outage time and unavailability per year of each power system component does not make the system adequacy analysis complete. This unit does not reflect the capability of the system to provide its customers with an acceptable level of supply. Thus, for a complete adequacy analysis, there are other indices. When analysing the reliability of the whole power system and, regarding the focus of this work, there are some important indices that are presented in Table 4 [33].

Table 4. System reliability indices.

Index	Unit	Description
SAIFI	[1/year]	System Average Interruption Frequency Index
SAIDI	[min/year]	System Average Interruption Index
CAIDI	[hour/int.]	Customer Average Interruption Index
ENS	[MWh/year]	Total Load Energy Not Supplied

These indices are mainly used for analysis of power systems (either for the whole or for a part) with generation points, distribution net and customers. However, for a reliability analysis of a wind farm, the related customer indices (SAIFI, SAIDI and CAIDI) are not used since there are not customers to evaluate. The topologies of the offshore wind farms only contain generation points and a distribution net, so the index used in this work was the ENS.

When executing the reliability analysis of a wind farm many variables need to be considered, such as generator capacity, wind variations, failure rate, outage time and many more. So, in the design phase, estimations of these variables are made to evaluate how much energy is likely to be produced on average. This average energy production can be easily converted into average expected income and be used to estimate the number of years until break even. For this evaluation, the ENS is an important index, because it is affected by both failure rate and outage time, which reflect the reliability of the project. The ENS is also useful when comparing topologies or reliability improvements, because it can easily be converted into economic benefits.

$$ENS = \sum U_i \times L_{avg,i} \tag{16}$$

where,

$L_{avg,i}$ – average load connected to load point i [MW],

U_i – unavailability of load point i [hour/year].

Chapter 3

Software Description

This chapter presents the software piece that was developed to compute the simulations and the calculations of the reliability indices and economic indicators. It starts with a brief explanation of the software and presents all the assumptions and scenarios that were considered so that trustworthy results could be simulated. These include: how much power is produced by the wind generators, the reliability data that was used, the faults considered for the simulations, what cables are used in the collector system, all costs associated with the necessary equipment to increase the reliability of the wind farm and how the economic evaluation was made. Finally, it also presents a validation of the software developed for this work.

3.1 Brief Description

For a reliability analysis and economic evaluation of the proposed topologies, a software was developed in MATLAB® (its open-source package MATPOWER®[1] [35] was also used). This developed software calculates the reliability indices and investment costs of a proposed topology, and with those results proceeds to do the economic evaluation. All the processes made by the software are presented in the flowchart in Figure 18. For the reliability analysis, it calculates the power flow for each possible scenario. In order to do the economic evaluation, the software needs a base reference topology to compare with the one being analysed, so that the added income and additional investment can be calculated. This base topology is created from the proposed topology, excluding all the elements added for reliability increase, namely the redundancies and the added equipment. The resulting base topology is known as the radial design. This is the design with less reliability levels, for which the occurrence of a fault causes all the equipment in a string to be out of service.

[1] Available at http://www.pserc.cornell.edu/matpower/

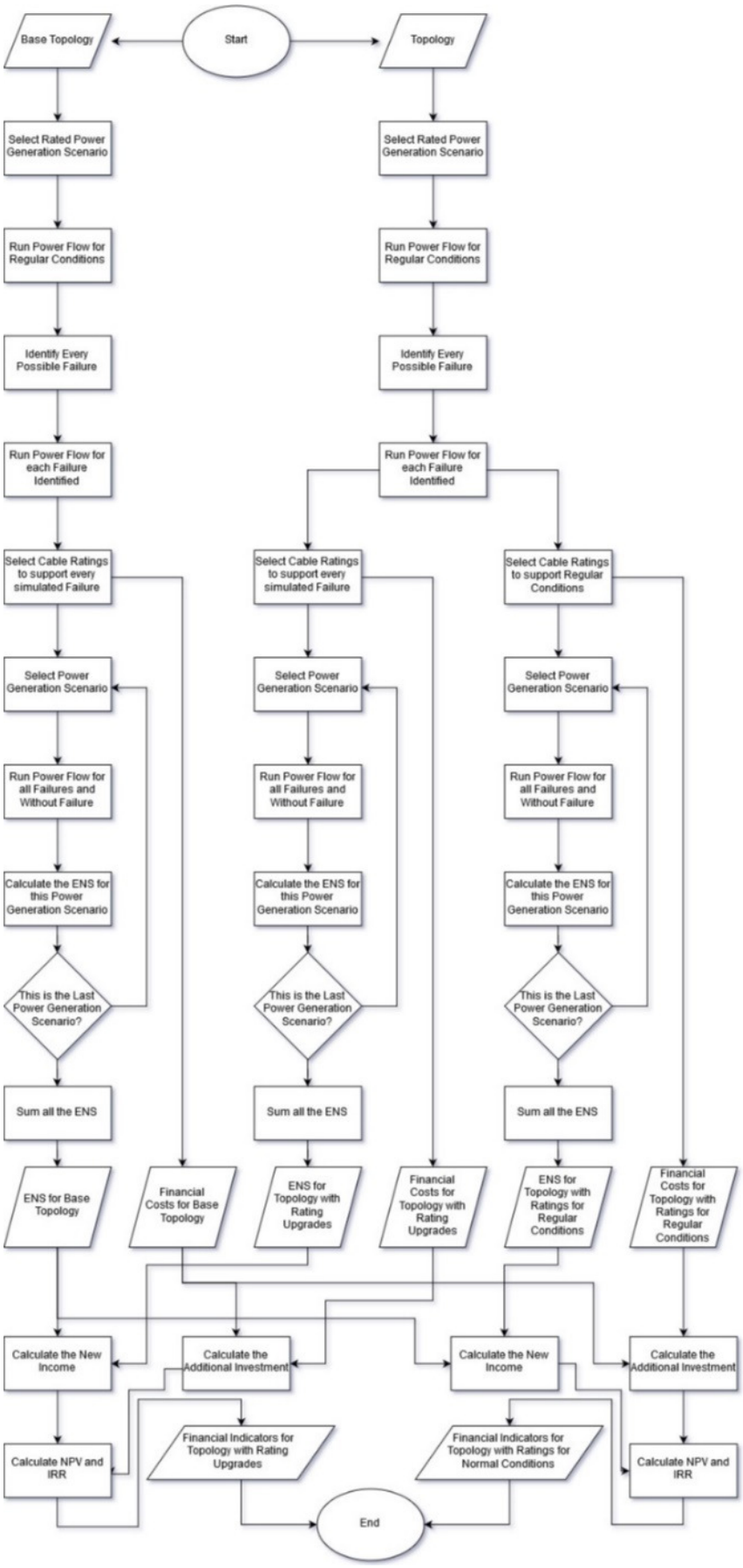

Figure 18. Software flowchart.

The software considers the variation of the wind by simulating twenty-two scenarios, each one associated with a probability. All these scenarios give the opportunity to consider wind variations in a trustworthy way and to reliably analyse all the topologies proposed. For a proposed topology, the software identifies every possible failure caused by protection elements and submarine cables, simulating each one for the twenty-two wind scenarios. Associating the results of all the simulations with the reliability data, the software calculates all reliability indices and investment costs. Finally, with those results the software proceeds to do the economic evaluation.

When choosing the topology to be analysed, a user does not need to specify the cable ratings, since they are automatically selected by the developed software, which identifies the most suitable ratings for each topology. This ensures that no money is wasted on improving ratings when it is not needed. The software selects the cable ratings from two different approaches. The ratings selected in the first approach are those necessary to handle every faulty scenario that may occur. The ratings selected in the second approach are those necessary to handle all scenarios for regular conditions (with no faults).

3.2 Power Generation Scenarios

For a trustworthy reliability analysis, it is necessary to simulate various scenarios for the output power of the wind generators. It is not enough to simulate just the rated power or even the average power. To compare different topologies, it is necessary to consider a wind probability density function.

So, it is necessary to define the power generation scenarios that will be used in the software for the reliability analysis and the economic evaluation of the proposed topologies. To accomplish that some assumptions are made and presented below.

Analysing the European Wind Atlas Offshore (Figure 3) and choosing the coast of Portugal, the annual average wind speed for a height of 100 m in open sea (more than 10 km offshore) is between 7.5 m/s to 8.5 m/s. So, selecting one value from this interval, the assumption considered in the simulations for the annual average wind speed is:

$$u_{avg\_annual}(100\ m) = 8.5\ m/s$$

The selected wind turbine was the Vesta V90-3MW [36], which is the turbine used in one of the biggest Offshore Wind farms, Thanet (300 MW) [37]. This turbine is characterized by a rated power of 3.0 MW, a cut-in speed of 3.5 m/s, a rated wind speed of 15 m/s and a cut-out speed of 25 m/s. The height of the tower is 105 m and the considered power factor was always 0.96 inductive (injective reactive power). The Power curve of this wind turbine is presented in Figure 19.

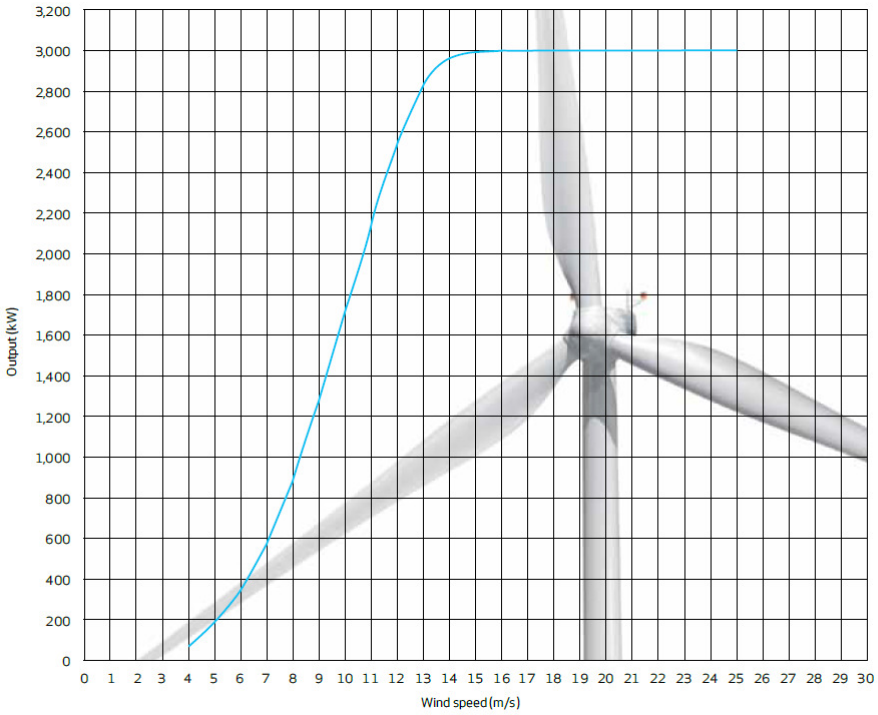

Figure 19. Power curve for V90-3MW [36]**.**

Since the height of the hub is different from the height of the assumed annual average wind speed, it is necessary to extrapolate it through the Prandtl law. In order to do that a surface roughness needs to be selected. According to Table 1, the surface roughness for a calm open sea is:

$$z_0 = 0.0002\ m$$

Using Equation 8, the assumed average annual wind speed at the hub height is:

$$u_{avg\_annual}(105\ m) = u_{avg\_annual}(100\ m) \times \frac{ln\left(\frac{105}{z_0}\right)}{ln\left(\frac{100}{z_0}\right)} = 8.532\ m/s$$

Now it is possible to define the probability distribution of the wind speed using the Rayleigh distribution. The only parameter of this distribution is the annual average wind speed, which was just calculated. With this distribution and using the cumulative probability (presented in Equation 6), it is possible to calculate a probability of a wind speed interval:

$$Probability\ [a;b] = F(a) - F(b) \tag{17}$$

where,

$Probability\ [a;b]$ – probability of the wind speed to be in the interval defined between a and b [%],

a – initial value for wind speed interval [m/s],

b – final value for wind speed interval [m/s],

$F(a)$ – cdf for wind speed a [%],

$F(b)$ – cdf for wind speed b [%].

Using this definition, it is possible to set twenty-two wind scenarios and associate each one with a probability [38]. From the power curve of the turbine, the average power generation for each wind speed interval can be calculated. Finally, it is possible to define the power generation scenarios to be simulated, with the average power generation and the probability associated with each wind speed interval. The numerical values are presented in Table 5.

Table 5. Each power generation scenario for the wind generators associated with a probability.

Initial Value [m/s]	Final Value [m/s]	Probability [%]	Power at Initial Value [MW]	Power at Final Value [MW]	Avg. Power [MW]
3.5	4.0	3.47	0.000	0.077	0.0385
4.0	5.0	7.79	0.077	0.190	0.1335
5.0	6.0	8.55	0.190	0.353	0.2715
6.0	7.0	8.87	0.353	0.581	0.4670
7.0	8.0	8.81	0.581	0.886	0.7335
8.0	9.0	8.40	0.886	1.273	1.0795
9.0	10.0	7.73	1.273	1.710	1.4915
10.0	11.0	6.89	1.710	2.145	1.9275
11.0	12.0	5.96	2.145	2.544	2.3445
12.0	13.0	5.00	2.544	2.837	2.6905
13.0	14.0	4.08	2.837	2.965	2.9010
14.0	15.0	3.24	2.965	2.995	2.9800
15.0	16.0	2.51	2.995	3.000	2.9975
16.0	17.0	1.89	3.000	3.000	3.0000
17.0	18.0	1.39	3.000	3.000	3.0000
18.0	19.0	1.00	3.000	3.000	3.0000
19.0	20.0	0.70	3.000	3.000	3.0000
20.0	21.0	0.48	3.000	3.000	3.0000
21.0	22.0	0.32	3.000	3.000	3.0000
22.0	23.0	0.21	3.000	3.000	3.0000
23.0	24.0	0.13	3.000	3.000	3.0000
24.0	25.0	0.08	3.000	3.000	3.0000

So, the software simulates each scenario, where the power generated in the wind turbines is the average power generation for each of them, and multiplies the reliability results with their associated probability:

$$ENS_{Topology} = \sum_{i} ENS_{Scenario\ i} \times Probability_{Scenario\ i} \quad (18)$$

where,

$ENS_{Topology}$ – Energy Not Supplied for the analysed topology [MWh],

$ENS_{Scenario\ i}$ – Energy Not Supplied for the analysed topology and the power generation scenario i [MWh],

$Probability_{Scenario\ i}$ – probability of the wind speed to be in the interval defined for the power generation scenario i [%] (see Table 5).

3.3 Reliability Analysis

To increase the reliability of a topology, different types of protection elements can be used, such as circuit breakers, load switches and disconnectors. An example of a topology that uses all these elements is present in Figure 20. The circuit breakers are the elements that take automated action, switching on and off automatically to protect all other elements when a fault occurs. Their switching action can also be remotely controlled. The load switches are protection elements that are only remotely controlled, this means that a status change only takes place through a remote command. The disconnectors are protection elements that can only be controlled manually, meaning that their switching status only change if someone goes to the site directly. All these elements are considered correctly dimensioned and treated as ideal elements during the power flow calculation.

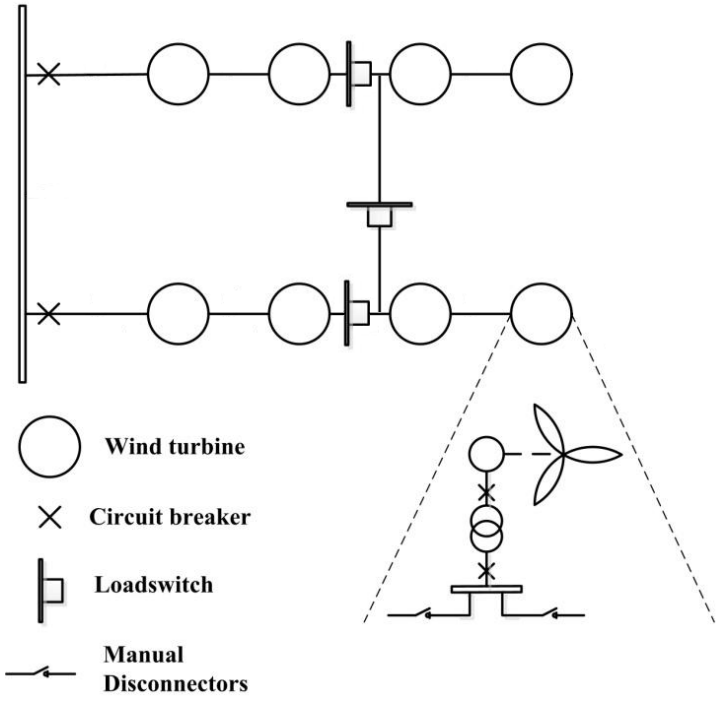

Figure 20. Example of a topology with all types of protection elements.

Since all the protection elements and the submarine cables have failures, the failure rates for each one are considered in the reliability analysis [39], [40]. The software identifies all possible failures caused by each element and simulates them all. The reliability results from each failure are then multiplied by their associated probability - their failure rate:

$$ENS_{Scenario\ i} = \sum_{k} ENS_{Failure\ k} \times Failure\ Rate_{Failure\ k} \quad (19)$$

where,

$ENS_{Scenario\ i}$ – Energy Not Supplied for the analysed topology and the power generation scenario i [MWh],

$ENS_{Failure\ k}$ – Energy Not Supplied for the analysed topology and the power generation scenario i when the failure k occurs [MWh],

$Failure\ Rate_{Failure\ k}$ – probability of a fault occurring in the equipment that caused the failure k [%].

The failure rates for each equipment are presented in Table 6. This table also presents the repair time needed to repair an element when a failure occurs, and the switching time needed to switch the status of a protection element (this time varies if the element is remotely controlled or manually operated) [39], [40].

Table 6. Reliability data.

Equipment	Failure Rate [failure/year]	Repair Time [hours]	Switching Time [min]
Submarine Cables	0.004	672	-
Disconnectors	0.02	168	10080
Circuit Breakers	0.03	168	20
Load Switches	0.03	168	20

The automated action of the circuit breaker that protects all the elements when a fault occurs is assumed to be instantaneous. However, the switching action of this equipment that is remotely controlled is not and the assumed time for that action to take place is 20 minutes. The disconnector's switching time is very high because it needs to be performed by service personnel going to the turbine by boat.

3.4 Fault Analysis

The faults that are considered in the reliability analysis are cable faults, circuit breaker faults, disconnector faults and load switch faults. Each possible failure is identified by the software, then all of them are simulated and the reliability indices are calculated according to Equation 19. The description

of the faults considered for the reliability analysis described below becomes easier to comprehend with the reading of Appendix B, where one example is thoroughly detailed.

Analysing the reliability data in Table 6, for the submarine cable faults, three periods in which the number of online turbines is different can be seen. The first period is characterized by the automated action of the protection equipment when the fault occurs. So, in this period, the string of wind turbines where the fault occurs will be out of service. The second period is characterized by the switching of the remote protection equipment. In this period, depending on the location of the redundancy, an increase in the number of online turbines may happen. The third and final period happens when the disconnector is manually switched and an increase in the number of online turbines may also happen. This period ends when the cable is finally repaired.

So, the calculation of the total Energy Not Supplied if a failure occurs, considering all the three identified periods, can be made by:

$$ENS_{Failure\ k} = \sum_{p} ENS_{Period\ p} \tag{20}$$

where,

$ENS_{Failure\ k}$ – Energy Not Supplied for the analysed topology and the power generation scenario i when the failure k occurs [MWh],

$ENS_{Period\ p}$ – Energy Not Supplied for the analysed topology and the power generation scenario i when the failure k occurs for the situation o period p [MWh].

The calculation of the Energy Not Supplied if a failure occurs for each period can be made by:

$$ENS_{Period\ p} = \Delta t_{Period\ p} \times \left(Power\ Supplied_{Regular\ Conditions} - Power\ Supplied_{Period\ p}\right) \tag{21}$$

where,

$ENS_{Period\ p}$ – Energy Not Supplied for the analysed topology and the power generation scenario i when the failure k occurs for the situation at period p [MWh],

$\Delta t_{Period\ p}$ – duration of the period p when the failure k occurs [h],

$Power\ Supplied_{Regular\ Conditions}$ – power supplied for the analysed topology for the power generation scenario i for regular conditions (with no failures) [MW],

$Power\ Supplied_{Period\ p}$ – power supplied for the analysed topology for the power generation scenario i when the failure k occurs for the situation at period p [MW].

For an easier comprehension, an example is now calculated for the topology presented in Figure 20. If a cable fault occurs in the first cable in the topology, the state of the topology during the first period can be seen in Figure 21. Analysing the data in Table 6, the first period starts with the automated action of the circuit breakers (which is instantaneous) and ends when the switching of the remote protection equipment (circuit breakers and load switches) happens, so the duration of this period is:

$$\Delta t_{Period\ 1} = \frac{20}{60} h = 0.33\ h$$

The characterization of the second period can be seen in Figure 22. This period starts with the switching action of the circuit breakers and the load switches and ends when the disconnector's manual switching takes place, so its duration is:

$$\Delta t_{Period\ 2} = \left(\frac{10080}{60} h - \frac{20}{60} h\right) = 167.67\ h$$

And finally, the characterization of the third period can be seen in Figure 23, which ends when the cable failure is repaired:

$$\Delta t_{Period\ 3} = \left(672\ h - \frac{10080}{60} h\right) = 504\ h$$

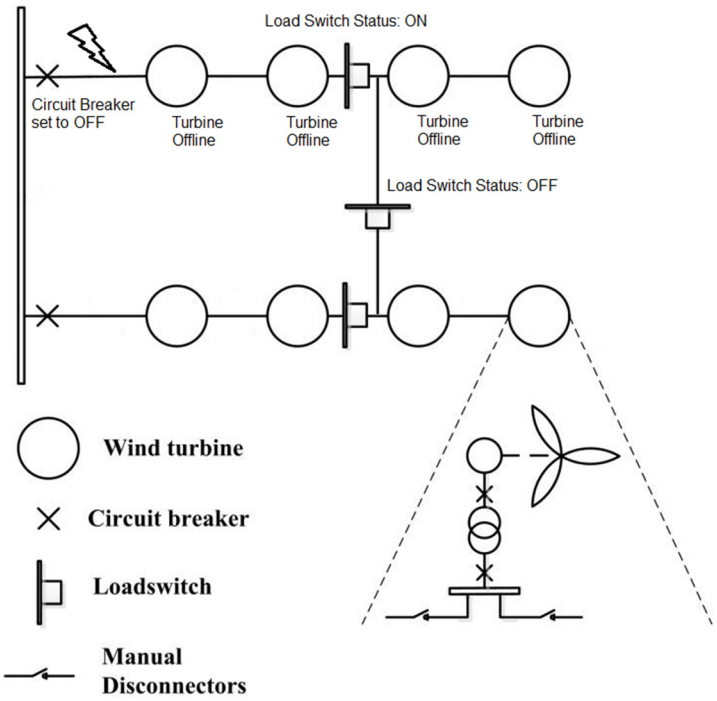

Figure 21. The first period when a fault occurs in the first submarine cable.

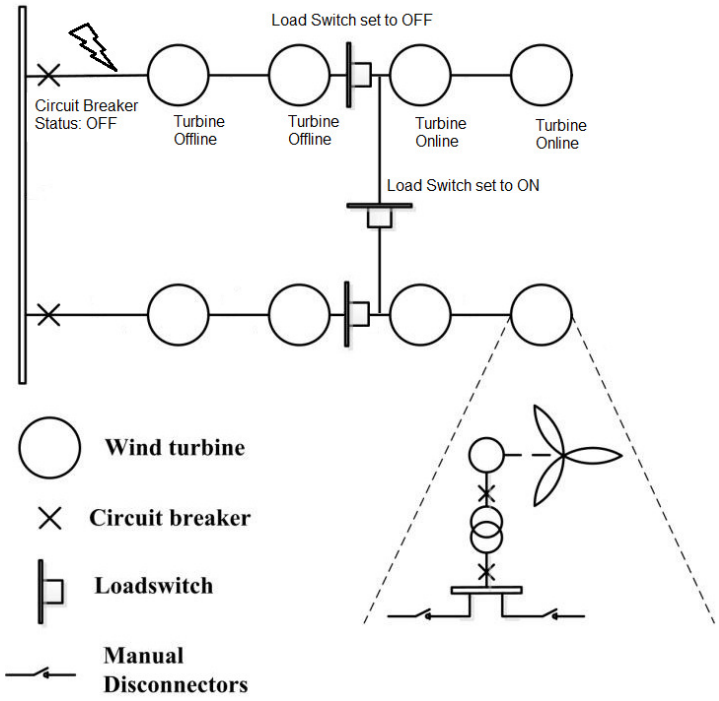

Figure 22. The second period when a fault occurs in the first submarine cable.

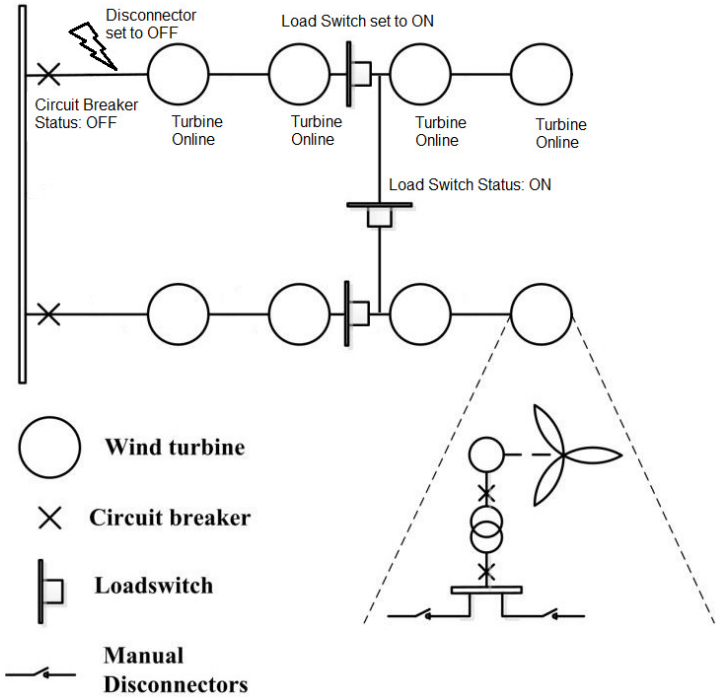

Figure 23. The third period when a fault occurs in the first submarine cable.

A similar reasoning than the one done for a cable fault can be made for circuit breaker faults, disconnector faults and load switch faults. However, instead of having three periods, only the first two occur. This happens because the repair time of these equipments is not greater than the switching time of the disconnectors, which is when the third period starts. So, the second period when a failure occurs in circuit breakers, disconnectors and load switches ends when the protection equipment is repaired.

It is important to note that the redundancies which are included in the proposed topologies are out of service during the regular operation of the wind farm. This means the reliability analysis does not analyse the occurrence of a fault in the redundancy cables.

The focus of this work is to perform a reliability analysis of the internal grid of an offshore wind farm. This means that for faults that occur outside the internal grid, the analysis is outside the scope of this work, because the additional elements added in the internal grid will not bring any increase of reliability to those failures.

3.5 Cable Ratings

Another important element to select is the cables that are to be used for the collector system. For this, it is necessary to calculate the power flow and the power losses of the system. Since the most common rated voltage used in the wind farm collector system is 33 kV, the selected submarine cable is the three-core cable with copper wire screen [41]. This type of cable has a wide range of available cross-sections, which are presented in Table 7. However, the selection is made by the software according to the power capacity that each cable must collect.

The software calculates simultaneously reliability and economic indicators from two different approaches for the selection of the cable ratings. The ratings selected in the first approach are those necessary to handle every faulty scenario that may occur. This means they are designed to handle all power produced by all online turbines when any fault occurs. The topologies with the first approach will be named Topologies with Rating Upgrades (TRU). From this approach, it is never necessary to turn off a wind turbine because the cable wouldn't be able to handle its power in the occurrence of a fault. The ratings selected in the second approach are those necessary to handle all scenarios for regular conditions (with no faults). The topologies with the second approach will be named Topologies with Ratings for Regular Conditions (TRRC). This means that if a failure occurs, it may be necessary to turn off some turbines because the cables are not capable of handling all the power. The reasoning behind the second approach is that both the failure rates and the probability of a wind turbine operating at the rated power are very low. So, the probability of a failure occurring while the wind turbines are operating at the rated power is even lower. Therefore, rating the cables at regular conditions means they will be able to handle most of the cases when the power produced by the wind turbines is less than the rated power. This means that in some scenarios it is not necessary to turn off turbines because of the cable ratings. In short, the reason for analysing this approach is to see if it is reasonable to increase the cable ratings (as in the first approach) just to account for some scenarios that are very unlikely.

Table 7. Three-core cable with cooper wire screen [41]**.**

Cross-section of conductor [mm^2]	Diameter of conductor [mm]	Insulation Thickness [mm]	Diameter over insulation [mm]	Cross section of screen [mm^2]	Outer diameter of cable [mm]	Cable weight (Aluminium) [kg/km]	Cable weight (Copper) [kg/km]	Capacitance [µF/km]	Charging current per phase at 50 Hz [A/km]	Inductance [mH/km]	Transmission capacity [MVA]
95	11.2	8.0	29.6	16	104.0	17.7	19.5	0.18	1.0	0.44	20
120	12.6	8.0	31.0	16	107.0	18.4	20.7	0.19	1.0	0.42	23
150	14.2	8.0	32.6	16	110.5	19.3	22.1	0.21	1.1	0.41	25
185	15.8	8.0	34.2	16	114.0	20.1	23.6	0.22	1.2	0.39	28
240	18.1	8.0	36.5	16	118.9	21.4	25.9	0.24	1.3	0.38	33
300	20.4	8.0	38.8	16	123.9	22.6	28.2	0.26	1.4	0.36	37
400	23.2	8.0	41.6	16	129.9	24.6	32.0	0.29	1.6	0.35	41
500	26.2	8.0	45.0	16	137.3	26.7	36.0	0.32	1.7	0.34	46
630	29.8	8.0	48.6	16	145.1	29.2	40.9	0.35	1.9	0.32	52
800	33.7	8.0	52.5	16	154.4	32.2	47.2	0.38	2.1	0.31	57
1000	-	-	-	-	-	-	-	0.41	-	0.30	65
1200	-	-	-	-	-	-	-	0.43	-	0.29	71

* An extrapolation of the capacitance, inductance and transmission capacity was performed for cable ratings 1000mm^2 and 1200mm^2 (see Appendix A).

For an easier comprehension, an example can be calculated for the TRRC approach, for the topology presented in Figure 20. For regular conditions (with no faults) the first cable of the second string must handle the power of four turbines, resulting in a maximum power transmitted of $4\times\frac{3\ MW}{0.96}=12.5\ MVA$. According with Table 7, the selected cross-section of the cable will be 95 mm^2 and the transmission capacity will be 20 MVA. If a fault occurs in the first cable of the first string, for the third period the characterization of the topology is the one already presented in Figure 23. Considering the power generation scenario at rated power (3 MW), all the wind turbines are generating 3.125 MVA. So, according to the characterization of the topology in the third period, the first cable of the second string would need to handle the power generated by 8 turbines (25 MVA). But, according to the selected cross-section of the cable, it can only handle 6 turbines (18.75 MVA), meaning that 2 turbines must be switched off due to the rating chosen for the cable, as presented in Figure 24. Considering now the power generation scenario at 2.34 MW, the power generated by all the turbines is 2.44 MVA. So, now the first cable of the second string can handle all the 8 turbines (19.53 MVA), meaning that there is no need to turn off any turbine because of the rating chosen for the cable, as presented in Figure 25. In conclusion, this approach limits the power supplied in case of a failure in the first cable of the first string, for some power generation scenarios, but it behaves like the first approach at a lower investment cost for power generation scenarios below 2.34 MW. This means that here the TRRC approach would have worst reliability indices just for wind speed scenarios that occur 21.03% of the time (the probability of the wind power to be greater than 2.34 MW, as can be computed from Table 5), but with a lower investment cost. It is important to note that a failure in cable one of the first string is one of the worst situations where this lack of rating upgrades is most noticeable. The reliability results will vary for each failure depending on the location of the equipment within the topology. Finally, the TRRC approach will have lower reliability indices (but not much lower, since this approach is limited for the less likely scenarios) than the TRU approach, but will have a lower investment cost.

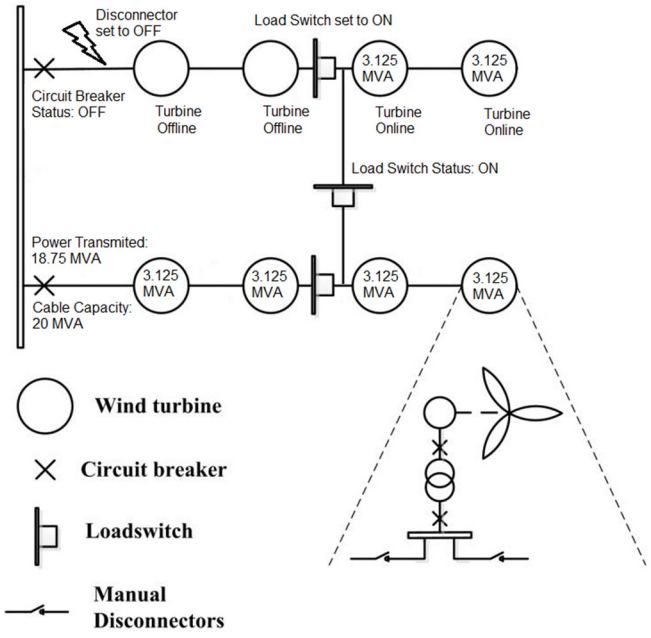

Figure 24. Topology with ratings for regular conditions for a power generation scenario of 3 MW.

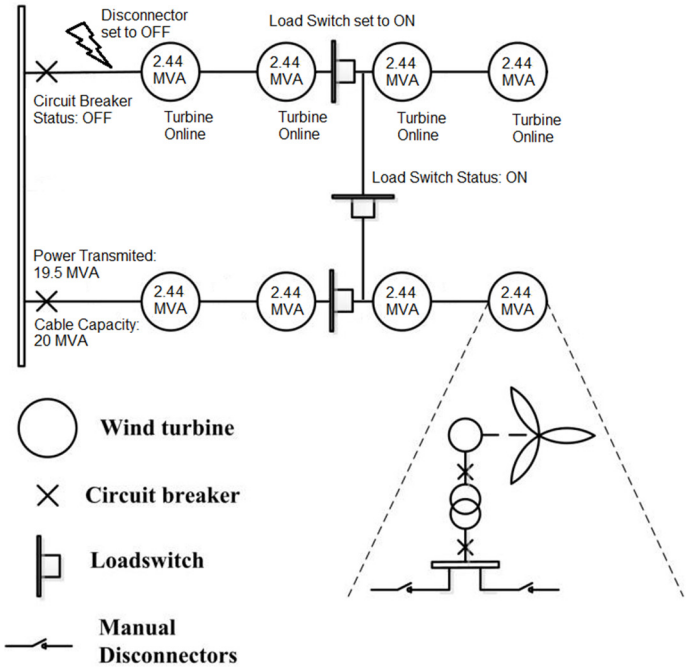

Figure 25. Topology with ratings for regular conditions for a power generation scenario of 2.34 MW.

3.6 Investment Costs

Since this work is analysing the reliability of the use of a redundancy, only the additional costs for introducing the reliability increment are considered and compared to the additional income made by the use of this redundancy. The cost of the additional equipment added to increase the reliability of the wind farm is presented in Table 8 [40].

Table 8. Data used for investment costs.

Equipment or Service	Cost
Vessel and Installation of the Cable	200 k€/km
Load Switch (with voltage and current measurement)	10 k€
Cable with a cross section of 95 mm^2	100 k€/km
Cable with a cross section of 120 mm^2	110 k€/km
Cable with a cross section of 150 mm^2	140 k€/km
Cable with a cross section of 185 mm^2	160 k€/km
Cable with a cross section of 240 mm^2	180 k€/km
Cable with a cross section of 300 mm^2	220 k€/km
Cable with a cross section of 400 mm^2	240 k€/km
Cable with a cross section of 500 mm^2	270 k€/km
Cable with a cross section of 630 mm^2	300 k€/km
Cable with a cross section of 800 mm^2	350 k€/km
Cable with a cross section of 1000 mm^2	360 k€/km
Cable with a cross section of 1200 mm^2	370 k€/km

3.7 Economic Evaluation

To proceed to the economic evaluation, it is necessary to compare the reliability indices and the investment costs with a reference base topology so that the new income (Cash Flow) and the additional necessary investment (I_0) are calculated. The topology used for comparison is called Base Topology. This topology is a radial design where all the elements added to the analysed topology to increase the reliability are excluded, namely the redundancies and the added equipment. An example of a Base Topology is presented in Figure 26, if the proposed topology is the one presented in Figure 20. The reason for choosing the radial design to be the Base Topology is because it is the design which has the lower reliability indices, so every single increment in reliability is considered when evaluating the proposed topology. All reliability processes are evaluated for the Base Topology too. However, it is not necessary to perform the two approaches for cable rating selection, since this topology does not have any redundancies, so the results for each would be the same.

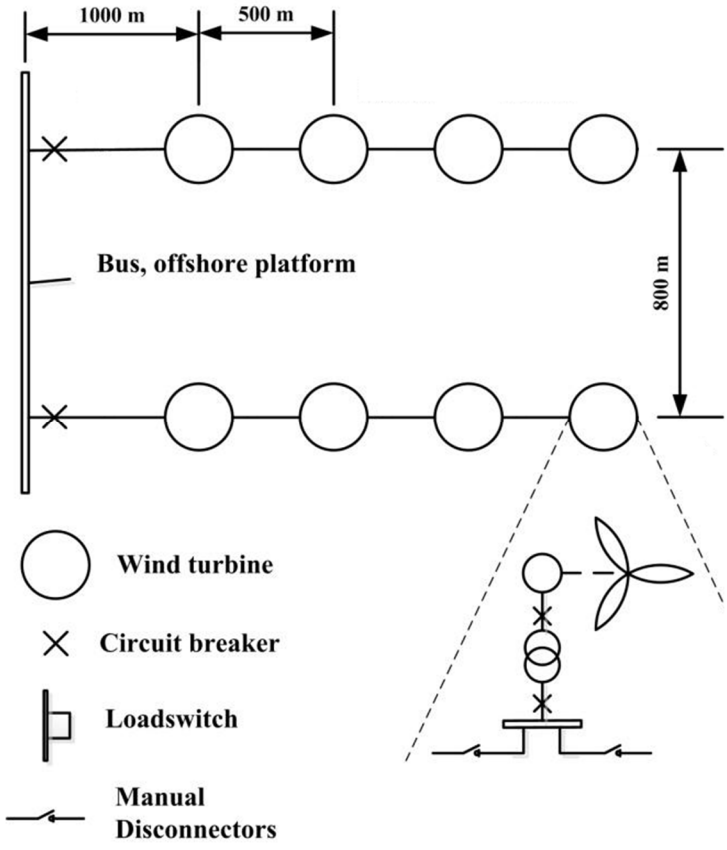

Figure 26. Base topology for an offshore wind farm with 2 strings each one with 4 turbines.

After calculating the reliability indices for the two topologies (proposed topology and base topology), it is possible to calculate the new income (Cash Flow) and additional investment (I_0) necessary to accomplish the proposed topology.

$$CF_y = \left(ENS_{Base\ Topology} - ENS_{Proposed\ Topology}\right) \times Selling\ Price \quad (22)$$

where,

CF_y – cash flow at year y [€],

$ENS_{Base\ Topology}$ – Energy Not Supplied for the base topology [MWh],

$ENS_{Proposed\ Topology}$ – Energy Not Supplied for the proposed topology [MWh],

$Selling\ Price$ – energy selling price (see Table 9) [€/MWh].

$$I_0 = Investment\ Cost_{Proposed\ Topology} - Investment\ Cost_{Base\ Topology} \quad (23)$$

where,

I_0 – additional investment at year 0 [€],

$Investment\ Cost_{Proposed\ Topology}$ – total investment cost for the base topology (see Table 8) [€],

$Investment\ Cost_{Base\ Topology}$ – total investment cost for the proposed topology (see Table 8) [€].

From these results, all economic indicators necessary for the evaluation of the proposed topology are calculated, such as the NPV and IRR. For the calculation, it is necessary to make assumptions for the expected lifetime of the wind farm, for the discount rate and for the expected income per MWh. These assumptions are presented in Table 9.

Table 9. Data used for economic evaluation.

Investment Data	Value
Expected lifetime of the wind farm	20 years
Discount rate	0.07
Selling price	100 €/MWh

3.8 Software Validation

The topology used for the validation of the software is much simpler than the ones that are being simulated in this work. It is presented in Figure 20 and it is a double-sided half ring design composed of two strings, each one with four Vestas V90-3MW wind turbines. The base topology used to compare this topology to and analyse the increase or decrease in reliability is the one presented in Figure 26. For an easier calculation, it was considered that the wind turbines were operating at the rated power (3 MW) all of the time.

Two different validations were conducted, one where all the calculations were made by hand and another one where all the calculations were made by a third-party reliability software. The first validation

is presented in Appendix B, in which all calculations and process steps made by the developed software are detailed. The aim of this is not only to validate the software but also to provide a basic understanding of how it executes its calculations. The second validation is presented in Appendix C.

The results obtained by the calculations made by hand are presented in Table 10 (reliability results and investment costs) and Table 11 (economic indicators). By looking at the reliability results, a small divergence in the ENS values (less than 0.31%) can be seen. This happens because in the hand calculations the power losses are not considered, for simplicity. The results of the investment cost are equal. The differences in the economic indicators are caused by the previously mentioned divergence in the ENS values.

Table 10. Hand calculations and software for reliability results and investment costs.

Topology	ENS [MWh]		Investment cost [k€]	
	Hand	Software	Hand	Software
Base Topology	1233.8	1230.0	500	500
TRU	650.2	650.8	870	870
TRRC	686.5	686.5	780	780

Table 11. Hand calculations and software economic indicators for the topology with redundancy.

Economic Indicators	TRU		TRRC	
	Hand	Software	Hand	Software
NPV [k€]	248.3	243.5	299.8	295.8
IRR [%]	14.77	14.63	18.94	18.79

The results obtained by the third-party software are presented in Table 12 (reliability results and investment costs) and Table 13 (economic indicators). By looking at the reliability results a small divergence in the ENS values (less than 0.63%) can be seen. This is due to the way the third-party software makes its reliability analysis calculations: since wind generators are modelled as loads and the delivery point as a generator, the power flows end up with directions opposite to the real ones. The results of the investment cost are equal, because the third-party software does not select the cable ratings, it only analyses the reliability for the given topology. The differences in the economic indicators are caused by the divergence within the ENS values.

Table 12. Third-party software and software for reliability results and investment costs.

Topology	ENS [MWh]		Investment cost [k€]
	Third-party Soft.	Software	
Base Topology	1237.7	1230.0	500
TRU	651.3	650.8	870
TRRC	686.6	686.5	780

Table 13. Third-party software and software economic indicators for the topology with redundancy.

Economic Indicators	TRU		TRRC	
	Third-party Soft.	Software	Third-party Soft.	Software
NPV [k€]	251.15	243.5	303.75	295.8
IRR [%]	14.85	14.63	19.08	18.79

Chapter 4

Wind Farm Proposed Topologies

This chapter presents the proposed topologies analysed in this work, which can be separated in two different groups. The first one is all the topologies with a redundancy between each pair of two strings (Redundancy between two strings). The other proposed topologies introduce a new design, which is characterized by a redundancy between the already redundantly paired sets of strings (Redundancy between two redundantly paired strings).

4.1 Redundancy between two Strings

The topology that was tested in this work is the double-sided half ring design (Figure 12), since this is the one which presents better reliability and economic results [16], even compared with the topologies presented in [9], which are radial (Figure 7), single-sided ring (Figure 8), double-sided ring (Figure 9) and single return (Figure 11). Since the reliability analysis needs a base topology to compare the increase or decrease in reliability to, the topology adopted for that is the one presented in Figure 27. The topologies that are being reliability analysed have a redundancy between the two strings and they are based on the double-sided half ring design. The purpose of this analysis is to evaluate which location is the best for the redundancy. There are eight possibilities for the location of the redundancy for this design which are presented in Figure 28. The first topology has a redundancy in location 1, the eighth topology has a redundancy in location 8 and the other six are the other possible locations between them.

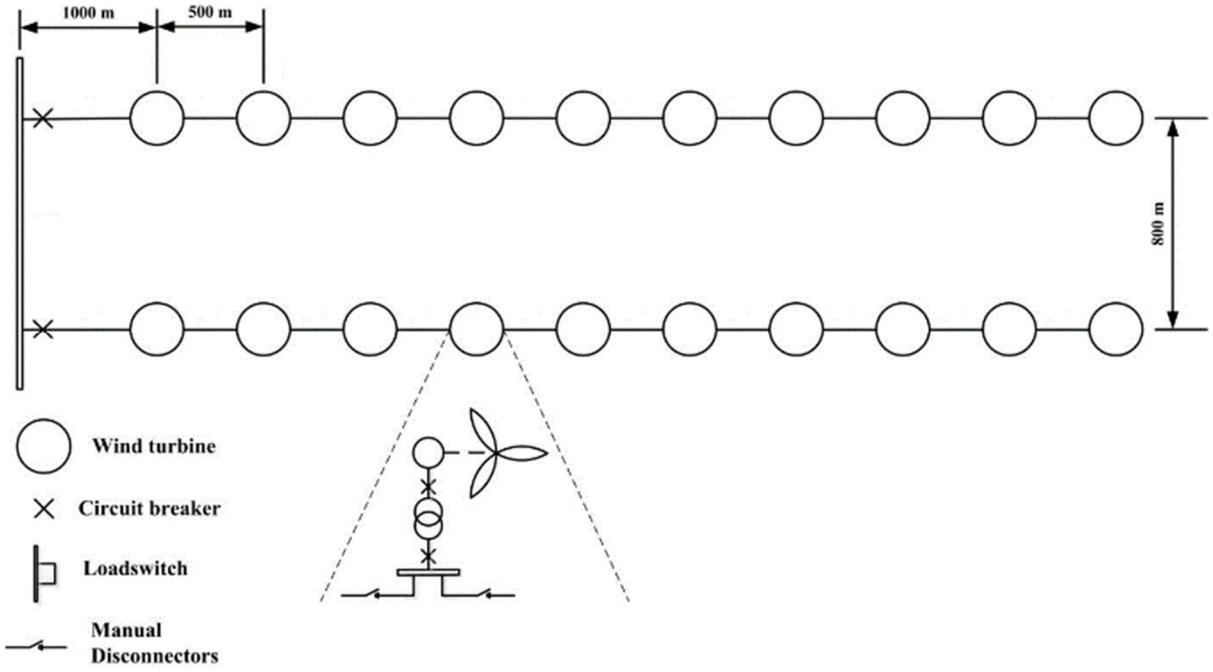

Figure 27. Base case: topology without redundancy.

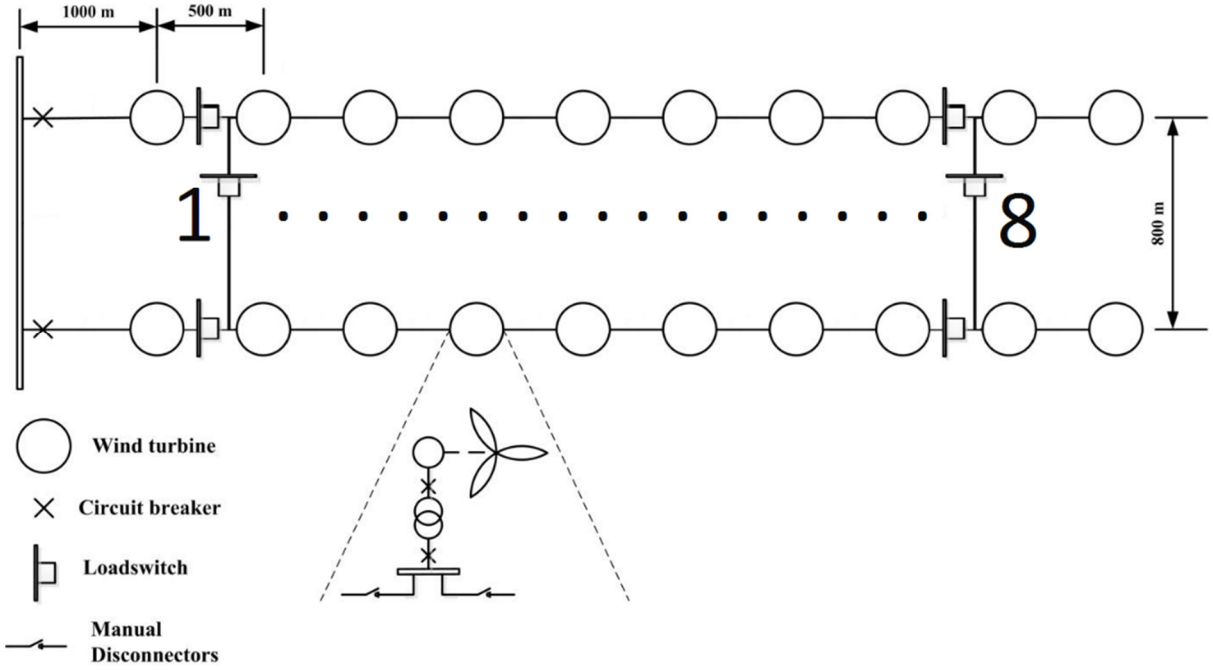

Figure 28. Proposed topology: topology with eight possible locations for redundancy.

4.2 Redundancy between two Redundantly paired strings

In most recent years, large offshore wind farms are appearing like the London Array (630 MW) in the United Kingdom or the Gemini (600 MW), in the Netherlands, which will be operational in 2017 (expected). This highlights the importance of using redundancies in wind farms and researching new topology designs. Until now, topologies only introduce redundancies between two isolate strings. In this work, a new type of topology design is proposed. These topologies analyse the introduction of a

redundancy between an already redundantly paired set of strings. At first glance, these topologies give an important advantage with the introduction of one more redundancy - if a fault occurs, the power generated by the wind turbines within the faulted string can be distributed to the others strings. This means that it will not be needed to increase the cable ratings much more for them to be able to handle all the generated power.

The first proposed topology of this kind is based on the double-sided half ring design and double-sided ring design and is presented in Figure 29. The second one is based only on the double-sided half ring design and is presented in Figure 30. The other four topologies proposed are based on the double-sided half ring design, but the location of the redundancy is different. The location of the redundancy for these topologies is between locations 3 and 6, as defined above. One example of these proposed topologies is one with a redundancy in location 5, presented in Figure 31. It is important to note that the topologies defined in Figure 28 only introduce redundancies between two strings, they do not introduce a redundancy between each redundantly paired set of strings, like the proposed topologies just mentioned.

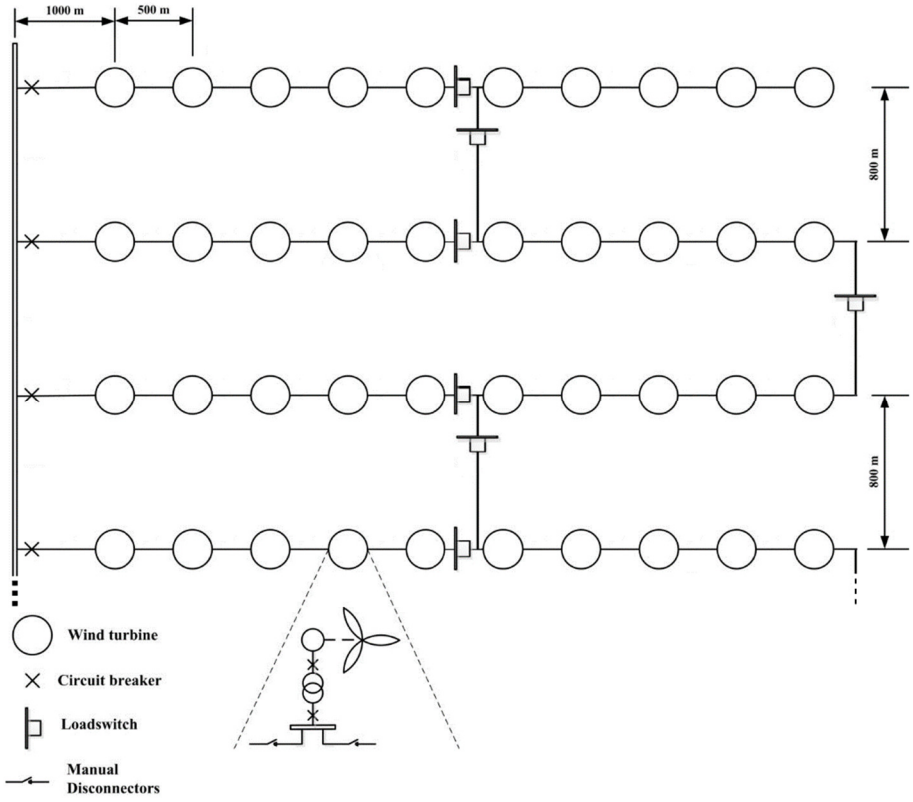

Figure 29. First proposed topology: based on double-sided half ring design and single-sided ring design.

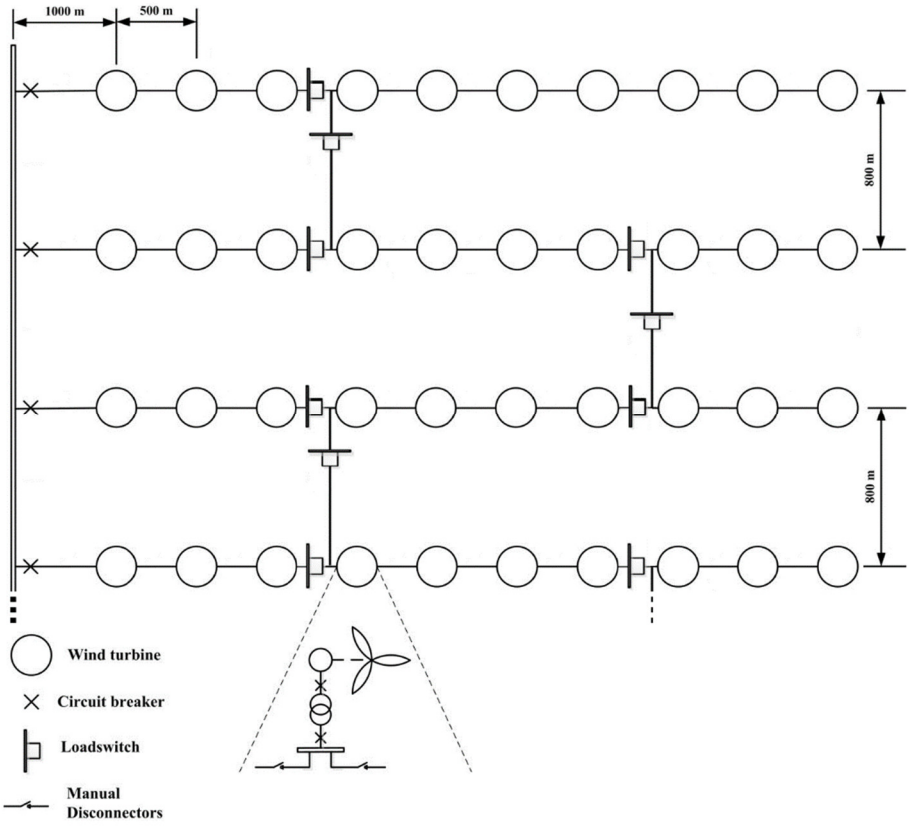

Figure 30. Second proposed topology: based on double-sided half ring design.

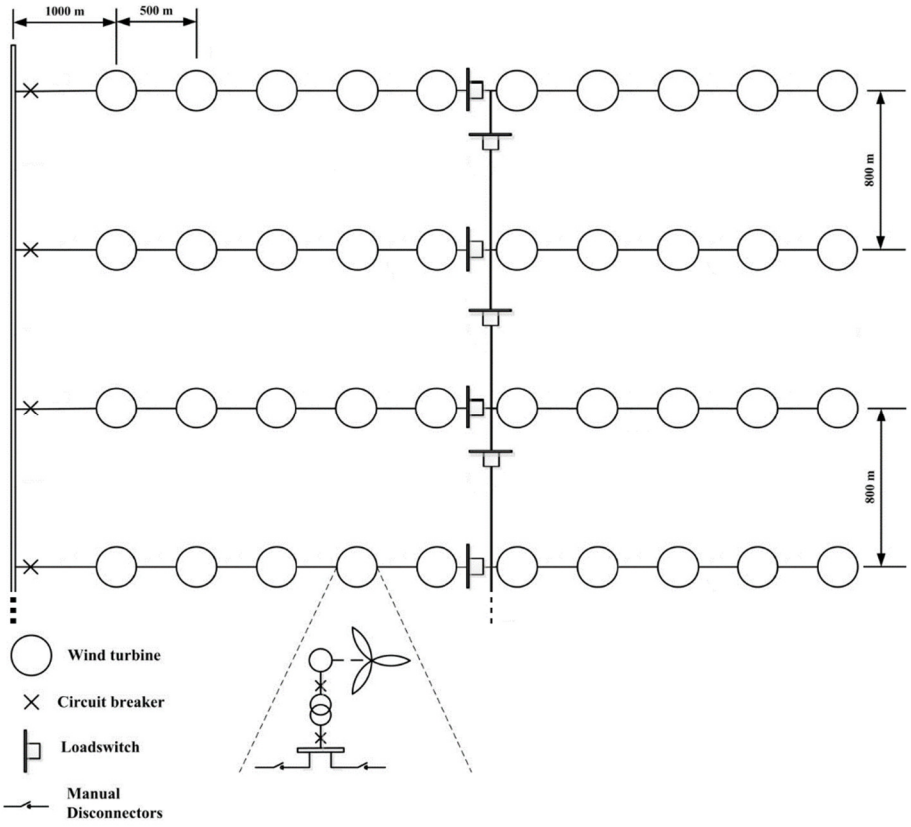

Figure 31. Fifth proposed topology: redundancy on location 5 and based on double-sided half ring design.

Chapter 5

Results

This chapter presents the reliability and economic results obtained from the developed software for the proposed topologies. The first analysis made was to evaluate the best location for the redundancy based on the double-sided half ring design (classical redundancy design), which is the design that has the best reliability and economic results from all the topologies presented in [9] and [16]. Since the developed software analyses two different approaches for the choosing of the cable ratings, this first analysis enables the evaluation of the best economic approach for the rating selection too. Also, a sensitivity analysis is developed for these topologies. Since the reliability data varies a lot in academic literature, it is important to ensure which is the best approach for cable rating selection and the best location for the redundancy. Finally, the last analysis made was to evaluate new designs which are characterized by a redundancy between the already redundantly paired sets of strings (new redundancy design – NRD). An additional simplified sensitivity analysis was then performed for the best topologies for both designs evaluated in this work.

5.1 Classical Redundancy Design

One of the focus of this work is to select the best location for the redundancy of all the possible locations on the double-sided half ring design. The double-sided half ring design which was presented in [16] only considered the location of the redundancy in the middle of the string. However, more possibilities exist, and each one has its pros and cons. So, it is necessary to analyse all of them and evaluate which one presents the best economic indicators. To accomplish that, eight different topologies were proposed (see Figure 28) and analysed. These are composed of two strings with 10 wind turbines each and one redundancy. Each proposed topology has a different location for this redundancy. As explained before, the developed software analyses two different approaches for the selection of the cable ratings that will lead to two different sets of results. These two approaches are named as Topologies with Rating Upgrades (TRU) and Topologies with Ratings for Regular Conditions (TRRC). Therefore, the results are being presented in two separated parts.

5.1.1 Topology with Rating Upgrades

The first approach for cable rating selection was named Topologies with Rating Upgrades (TRU), where the cables are rated to handle all the power produced by all online turbines when any failure occurs, so it is not needed to turn off wind turbines because a cable cannot handle the required power. From this approach, the developed software calculates the reliability indices (ENS) and the Investment Cost. After that it calculates the economic indicators which are the NPV and the IRR.

The reliability results for the TRU approach for all possible locations of the redundancy are presented in Figure 32. As it can be seen the location that has the best Energy Not Supplied (ENS) is the 5th. This result can be explained by the fact that this location divides the string into two equal parts, which gives the best ratio for all possible faults. For an easier understanding, consider the 6th location for the redundancy (see Figure 33). If a failure occurs in the first side of the string (first 6 turbines), in the second period (as defined in Chapter 3.4) all the 6 turbines are offline. But if a failure occurs in the second side of the string (last 4 turbines), in the second period only 4 turbines are offline. So, for this redundancy location a failure in the second side is less severe than in the first side. So, depending on the location, each side will have greater or less severe situations and it is only possible to determine the location which has the best adequate situations through numerical simulations.

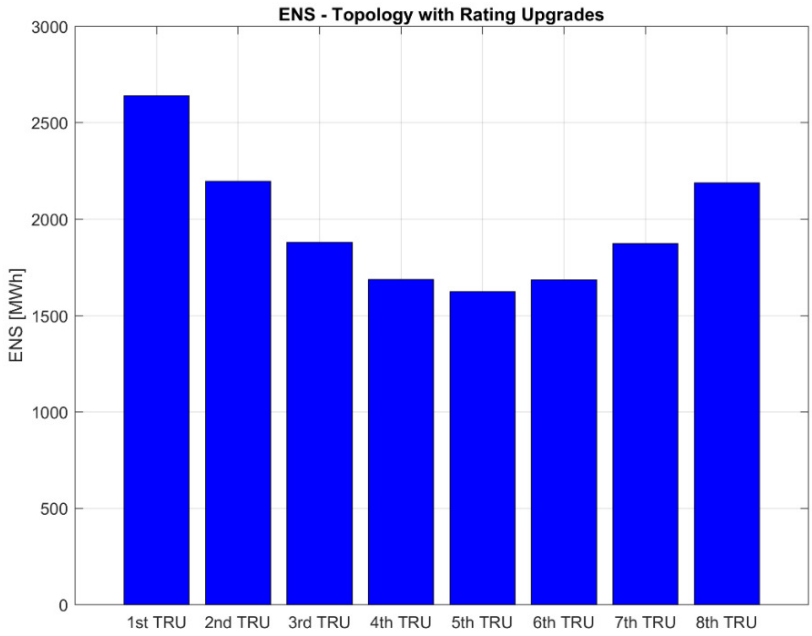

Figure 32. ENS for the proposed topologies with rating upgrades (TRU).

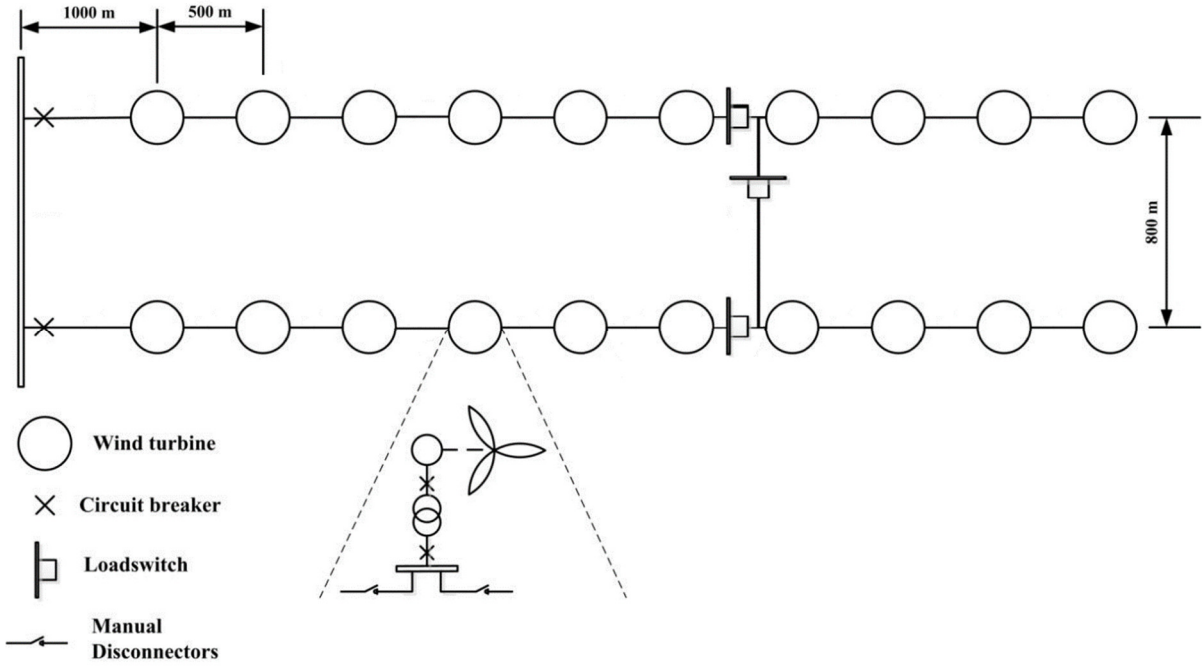

Figure 33. Topology based on double-sided half ring design with a redundancy in location 6.

For the Investment Cost and since this topology rates the cables to handle all of the power, depending on the redundancy location more cables may need upgrading. For example, if the location picked is the 1st (Figure 34), only the first two cables of each string need to have improved upgrades, since only they will handle more power when a fault occurs compared with the regular conditions (with no faults). If the location is moved on to the right, more cables must be upgraded. This justifies an increase in the Investment Cost when the redundancy is moved to the next spot. These results can be seen in Figure 35.

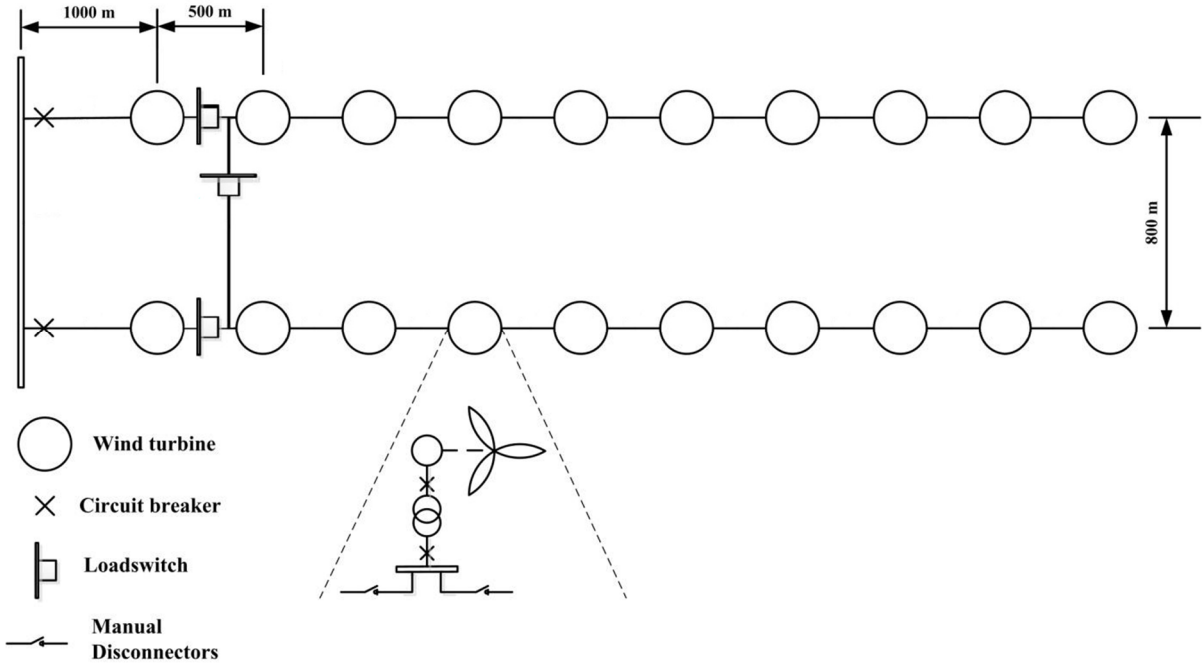

Figure 34. Topology based on double-sided half ring design with a redundancy in location 1.

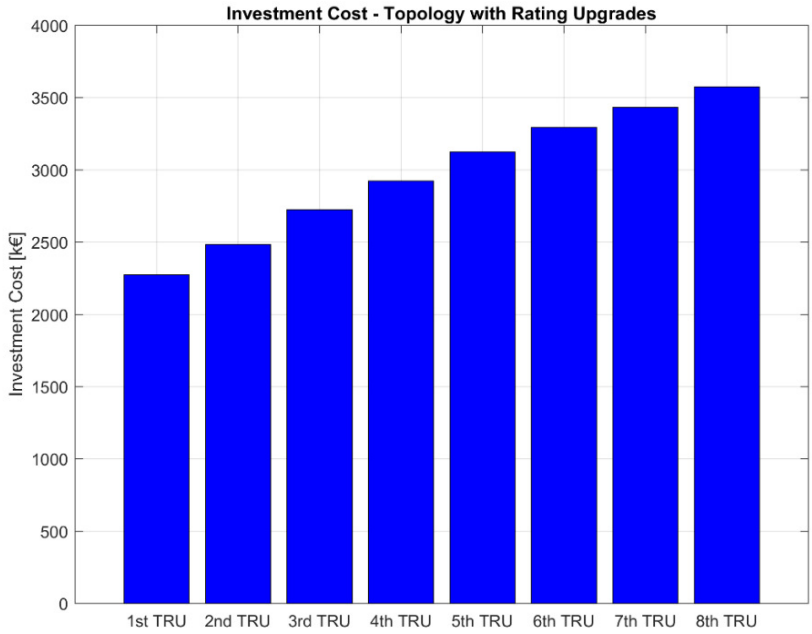

Figure 35. Investment cost for the proposed topologies with rating upgrades (TRU).

After the reliability results and the Investment Costs, the calculation of the economic indicators, which are the NPV (presented in Figure 36) and the IRR (presented in Figure 37), can now be made. Analysing both, it is possible to conclude that only the 3rd and 4th redundancy locations present positive results. Although the 4th location presents the best $NPV = 79.9\ k€$, the 3rd location is the one which has the best $IRR = 7.73\%$. So, from the investor's point of view, the topology which is more worth the invested cost is the 3rd one, whose single line diagram is presented in Figure 38.

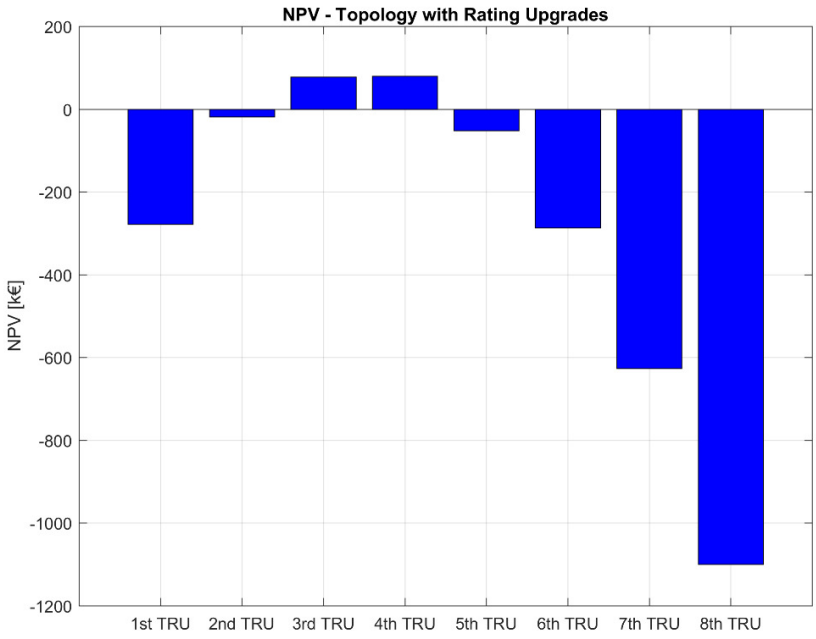

Figure 36. NPV for the proposed topologies with rating upgrades (TRU).

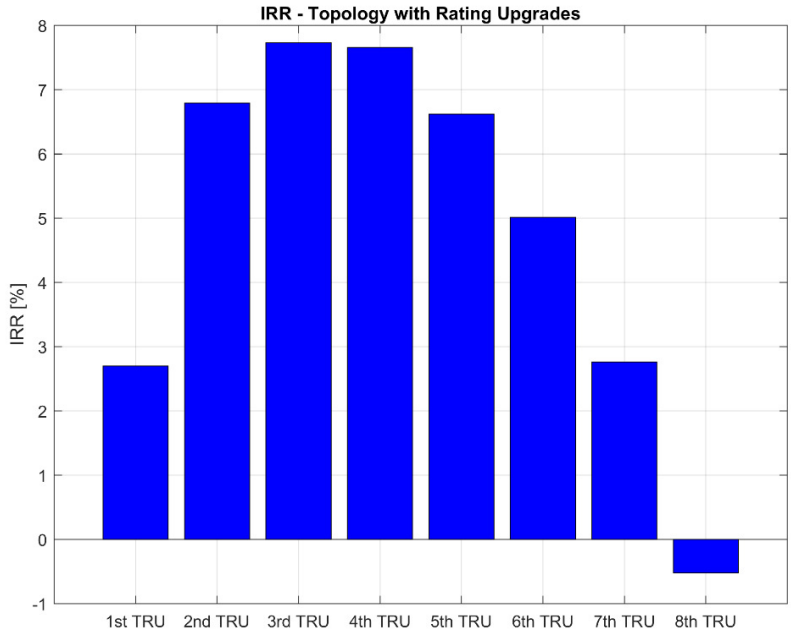

Figure 37. IRR for the proposed topologies with rating upgrades (TRU).

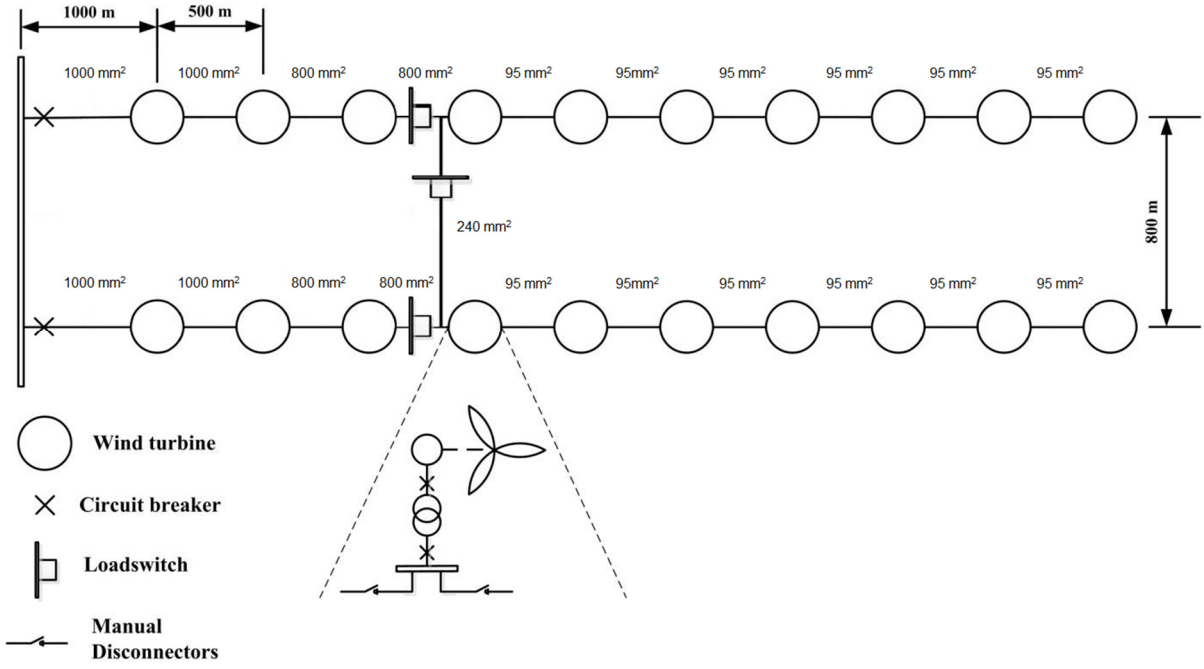

Figure 38. Best topology for the TRU approach (3rd TRU).

5.1.2 Topology with Ratings for Regular Conditions

The second approach for cable rating selection was named Topologies with Ratings for Regular Conditions (TRRC), where the cables are rated to handle all the scenarios for regular conditions (where no faults occur). That means that if a failure occurs, it may be necessary to turn off wind turbines because the cables are not capable of handling all of the power flowing through them. From this approach, the reliability indices (ENS) and the Investment Cost are calculated. After that it is possible to calculate the economic indicators which are the NPV and IRR.

The reliability results for the TRRC approach for all the possible locations of the redundancy are presented in Figure 39. As it can be seen, the location that has the best Energy Not Supplied (ENS) is the 5th. The explanation made above for the TRU approach also applies here. So, depending on the location, each side will have greater or less severe situations and it is only possible to determine the location which has the best adequate situations through numerical simulations.

The Investment Cost results are presented in Figure 40. As it can be seen, all possible locations have the same results. That is a consequence of the approach for cable rating selection that is being used. This selection is made for the regular conditions, that are the same for all possible redundancy locations. The only thing that could vary would be the rating of the redundancy, but, since the cable ratings within the strings limit the number of online turbines when a fault occurs, the rating for the redundancy is the same for all the topologies.

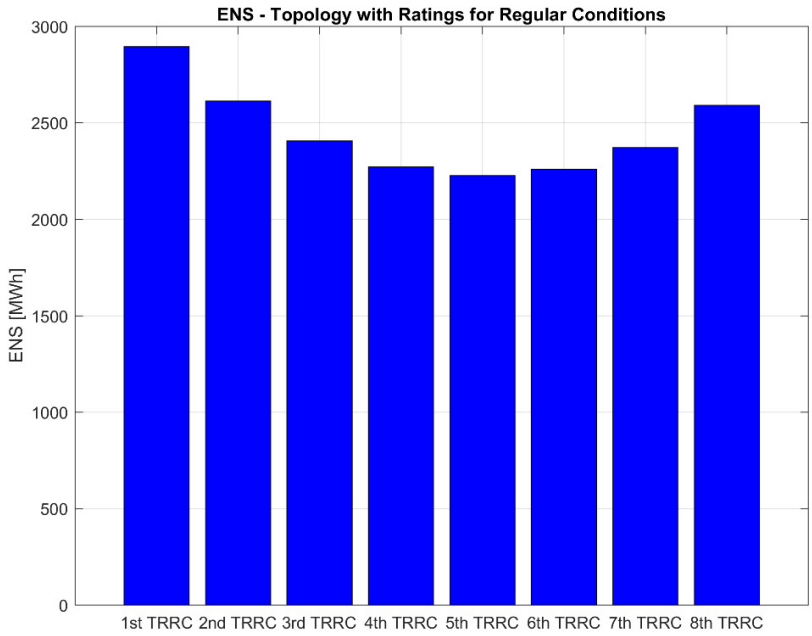

Figure 39. ENS for the proposed topologies with ratings for regular conditions (TRRC).

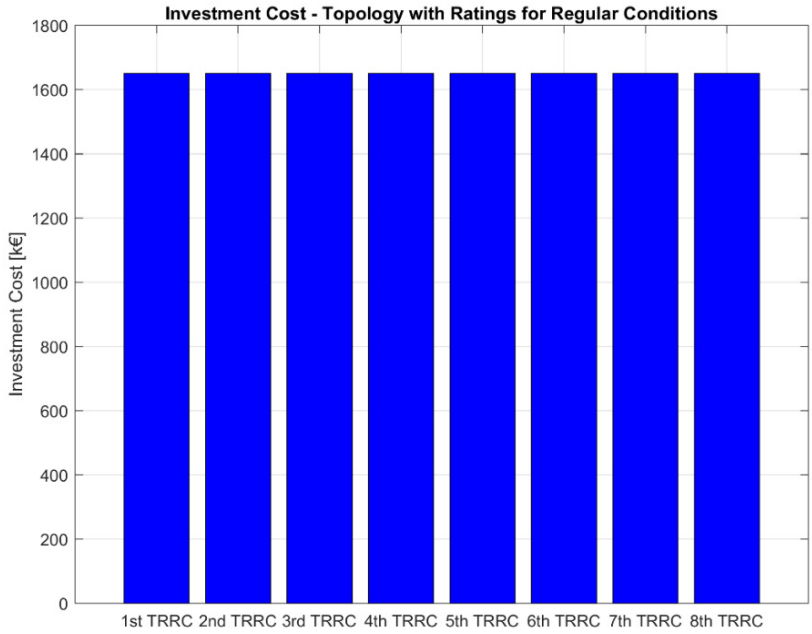

Figure 40. Investment cost for the proposed topologies with ratings for regular conditions (TRRC).

After the reliability results and the Investment Costs, the economic indicators (NPV presented in Figure 41 and IRR presented in Figure 42) can now be calculated. Analysing both, it is possible to conclude that all the possible redundancy locations present positive results. The one that presents the best economic results is the 5th location, with $NPV = 783.1\ k€$ and $IRR = 35.76\%$. So, this is the topology that is more worth the invested money for an investor, whose single line diagram is presented in Figure 43.

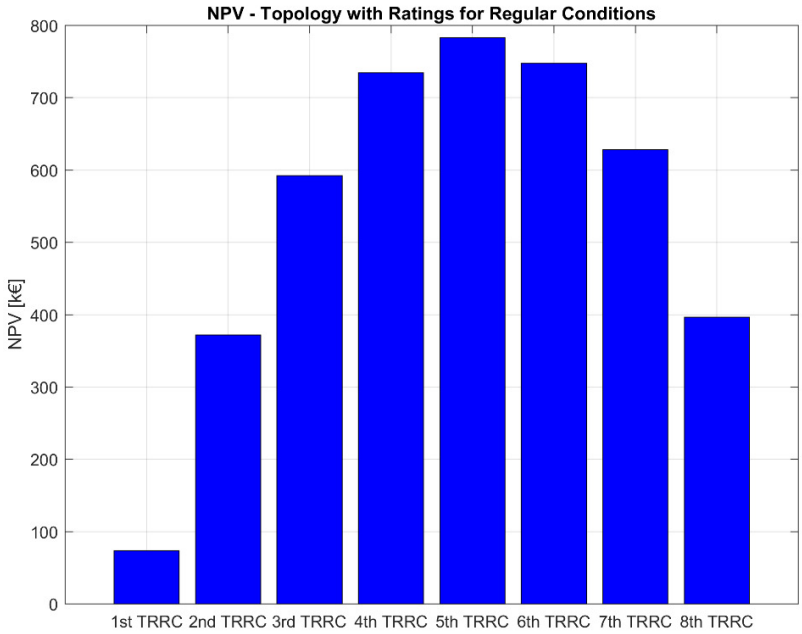

Figure 41. NPV for the proposed topologies with ratings for regular conditions (TRRC).

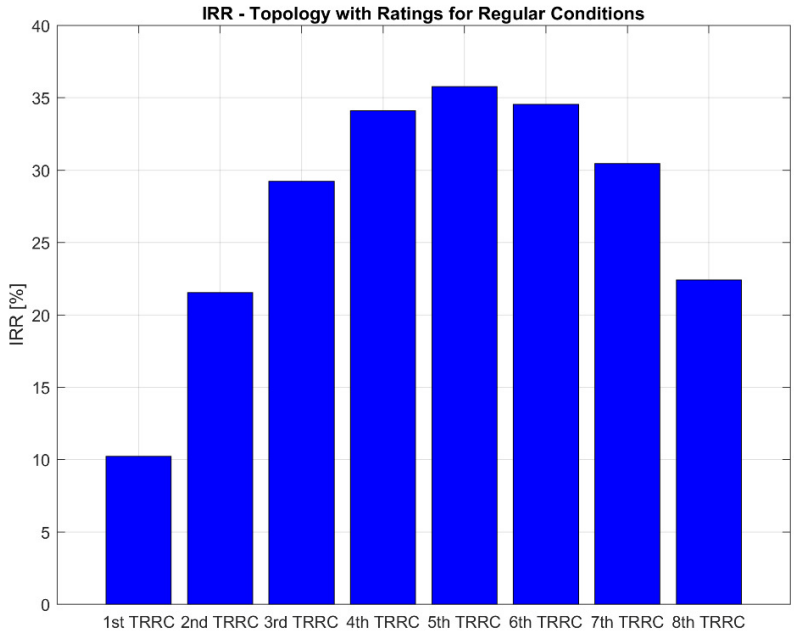

Figure 42. IRR for the proposed topologies with ratings for regular conditions (TRRC).

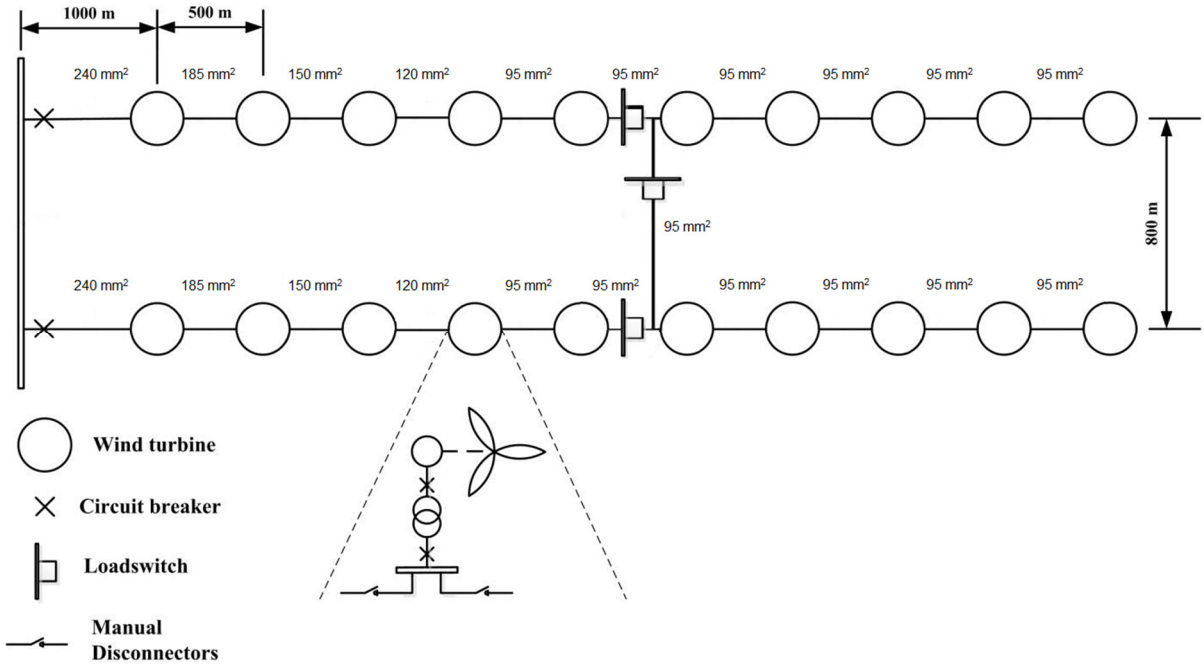

Figure 43. Best topology for the TRRC approach (5th TRRC).

5.1.3 Discussion

After analysing all the possible redundancy locations for both rating approaches, the pros and cons of each one become more evident. For the reliability results it is clear, comparing both approaches, that the TRU presents the best results as far as the ENS is concerned. This is a consequence of the ratings being chosen to handle all the power for all possible scenarios, unlike what happens for the TRRC.

The differences within the Investment Costs are significant and the TRRC approach is the one which presents the lower values, as expected. This can be explained by the fact that the cable ratings are the same for the regular conditions and the base topology, so the investment cost only represents the cost of the introduction of the redundancy. This does not happen for the TRU approach, where the cable upgrades represent an increase in the Investment Costs.

Analysing the economic indicators, it is clear that the TRRC approach presents the best results in this area. Comparing both approaches, the results can be explained by the fact that the higher ENS obtained for the TRRC approach is compensated by the decrease of the investment costs. These conclusions are represented in both economic indicators. One important thing to refer is that all the topologies within the TRRC approach are investor attractive - they all have positive economic indicators.

Comparing the economic indicators for the best topologies from both approaches, it is possible to conclude that overall the best topology is the TRRC approach with a redundancy in the 5th location (see Figure 43). The investment cost of this topology, according with [28]–[30], presents an increase between 0.13% and 0.20% compared with the one without redundancy (radial topology).

In conclusion, the topologies based on the TRU approach are the ones with best reliability results and the topologies based on the TRRC approach are the ones with best economic indicators. So, it is proven that the money invested to increase the cable ratings to handle all the possible faulty scenarios is not worth it for an investor, since the most severe scenarios have a really low probability.

5.2 Sensitivity Analysis

A sensitivity analysis is a tool for finding out how the results from the reliability analysis vary when the input parameters are changed. This type of analysis is suitable when the input data suffers from a high degree of uncertainty. This is the case for the reliability data (presented in Table 6), the investment costs (presented in Table 8) and the energy selling price (presented in Table 9). For the reliability data there is a lack of information and the one that exists is not coherent [12], [16], [39], [40]. The main reason for this variation is the uncertainty of the weather conditions, which leads to uncertain failure rates and outage times. There is a lack of information for the investment costs too, which can be explained by the confidentiality involved in the Offshore Wind Farm projects. For the selling energy price as seen in Table 3, the values can vary a lot depending on the country which is being considered.

So, to reach trustworthy results, the sensitivity analysis was performed through various simulations where each identified input varied separately. For the reliability data, a separate analysis was performed for the failure rates of the submarine cable, the disconnector, the circuit breaker, the load switch and the outage time (presented as repair time). An analysis varying the investment costs and the selling price was also performed. The range of variation of the selected inputs are based on the values presented in the academic literature [12], [16], [39], [40].

The sensitivity analysis was performed for the two cable rating approaches for all proposed topologies with a redundancy between two strings. Although there are eight proposed topologies for each approach, in this analysis the results only consider the bests ones for each approach. The best results for the TRU approach are the 3rd and 4th redundancy locations (as seen in Figure 37) and the ones for the TRRC approach are the 5th and 6th redundancy locations (as seen in Figure 42).

5.2.1 Cable Failure Rate

In this work, the failure rate considered for the submarine cables is 0.4%, as presented in Table 6. According to study [39], the failure rate for this equipment is 0.8%. It is considered even higher in [12], which presents a rate of 1.5%. However, the failure rate variation considered in this work is the same as in [16], [40], varying from 0.2% to 1.2%. The economic indicators resulting from this simulation are presented in Figure 44 (NPV) and in Figure 45 (IRR).

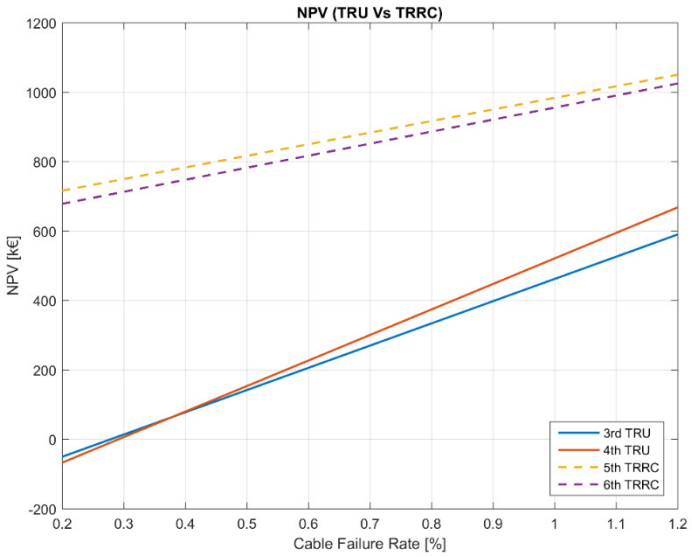

Figure 44. NPV for TRU and TRRC as a function of the cable failure rate.

Evaluating the economic indicators, it is visible they always increase with the cable failure rate. This results from the fact that more failures lead to a higher income cash flow with the same Investment Cost, resulting in better economic indicators. Analysing Figure 44, it is visible that the increase of the cable failure rate will lead to a higher NPV increase for the TRU approach than for the TRRC. This happens because the failures occur more often and the investment made in the ratings will compensate. However, the same does not happen in Figure 45, since the investment cost for the TRU approach is much higher than for the TRRC.

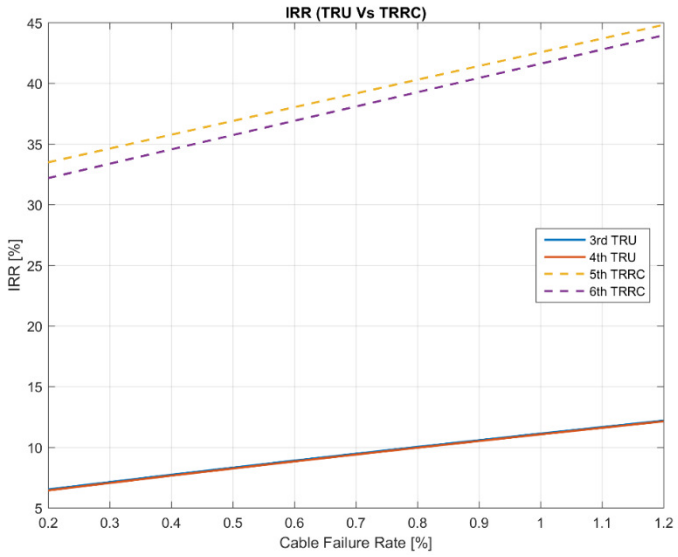

Figure 45. IRR for TRU and TRRC as a function of the cable failure rate.

5.2.2 Disconnector Failure Rate

In this work, the failure rate considered for the disconnectors is 2%, as presented in Table 6. This failure rate is considered higher in study [40] (3%) and even higher in [12] (6.67%). In [16] the disconnector failure rate considered is 1%, which is lower than the value considered in this work. The range considered for the variation of the disconnector failure rate was from 0.5% to 4%. The economic indicators resulting from this simulation are presented in Figure 46 (NPV) and in Figure 47 (IRR).

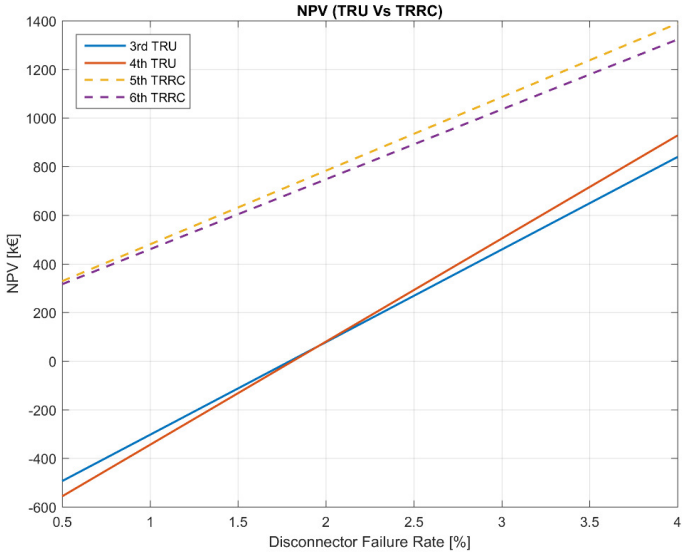

Figure 46. NPV for TRU and TRRC as a function of the disconnector failure rate.

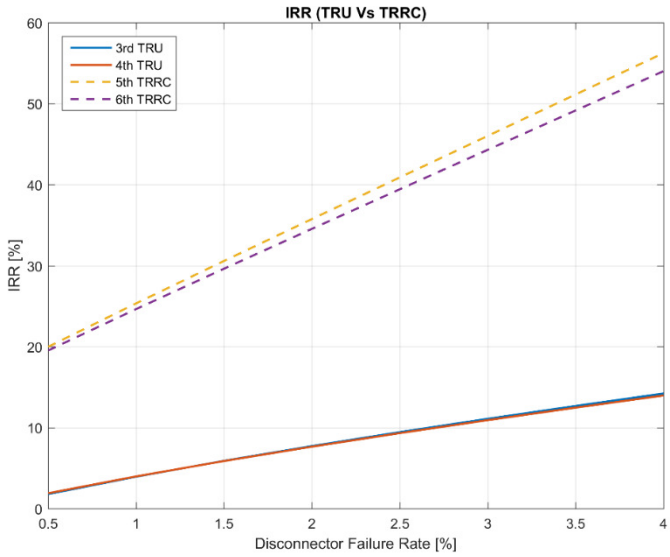

Figure 47. IRR for TRU and TRRC as a function of the disconnector failure rate.

The conclusions are the same than the ones derived from the variation of the cable failure rate.

5.2.3 Circuit Breaker Failure Rate

The failure rate considered for the circuit breakers was 3%, as presented in Table 6, as in studies [16], [40]. However in studies [12], [39] the circuit breaker failure rate is lower – 2.4% and 2.5%, respectively. The range considered for the variation of the circuit breaker failure rate was from 1.5% to 6%. The economic indicators resulting from this simulation are presented in Figure 48 (NPV) and in Figure 49 (IRR).

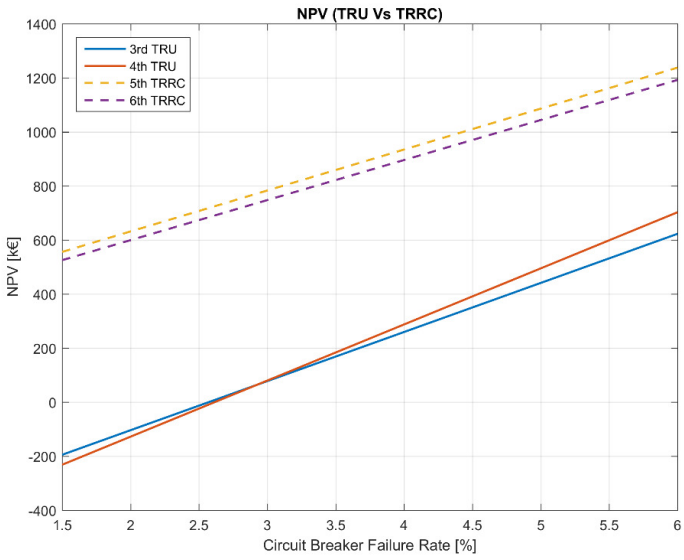

Figure 48. NPV for TRU and TRRC as a function of the circuit breaker failure rate.

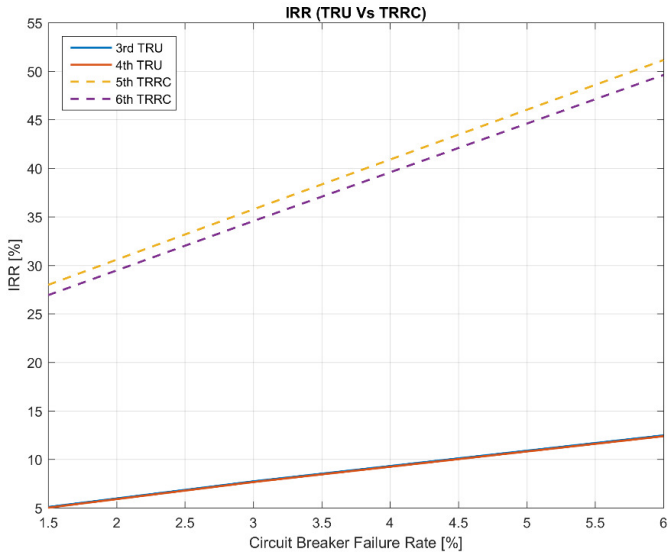

Figure 49. IRR for TRU and TRRC as a function of the circuit breaker failure rate.

Evaluating the economic indicators, the conclusions are the same than for the variation of the cable failure rate and the disconnector failure rate.

5.2.4 Load Switch Failure Rate

The failure rate considered for the load switch was 3%, as presented in Table 6. All the values in the academic literature [12], [16], [39] are lower – 1%, 2% and 2.5%, respectively. The range considered for the variation of the load switch failure rate was from 0.5% to 4%. The economic indicators resulting from this simulation are presented in Figure 50 (NPV) and in Figure 51 (IRR).

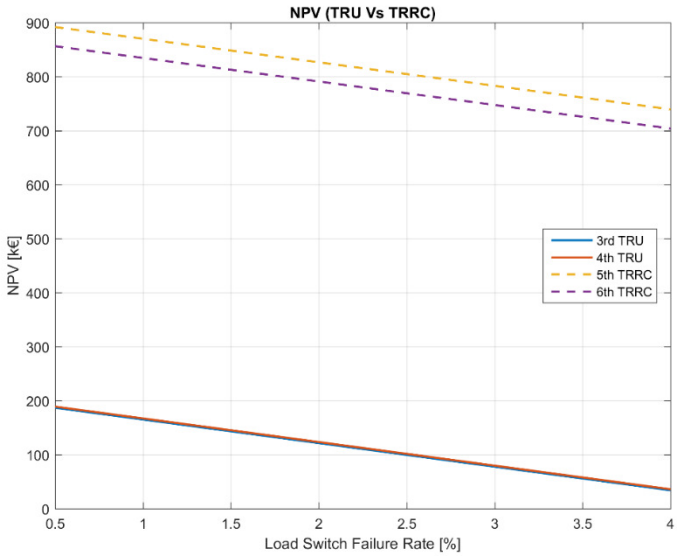

Figure 50. NPV for TRU and TRRC as a function of the load switch failure rate.

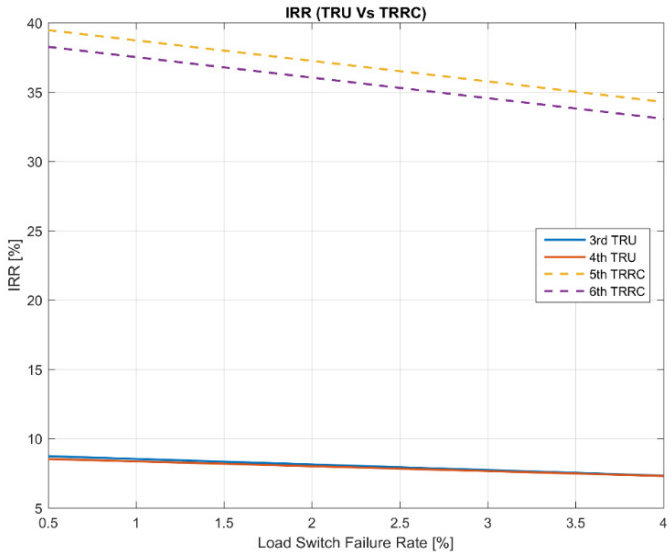

Figure 51. IRR for TRU and TRRC as a function of the load switch failure rate.

Evaluating the economic indicators, it is visible the indicators decrease with the increase of the load switch failure rate. This can be easily explained since only the topologies with redundancies have load switches, so increasing the failure rate will result in more failures that did not exist in the Base Topology, resulting in worst economic indicators.

5.2.5 Outage Time

In order to take into account the uncertainty of the weather conditions, which can lead to an increase of the repair time of the equipments, the sensitivity analysis also varied the outage time. This time is correlated to the repair time of the submarine cable, the disconnector, the circuit breaker and the load switch. The weather conditions also impact the switching time of the disconnector. All these times are presented in Table 6 – 672h for the repair of the cable, 120h (one quarter of the repair time of the cable) for the repair of the disconnector, circuit breaker and load switch and for the switching time of the disconnector when a fault occurs in other equipments. For the variation that was made, all these times maintain the ratios between them.

In academic literature [12], [16], [39], [40] the repair time of the submarine cable is between 672h and 2160h and for the other ones between 120h to 2160h. So, the range of variation of the outage time will be represented as a ratio, considered from 1 to 3. This means that, when the outage time ratio is equal to 1, the repair times and the switching time are the ones considered in this work and when the outage time ratio is equal to 3, the repair time of the cable is 2016h and the repair time for the other equipments and the switching time of the disconnector are 504h. The economic indicators resulting from this simulation are presented in Figure 52 (NPV) and in Figure 53 (IRR).

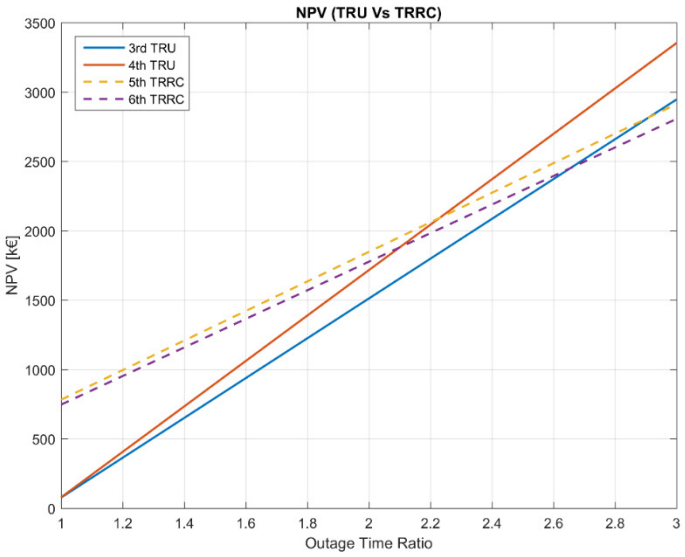

Figure 52. NPV for TRU and TRRC as a function of the outage time.

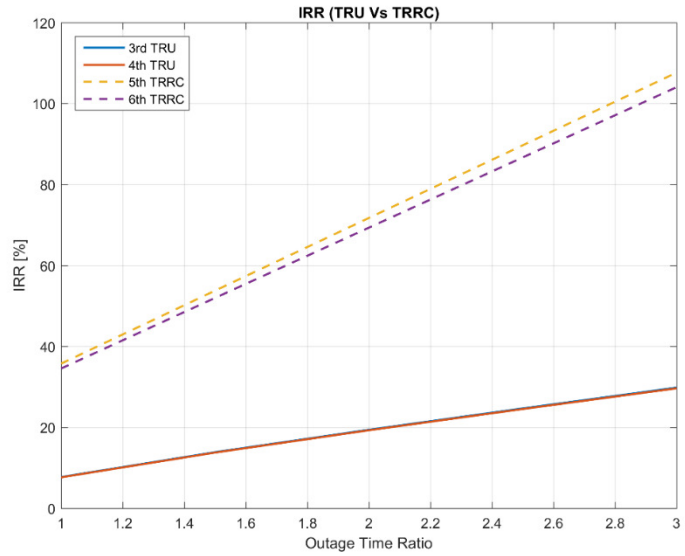

Figure 53. IRR for TRU and TRRC as a function of the outage time.

It is visible that the indicators increase with the outage time. This can be explained since if the duration of the failure is higher, the benefits of the use of the redundancy are seen in a higher income cash flow for the same investment, resulting in better economic indicators. Analysing Figure 52, it is visible that the increase of the outage time will lead to a higher NPV increase for the TRU approach than for the TRRC. This happens because the duration of the failures will be higher and the investment made in the ratings will compensate. For an outage time ratio above 2.2, it is clear that the TRRC approach begins to present better results than the TRU approach. However, the same does not happen in Figure 53, since the investment cost for the TRU approach is much higher than for the TRRC.

5.2.6 Investment Cost

Due to the confidentiality involved in the Offshore Wind Farm projects, there is a lack of information for the investment costs. The range of variation for the Investment Cost is represented as a ratio and the considered variation was from one half to double (0.5 to 2). The economic indicators resulting from this simulation are presented in Figure 54 (NPV) and in Figure 55 (IRR).

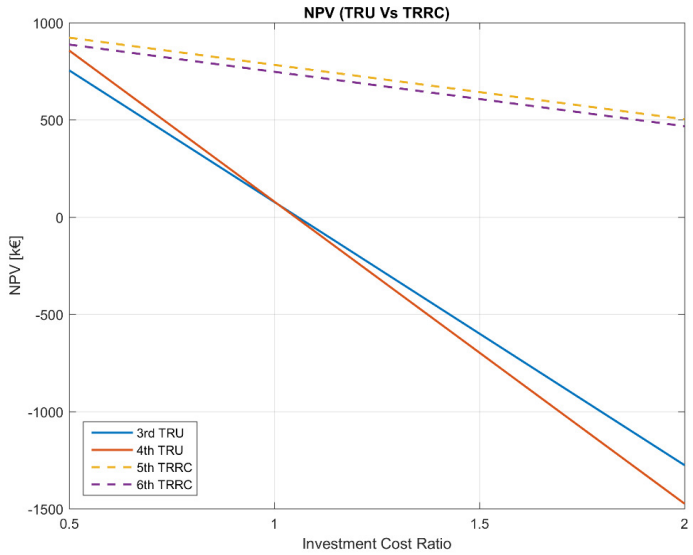

Figure 54. NPV for TRU and TRRC as a function of the investment cost.

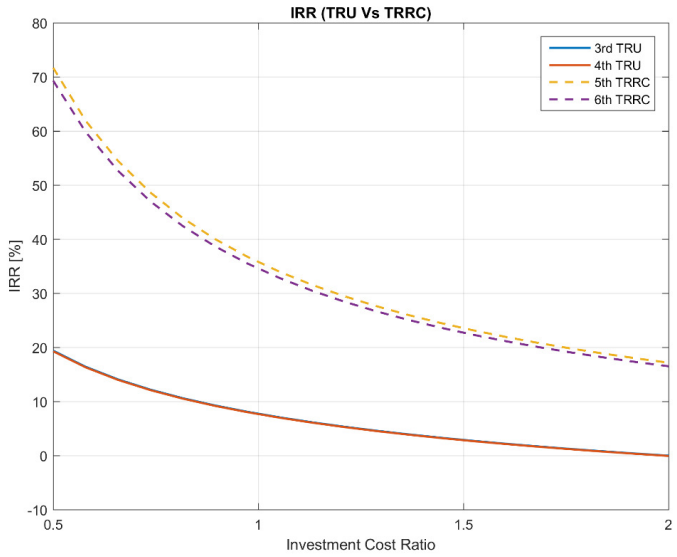

Figure 55. IRR for TRU and TRRC as a function of the investment cost.

It is visible these indicators decrease with the increase of the investment cost. Analysing Figure 54, the increase of the investment cost will lead to a higher NPV decrease for the TRU approach than for the TRRC. This happens because the TRU approach increases the cable rating, resulting in a bigger investment compared to the TRRC approach.

5.2.7 Selling Price

The energy selling price can vary a lot depending on the country which is considered, as seen in Table 3. Analysing this table, it is possible to verify that the selling energy price can vary from 67.6 €/MWh (if the location of the Offshore Wind Farm project is Sweden) to 180 €/MWh (if the country involved is the United Kingdom). So, the range considered for the variation of the selling price was from 50 €/MWh to 200 €/MWh. The economic indicators resulting from this simulation are presented in Figure 56 (NPV) and in Figure 57 (IRR).

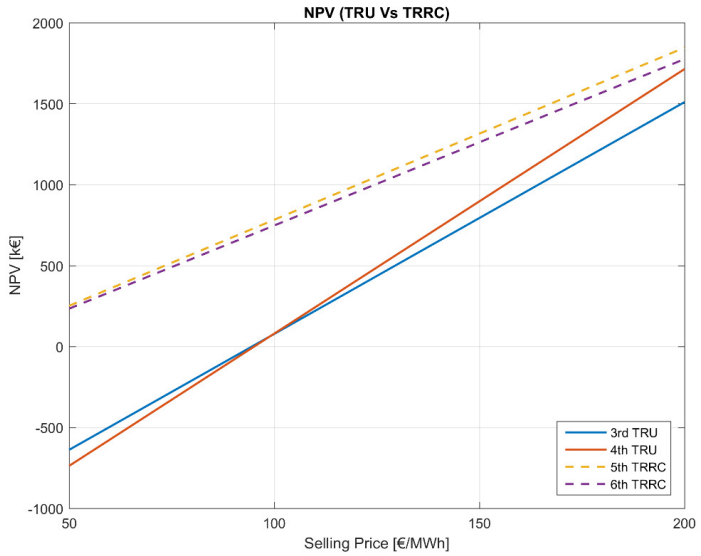

Figure 56. NPV for TRU and TRRC as a function of the selling price.

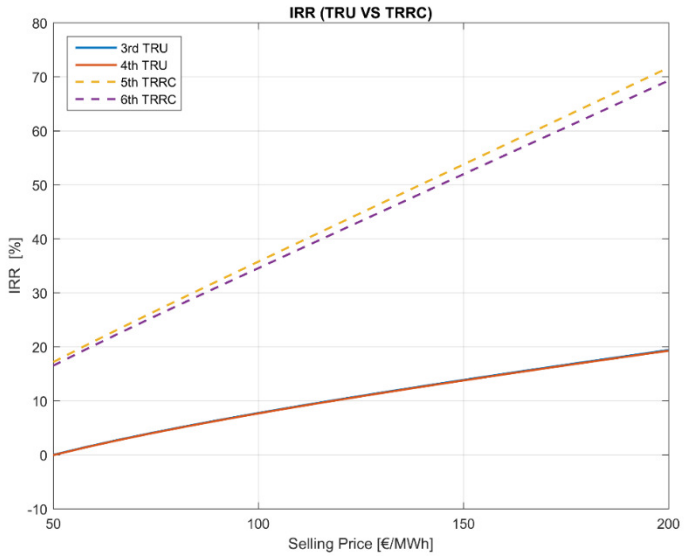

Figure 57. IRR for TRU and TRRC as a function of the selling price.

The conclusions for the selling price variation are the same than for the outage time variation. This happens because the increase of the outage time will lead to a higher income cash flow and the increase of the selling price will lead to the same.

5.2.8 Discussion

For the NPV results, it is visible that the variations on the input parameters will lead to higher variations for the TRU approach than for the TRRC. This happens because the TRU approach handles more power scenarios leading to a higher increase of the income cash flow. However, the opposite happens for the IRR. Since the investment cost for the TRU approach is much higher than for the TRRC, the additional extra income cash flow for the TRU is lower when indexed to the investment made. In conclusion, for all the variations that were simulated within the assumed ranges, the topologies based on the TRRC approach are the ones with best economic indicators. So, the money invested to increase the cable ratings to handle all the possible scenarios is not worth it from the investor's point of view, even if the input parameters are changed to handle more severe scenarios.

It can also be claimed that the assumed values for the reliability data were not too optimistic, since they are some of the lowest possible values present in the academic literature.

Analysing all the results from these variations, the best topology is the topology with the cable ratings based on the TRRC approach with a redundancy in the 5th location, for all the ranges considered.

5.3 New Redundancy Design

This last analysis was made to evaluate a new type of design, characterized by introducing redundancies across sets of two strings already paired by one redundancy. These topologies give an important additional advantage – if a fault occurs, the power generated by the wind turbines within the faulted string can be distributed to the others strings. Only the Topologies with Rating Upgrades (TRU) will be analysed. The proposed topologies analysed here are presented and explained in Chapter 4.2. These are composed of ten strings with 10 wind turbines each, and have been called 1st NRD, 2nd NRD, 3rd NRD, 4th NRD, 5th NRD and 6th NRD. In order to compare the results obtained from this analysis with the results already shown above for the best classical topologies in the previous sections (TRRC with redundancy in the 5th location and TRU with redundancy in the 3rd location), all of them are shown side by side.

The reliability results for the new redundancy design topologies are presented in Figure 58. The location that gives the lowest Energy Not Supplied (ENS) is the 2nd (Figure 30). This has the same explanation than the one presented before – the location of the redundancies divide each string into 3 equal parts. It is visible that all the new proposed topologies present better ENS results than the ones which only had one redundancy between each pair of strings.

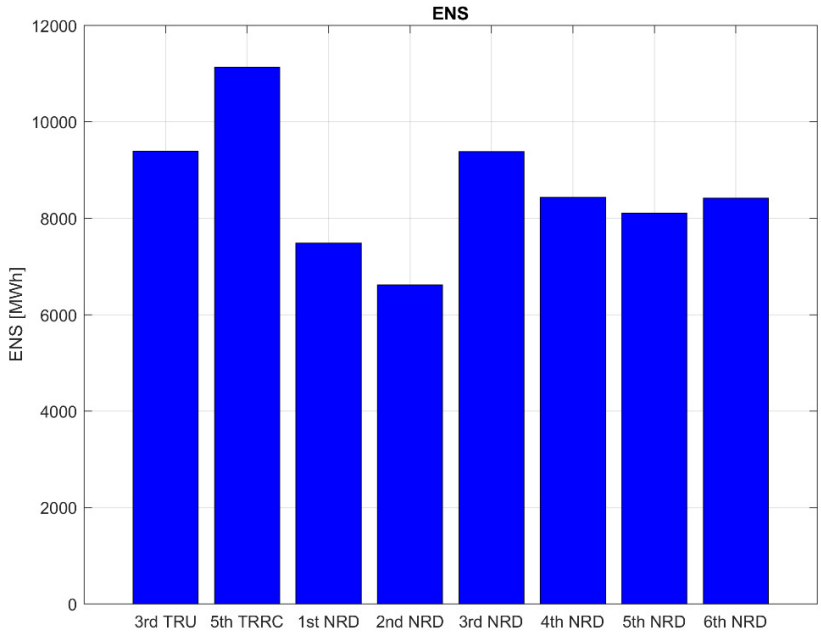

Figure 58. ENS for the proposed topologies with redundancy between two redundantly paired of strings.

For the Investment Cost, and since the topology approach for the cable rating was the TRU, depending on the redundancy locations different cables must be upgraded. All the results can be seen in Figure 59. It is visible that the 1st and 2nd NRD are the ones which show higher investment costs. This can be explained because in case of a failure all the distributed generator power of the faulted string needs to flow over to the cables in the centre of the strings, so the rating of these cables and the ones on the left side must be upgraded, resulting in higher investment costs. The difference between these two is that the 2nd NRD needs to use more load switches compared with the 1st topology, as seen in Figure 29 and Figure 30. For the other ones, since the location is the same for every redundancy, all the strings are only divided into two, so there are not cables in the middle of the string that are necessary for the distribution of the power when a failure occurs. This will result in lower investment costs.

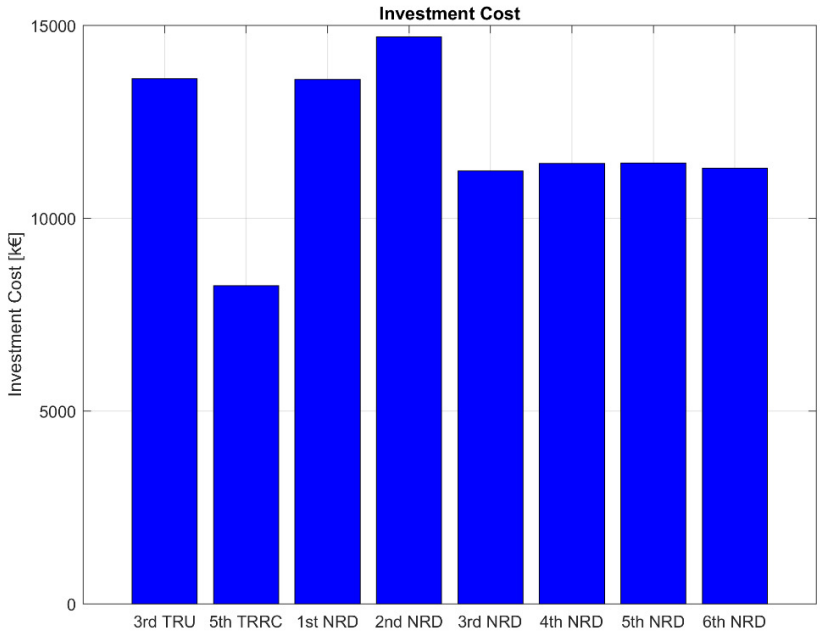

Figure 59. Investment cost for the proposed topologies with redundancy between two redundantly paired of strings.

After the reliability results and the Investment Costs, the economic indicators, which are the NPV (presented in Figure 60) and the IRR (presented in Figure 61), can now be calculated. Analysing both indicators, the topology that presents the best economic results is the 5th NRD (Figure 62), with $NPV = 3934.7\ k€$ and $IRR = 16.75\%$. The investment cost of this topology, according with [28]–[30], presents an increase between 0.42% and 0.65% compared with the one without redundancy (radial topology). One important thing to note is that all the new proposed topologies are investor attractive – they all have positive economic indicators.

Comparing these topologies with the topologies that only have one redundancy between every two strings, it can be seen that the 5th NRD topology is the one which presents the higher NPV from all the topologies studied in this work. As far as the IRR is concerned, it is visible that the topology with the cable ratings based on the TRRC approach with a redundancy in the 5th location is the one which shows the best results. This is caused by its lower investment cost, compared to the others. So, this is the topology that is more worth the invested money for an investor (with $NPV = 3915.7\ k€$ and $IRR = 35.76\ \%$), and is presented in Figure 63.

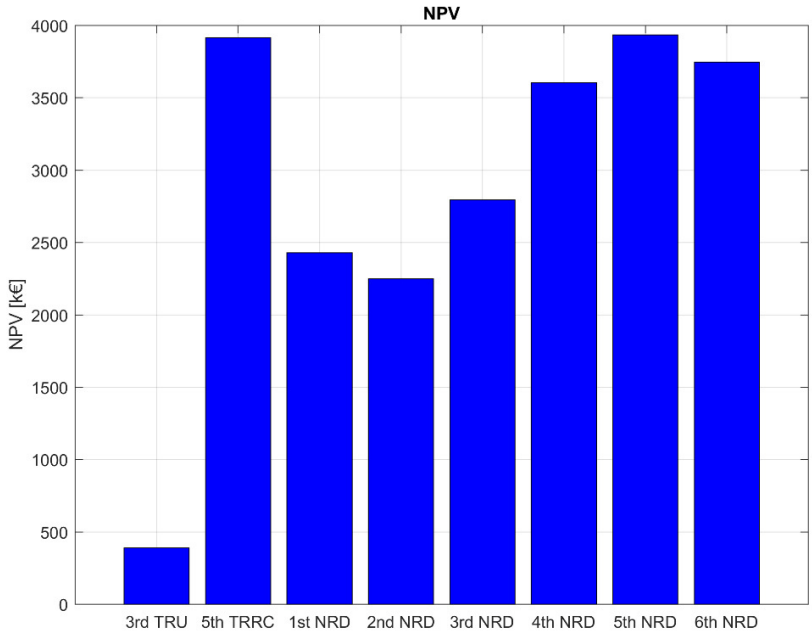

Figure 60. NPV for the proposed topologies with redundancy between two redundantly paired of strings.

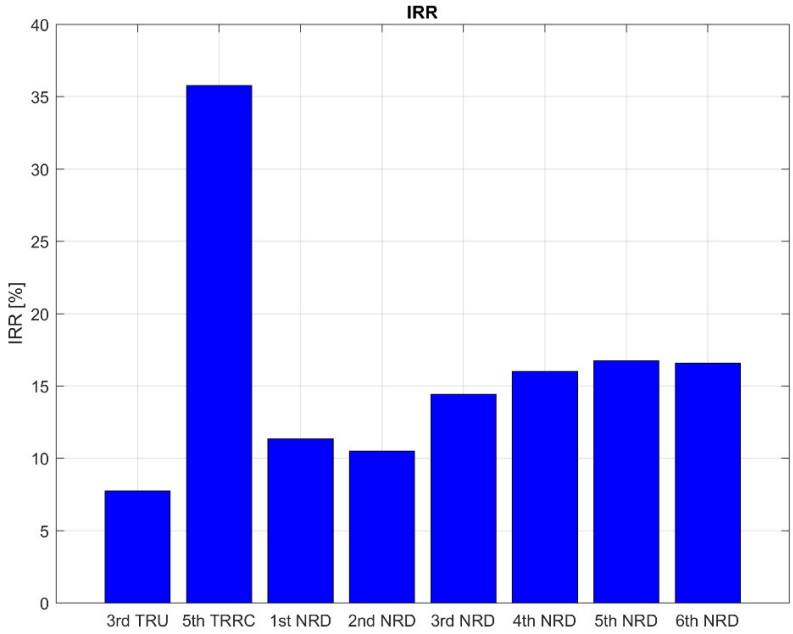

Figure 61. IRR for the proposed topologies with redundancy between two redundantly paired of strings.

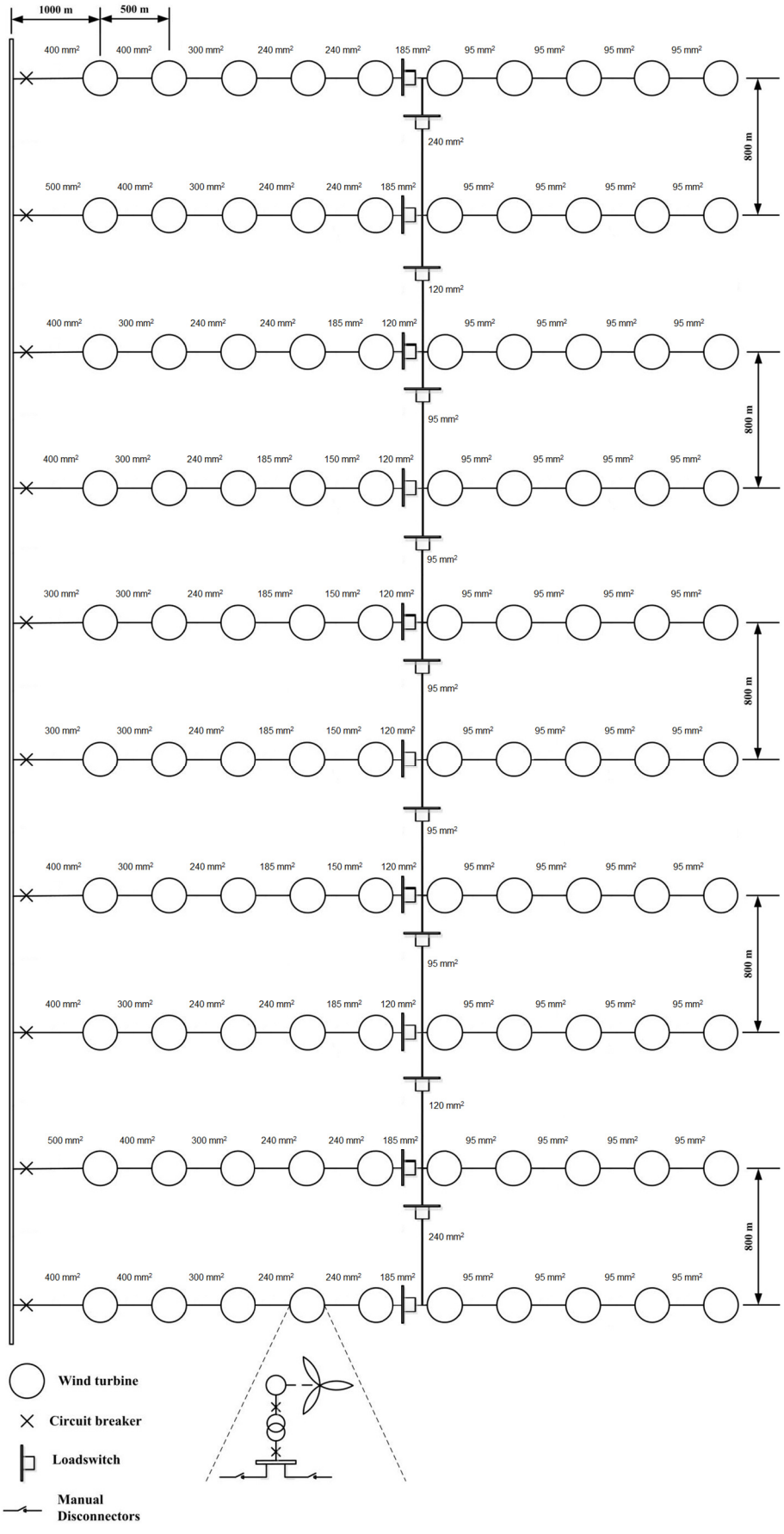

Figure 62. Best topology from the NRD topologies (5th NRD).

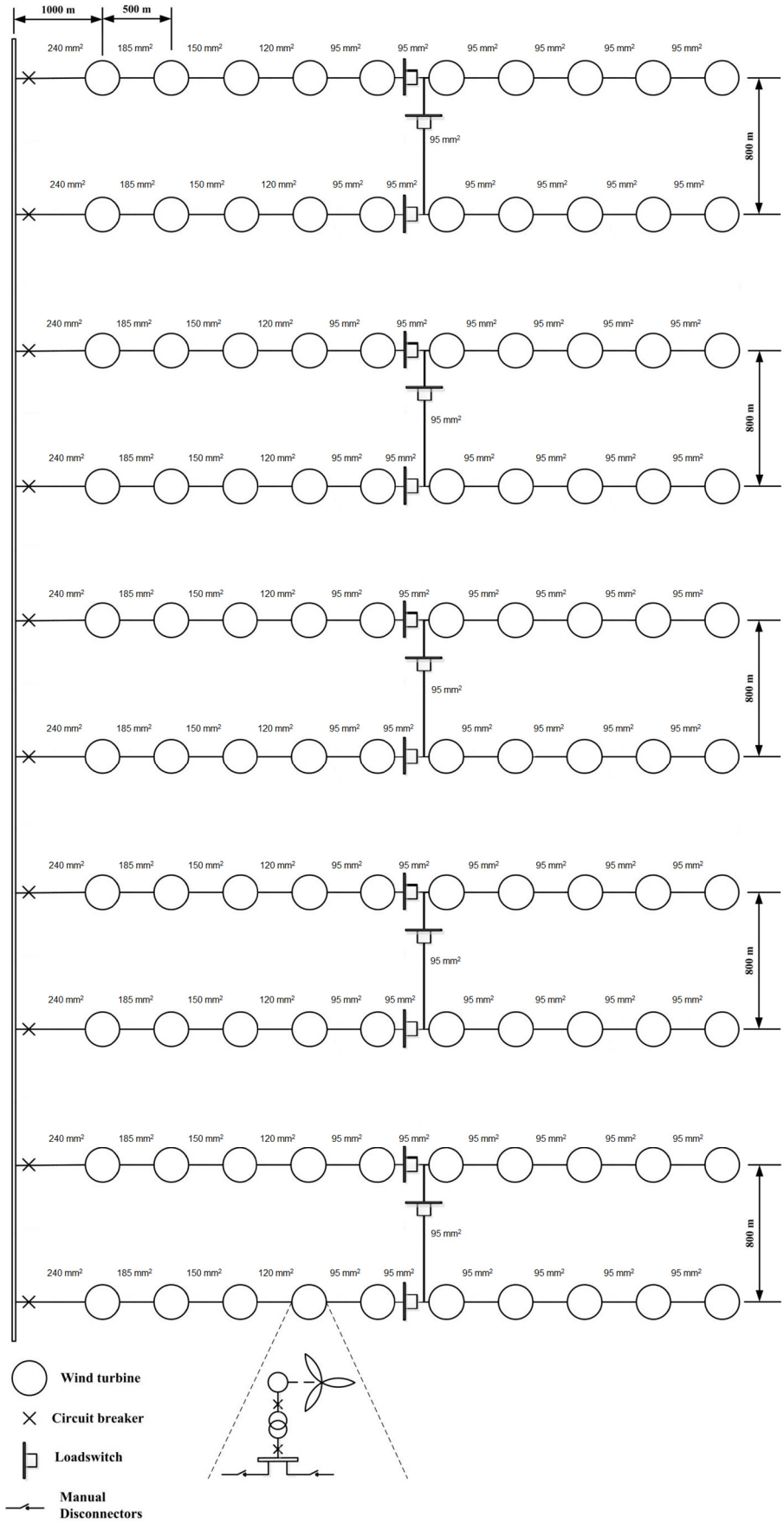

Figure 63. Best topology: Wind Farm composed by 100 turbines and cable rating based on TRRC approach.

5.3.1 Sensitivity Analysis

A simplified sensitivity analysis was performed to evaluate how the results from the reliability analysis vary for the best classical redundancy design topology (5th TRRC – presented in Figure 63) and the best new redundancy design topology (5th NRD – presented in Figure 62). Since this is a simplified analysis, the input parameters chosen to be variable are the ones which present more sensitivity variation on the output. These parameters are the outage time, the investment cost and the selling price.

For the outage time, the range considered was the same presented in Chapter 5.2.5, where the outage time ratio was changed from 1 to 3. This represents a repair time of the submarine cable between 672h and 2160h and a repair time for the others equipments between 120h and 2160h (same as for the switching time of the disconnector). The economic indicators resulting from this simulation are presented in Figure 64 (NPV) and Figure 65 (IRR).

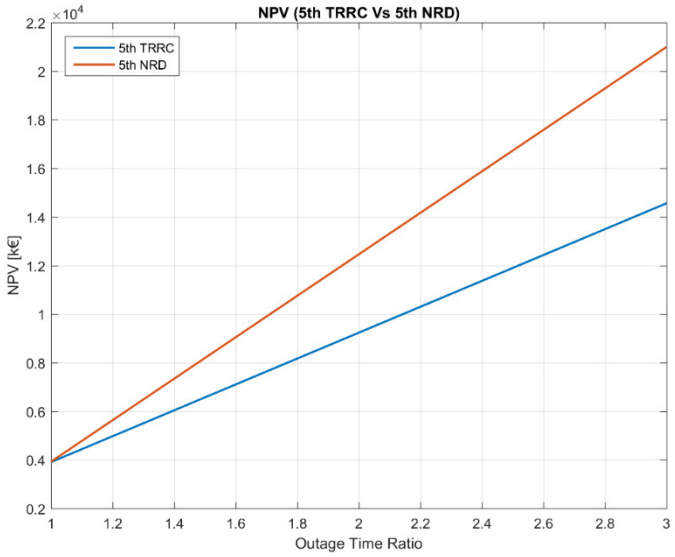

Figure 64. NPV for best TRRC and NRD as a function of the outage time.

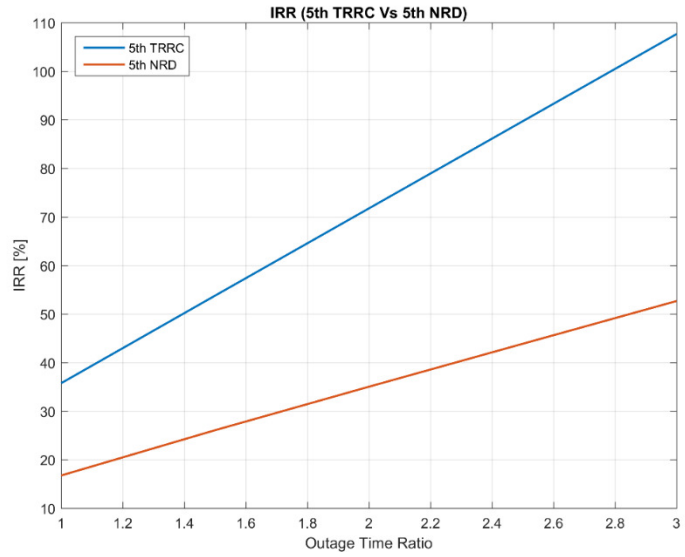

Figure 65. IRR for best TRRC and NRD as a function of the outage time.

Analysing Figure 64, it is visible that the increase of the outage time leads to a higher NPV increase for the 5th NRD than for the 5th TRRC. This happens because the duration of the failures will be higher and, since the ENS for the 5th NRD is lower, the additional investment made for this topology will compensate. However, the opposite happens for the IRR (Figure 65), since the investment cost for the 5th TRRC is much lower than for the 5th NRD, the Internal Rate of Return for the investor will be higher for the 5th TRRC.

For the investment cost, the range considered was the same presented in Chapter 5.2.6. It is represented as a ratio and the considered variation was from one half to double (0.5 to 2). The economic indicators resulting from this simulation are presented in Figure 66 (NPV) and in Figure 67 (IRR).

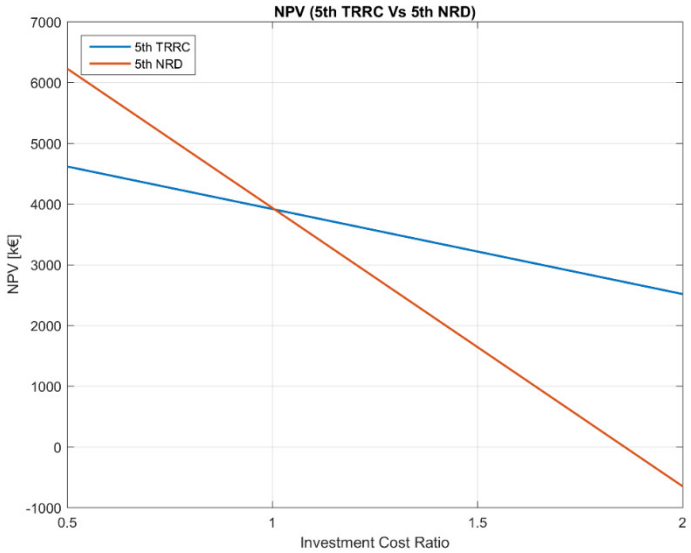

Figure 66. NPV for best TRRC and NRD as a function of the investment cost.

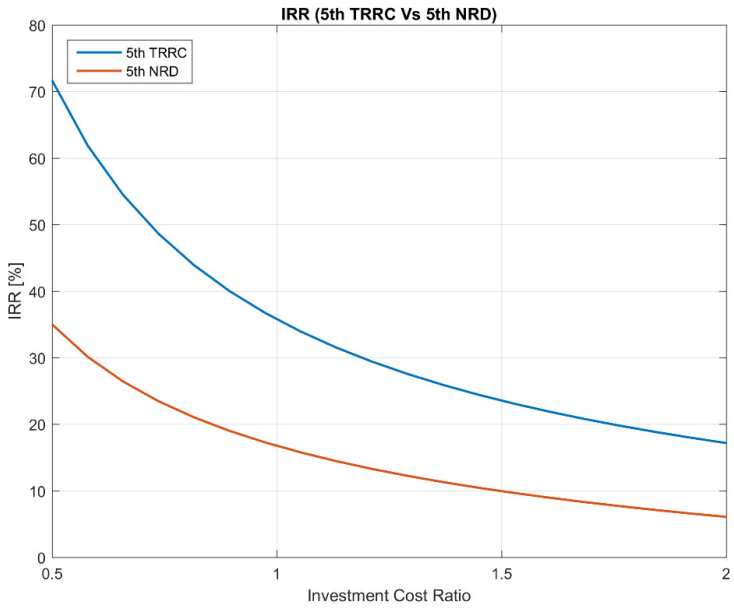

Figure 67. IRR for best TRRC and NRD as a function of the investment cost.

Analysing Figure 66, it is visible that the increase of the investment cost will lead to a higher NPV decrease for the 5th NRD than for the 5th TRRC. This happens because the 5th NRD has more redundancies, resulting in a bigger investment compared to the 5th TRRC.

For the selling price, the range considered was the same presented in Chapter 5.2.7 – from 50 €/MWh to 200 €/MWh. The economic indicators resulting from this simulation are presented in Figure 68 (NPV) and in Figure 69 (IRR).

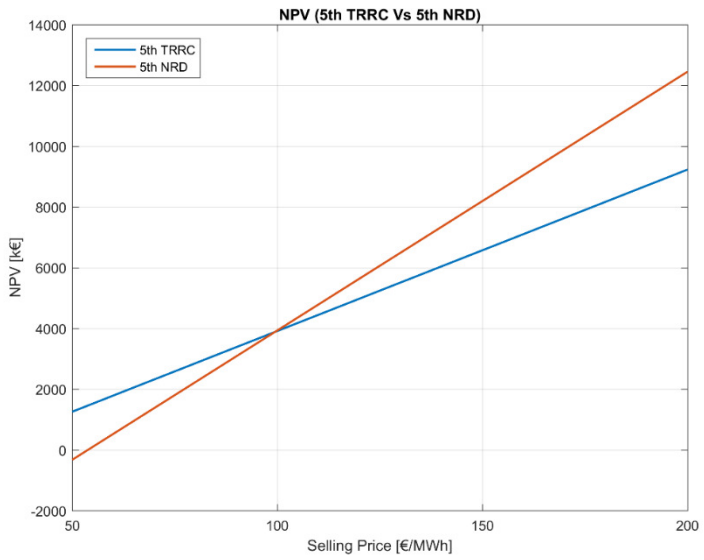

Figure 68. NPV for best TRRC and NRD as a function of the selling price.

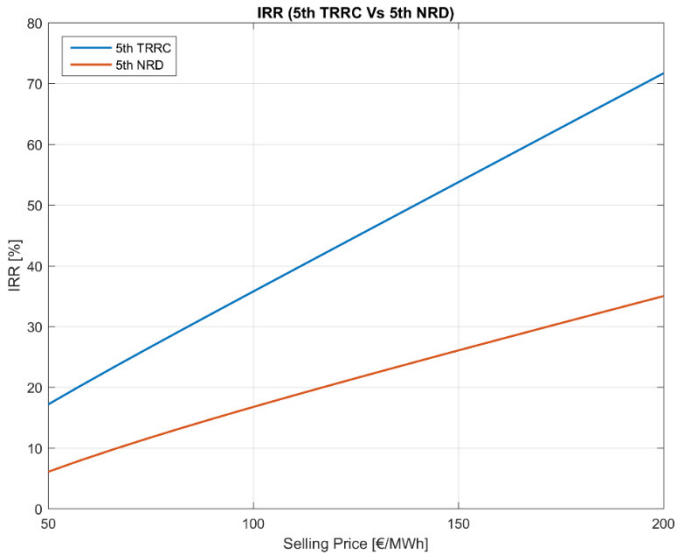

Figure 69. IRR for best TRRC and NRD as a function of the selling price.

The conclusions for the selling price variation are the same than for the outage time variation. This happens because the increase of the outage time will lead to a higher income cash flow and the increase of the selling price will lead to the same.

5.3.2 Discussion

Since the NRD topologies are based on the TRRC approach, the conclusions from the NPV and IRR results are the same as the ones that are presented in Chapter 5.2.8. For the NPV results, it is visible that the variations on the input parameters will lead to higher variation for the 5th NRD approach than for the 5th TRRC. For the IRR results, the variations on the input parameters will lead to higher variation for the 5th TRRC approach than for the 5th NRD.

In conclusion, the topologies characterized by a redundancy between already redundantly paired sets of strings are the ones with best reliability results. However, the topology with cable ratings based on the TRRC approach with a redundancy in the 5th location is the one that is more attractive for an investor (high NPV and highest IRR), because it is more worth the invested money.

Chapter 6

Conclusions

The objective of this thesis was to perform a reliability analysis of the internal grid of an offshore wind power system, comparing different topologies and their potential economic benefits. To perform such a reliability assessment, a software piece was developed to simulate the reliability for each component in the system and determine the impact of each contingency on each load point, the frequency of production interruption and sum up the impact of all contingencies. This study addressed the reliability impact of different topological solutions while maintaining an economic rationale between the layout design and the energy production output. This was accomplished with the evaluation of the economic indicators as shown in Chapter 5.

One of the focuses of this work was to select the best location for a redundancy for a topology with a redundancy between each pair of two strings. To accomplish that, all the possible locations on the double-sided half ring design were studied, in order to find out which is the topology that presents the best reliability and economic indexes. The developed models considered two different approaches for the selection of the cable ratings. The ratings selected in the first approach are those necessary to handle every faulty scenario that may occur. This means they are designed to handle all power produced by all online turbines when any fault occurs. The topologies with the first approach were named Topologies with Rating Upgrades (TRU). The ratings selected in the second approach are those necessary to handle all scenarios for regular conditions (with no faults). The topologies with the second approach were named Topologies with Ratings for Regular Conditions (TRRC). This means that if a failure occurs, it may be necessary to turn off some turbines because the cables are not capable of handling all the power. The reasoning behind the second approach is that both the failure rates and the probability of a wind turbine operating at the rated power are very low. So, the reason for analysing this approach is to see if it is reasonable to increase the cable ratings (as in the first approach) just to account for some scenarios that are very unlikely. After analysing all the topologies proposed for both ways of rating cables, it was concluded that the topologies based on the TRU approach are the ones with the best reliability results and the topologies based on TRRC approach are the ones with the best economic indicators. These results can be explained by the fact that the higher Energy Not Supplied (ENS) obtained for the TRRC approach is compensated by the decrease of the investment costs. So, it is proven that the money invested to increase the cable ratings to handle all the possible faulty scenarios

is not worth it for an investor, since the most severe scenarios have a really low probability. One important thing that stands out is that all the topologies within the TRRC approach have viable economic indicators. Overall the topology that presents the best economic results combined with a good reliability result is the topology with cable ratings based on TRRC approach with a redundancy in the 5th location. This is the most profitable one for the investors.

As stated previously in this work, the data suffers from a high degree of uncertainty. This is the case for the reliability data, for which there is a lack of information and the one that exists is not coherent. The main reason for this variation is the uncertainty of the weather conditions, which leads to uncertain failure rates and outage times. There is a lack of information for the investment costs too, which can be explained by the confidentiality involved in the Offshore Wind Farm projects. For the selling energy price, the values can vary a lot depending on the country which is being considered. So, in order to take these uncertainties into account, a sensitivity analysis was also made to all proposed topologies with a redundancy between each pair of two strings. In the sensitivity analysis performed, each identified input suffering from a considerable degree of uncertainty was changed separately. Therefore, a separate analysis was performed changing the failure rates of the submarine cable, the disconnector, the circuit breaker, the load switch and the outage time. An analysis changing the investment costs and the selling price was also performed. Analysing all the results from these variations and comparing the TRU with the TRRC approach, the money invested to increase the cable ratings to handle all the possible scenarios is not worth it from the investor's point of view. For all the ranges considered, the topology with better economic indexes is the topology with the cable ratings based on the TRRC approach with a redundancy in the 5th location.

A final research was conducted to evaluate new designs characterized by having a redundancy between already redundantly paired sets of strings. These topologies give the important advantage of distributing all the power generated by the wind turbines within the faulted string to others strings. All the new proposed topologies are investor attractive – they all have viable economic indicators. The one that presents the best economic results is the new proposed topology that has all the redundancies located in the 5th location. Although this topology is the one which presents the best NPV from all the topologies studied in this work, the topology with the cable ratings based on the TRRC approach with a redundancy in the 5th location is the one with the best IRR of them all. A simplified sensitivity analysis was performed on these two topologies – the best classical redundancy design topology (5th TRRC) and the best new redundancy design topology (5th New Redundancy Design – NRD). The conclusion is that the topologies characterized by a redundancy between already redundantly paired sets of strings are the ones with best reliability results, but the topology with the cable ratings based on the TRRC approach with a redundancy in the 5th location is the one that is more attractive for an investor. Thus, it was proven that the money invested in a topology that is characterized by a redundancy between each pair of two strings is more worth it than the money invested in a topology that has one redundancy between already redundantly paired sets of strings.

For future studies, it would be interesting to refine the software piece to test other rating approaches. For example, an intermediate approach, to be capable of handling more scenarios than the TRRC, but

not to handle all of them like the TRU. It could also test every possible combination for the ratings and find out the best one. An interesting refinement that could also be made to the software piece would be to have it receive as an input just the locations of the wind turbines, and have it calculate the best topology arrangement. For this it would have to test every possible topology with every possible redundancy, perform a reliability analysis and calculate the respective economic indicators.

Bibliography

[1] R. Castro, *Uma Introdução às Energias Renováveis: Eólica, Fotovoltaica e Mini-hídrica*, 1st ed. Lisboa, PT: IST Press, 2011.

[2] "8 amazing things you probably didn't know about the Persians," 2014. [Online]. Available: http://www.hexapolis.com/2014/11/03/8-things-probably-didnt-know-persians/. [Accessed: 10-Apr-2017].

[3] I. Troen and E. Lundtang Petersen, *European Wind Atlas*. Roskilde: Risø National Laboratory, 1989.

[4] E. L. Petersen, "Wind resources part I: The European wind climatology," in *1993 European Community wind energy conference*, 1993, pp. 663–668.

[5] J. Johnson, "Offshore Wind Technology Overview," *BOEMRE North Carolina Task Force Meeting*, 2011. [Online]. Available: https://www.boem.gov/Renewable-Energy-Program/State-Activities/Johnson_NC-Task-Force-Mtg_11May2011.aspx. [Accessed: 11-Apr-2017].

[6] "Lodon Array." [Online]. Available: http://www.londonarray.com/. [Accessed: 14-Apr-2017].

[7] "Gemini." [Online]. Available: geminiwindfarm.com/. [Accessed: 14-Apr-2017].

[8] "Wind turbine power ouput variation with steady wind speed," *Wind Power Program*. [Online]. Available: http://www.wind-power-program.com/turbine_characteristics.htm. [Accessed: 11-Apr-2017].

[9] G. Quinonez-Varela, G. W. Ault, O. Anaya-Lara, and J. R. Mcdonald, "Electrical collector system options for large offshore wind farms," *IET Renew. Power Gener.*, vol. 1, no. 2, pp. 107–114, 2007.

[10] D. Mentis, S. Hermann, M. Howells, M. Welsch, and S. H. Siyal, "Assessing the technical wind energy potential in africa a GIS-based approach," *Renew. Energy*, vol. 83, no. November, pp. 110–125, 2015.

[11] J. Yang, J. O'Reilly, and J. E. Fletcher, "Redundancy analysis of offshore wind farm collection and transmission systems," in *International Conference on Sustainable Power Generation and Supply (SUPERGEN '09)*, 2009, pp. 1–7.

[12] A. Sannino, H. Breder, and E. K. Nielsen, “Reliability of collection grids for large offshore wind parks,” in *International Conference on Probabilistic Methods Applied to Power Systems (PMAPS 2006)*, 2006.

[13] G. J. W. van Bussel and C. Schöntag, “Operation and Maintenance Aspects of Large Offshore Windfarms,” Delft, 1994.

[14] M. Damen, P. Bauer, S. W. H. de Haan, and J. T. G. Pierik, “Steady State Electrical Design, Power Performance and Economic Modeling of Offshore Wind Farms,” *EPE J.*, vol. 16, no. 4, pp. 44–49, 2006.

[15] P. Gardner, L. M. Craig, and G. J. Smith, “Electrical Systems for Offshore Wind Farms,” in *Switch Onto Wind Power 20th (BWEA)*, 1998, pp. 309–317.

[16] T. Winter, “Reliability and economic analysis of offshore wind power systems - A comparison of internal grid topologies,” MSc Thesis, Göteborg: Chalmers University of Technology, 2011.

[17] T. Ackermann, “Transmission systems for offshore wind farms,” *IEEE Power Eng. Rev.*, vol. 22, no. 12, pp. 23–27, 2002.

[18] N. R. Ullah, A. Larsson, A. Petersson, and D. Karlsson, “Detailed modeling for large scale wind power installations - a real project case study,” in *Third International Conference on Electric Utility Deregulation and Restructuring and Power Technologies (DRPT 2008)*, 2008, pp. 46–56.

[19] “Cape Wind farm.” [Online]. Available: https://www.capewind.org/. [Accessed: 11-Apr-2017].

[20] I. Alegria, J. Martin, I. Kortabarria, J. Andreu, and P. Ereno, “Transmission alternatives for offshore electrical power,” *Renew. Sustain. Energy Rev.*, vol. 13, no. 5, pp. 1027–1038, 2009.

[21] “Polycab 2.5sq. mm 3 Core Aluminium Armoured Cable 100mtr.” [Online]. Available: http://www.urjakart.com/polycab-2-5sq-mm-3-core-aluminium-armoured-cable-100mtr.html. [Accessed: 11-Apr-2017].

[22] S. D. Wright, A. L. Rogers, J. F. Manwell, and A. Ellis, “Transmission Options for Offshore Wind Farms in the United States,” *AWEA*, pp. 1–12, 2002.

[23] “A Guide to an Offshore Wind Farm,” *The Crown Estate*, pp. 1–70, 2010.

[24] C. A. Morgan, H. M. Snodin, and N. C. Scott, “Economies of scale , engineering resource and load factors,” *Garrad Hassan Partners Ltd*, 2003.

[25] N. Nikolaos, “Deep water offshore wind technologies,” MSc Thesis, University of Strathclyde, 2004.

[26] Douglas Westwood Ltd, “Offshore Wind Asessment For Norway,” *Res. Counc. Norw.*, 2010.

[27] “Study of the costs of offshore wind generation: A Report to the Renewables Advisory Board & DTI,” *Offshore Des. Eng. Ltd*, 2007.

[28] “Cost of and financial support for offshore wind: A report for the Department of Energy and Climate Change,” *Ernst & Young*, 2009.

[29] Renewable UK, “Offshore wind: Forecasts of future costs and benefits,” *BWEA*, 2011.

[30] J. Limpo, “Assessment of Offshore Wind Energy in Portuguese Shallow Waters - Site Selection, Technical Aspects and Financial Evaluation,” MSc Thesis, Instituto Superior Tecnico, 2011.

[31] G. J. W. van Bussel, A. R. Henderson, C. A. Morgan, B. Smith, R. Barthelmie, K. Argyriadis, A. Arena, G. Niklasson, and E. Peltola, “State of the Art and Technology Trends for Offshore Wind Energy : Operation and Maintenance Issues,” *Concert. Action Offshore Wind Energy Eur.*, 2001.

[32] O. Koppe and K. Schulze, “Offshore wind in Europe - 2010 Market Report,” *KPMG*, 2010.

[33] R. Billinton, *Reliability Evaluation of Power Systems*, 2nd Editio., vol. 30, no. 6. Plenum Press, 1996.

[34] R. Billinton and L. Wenyuan, *Reliability Assessment of Electric Power Systems Using Monte Carlo Methods*. Plenum Press, 1994.

[35] R. D. Zimmerman and C. E. Murillo-Sánchez, “MATPOWER 6.0 User’s Manual.” Power Systems Engineering Research Center (PSerc), 2016.

[36] “V90 - 3.0 MW Brochure,” *Vestas*, 2017.

[37] Vattenfall, “Thanet.” [Online]. Available: https://corporate.vattenfall.co.uk/projects/operational-wind-farms/thanet/. [Accessed: 27-Apr-2017].

[38] “General Specification V90 - 3.0 MW,” *Vestas Wind Syst. A/S*, 2004.

[39] B. Frankén, “Reliability Study - Analysis of Electrical Systems within Offshore Wind Parks,” *Elforsk Rapp.*, vol. 7, no. 65, 2007.

[40] E. Eriksson, “Wind farm layout - a reliability and investment analysis,” Uppsala Universitet, 2008.

[41] “XLPE Submarine Cable Systems Attachment to XLPE Land Cable Systems - User’s Guide,” *ABB*, 2017.

Appendix A

Extrapolation for Higher Cable Ratings

Due to a lack of information on isolated cables for offshore wind farms, it was necessary to extrapolate the cable rating for higher cross-sections (1000 mm^2 and 1200 mm^2) that were needed for the analysis conducted in this work. This extrapolation was only made for the parameters that were necessary to compute the simulations – capacitance, inductance and transmission capacity. For each one, the coefficient of determination is calculated in order to evaluate the proportion of the variance in the dependent variable that is predictable from the independent variable.

A.1. Capacitance Extrapolation

Considering that $S_{Cable}\ [mm^2]$ is the cross-section of the conductor, the equation that results from the capacitance extrapolation is a power function:

$$Capacitance = 0.0347 \times S_{Cable}^{0.3565}\ [\mu F/km]$$

The data collected from the manufacture [41], the extrapolation that results from that data and the new data that was collected from the extrapolation for the higher cable ratings (1000 mm^2 and 1200 mm^2) can be seen in Figure 70. The coefficient of determination for the capacitance extrapolation is $R^2 = 0.9963$, meaning the results obtained from the extrapolation are reliable. The capacitance for the higher cross-section cables are:

$$Capacitance(S_{Cable} = 1000\ mm^2) = 0.41\ \mu F/km$$

$$Capacitance(S_{Cable} = 1200\ mm^2) = 0.43\ \mu F/km$$

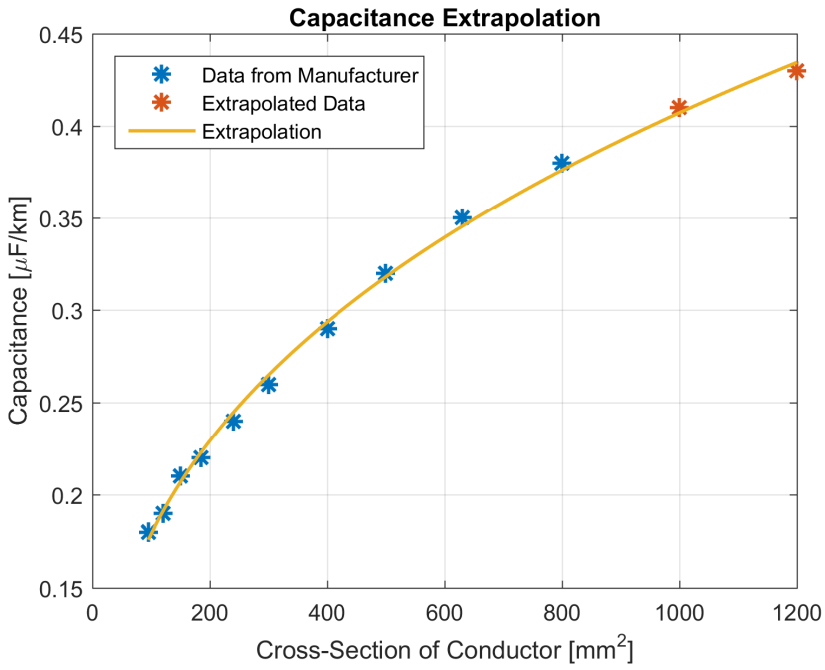

Figure 70. Capacitance extrapolation for higher cable rating (1000 mm² and 1200 mm²).

A.2. Inductance Extrapolation

Considering that S_{Cable} $[mm^2]$ is the cross-section of the conductor, the equation that results from the inductance extrapolation is a power function:

$$Inductance = 0.9161 \times S_{Cable}^{-0.162} \; [mH/km]$$

The data collected from the manufacture [41], the extrapolation that results from that data and the new data that was collected from the extrapolation for the higher cable ratings (1000 mm² and 1200 mm²) can be seen in Figure 71. The coefficient of determination for the inductance extrapolation is $R^2 = 0.9945$, meaning the results obtained from the extrapolation are reliable. The inductance for the higher cross-section cables are:

$$Inductance(S_{Cable} = 1000\, mm^2) = 0.30\, mH/km$$

$$Inductance(S_{Cable} = 1200\, mm^2) = 0.29\, mH/km$$

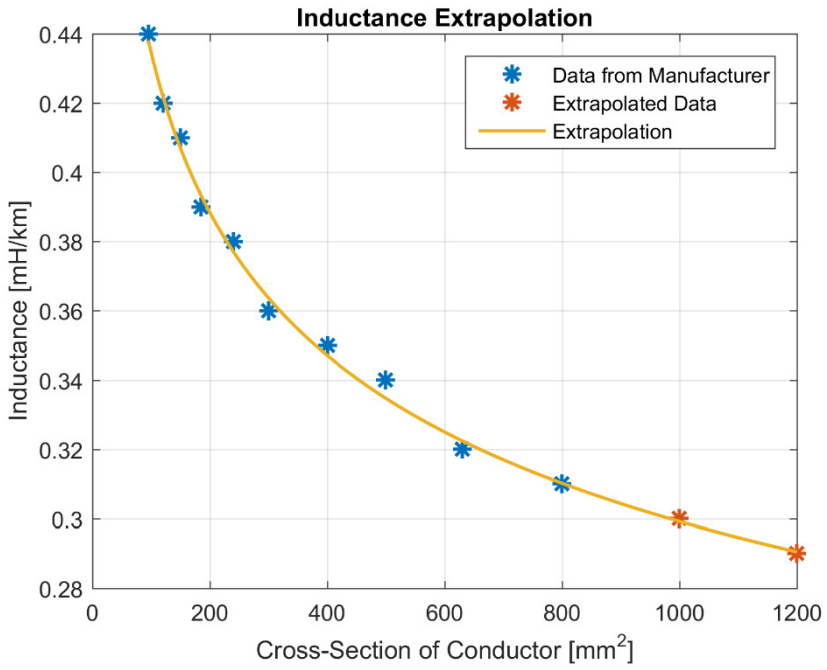

Figure 71. Inductance extrapolation for higher cable rating (1000 mm² and 1200 mm²).

A.3. Transmission Capacity

Considering that $S_{Cable}\ [mm^2]$ is the cross-section of the conductor, the equation that results from the transmission capacity extrapolation is a power function:

$$Transmission\ Capacity = 2.1419 \times S_{Cable}^{0.494}\ [MVA]$$

The data collected from the manufacture [41], the extrapolation that results from that data and the new data that was collected from the extrapolation for the higher cable ratings (1000 mm² and 1200 mm²) can be seen in Figure 72. The coefficient of determination for the transmission capacity extrapolation is $R^2 = 0.9974$, meaning that the results obtained from the extrapolation are reliable and the transmission capacity for the higher cross-section cables are:

$$Transmission\ Capacity\ (S_{Cable} = 1000\ mm^2) = 65\ MVA$$

$$Transmission\ Capacity\ (S_{Cable} = 1200\ mm^2) = 71\ MVA$$

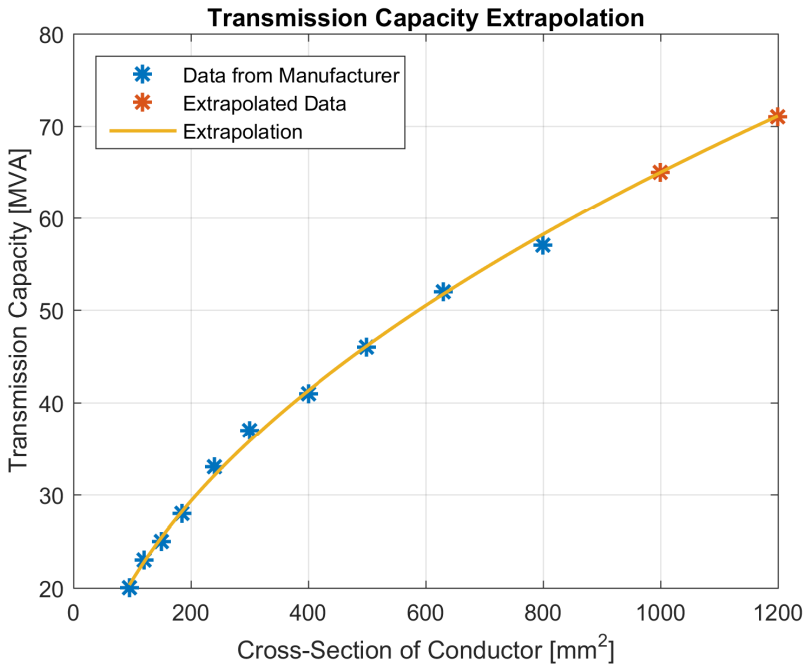

Figure 72. Transmission capacity extrapolation for higher cable rating (1000 mm^2 and 1200 mm^2).

Appendix B

Software Validation by Hand

The calculations in this appendix detail the calculations made by hand for the base and proposed topologies, their cables and strings, disconnectors, circuit breakers and load switches when a fault occurs, following the three periods of action described in Chapter 3. For an easier calculation, it was considered that the wind turbines were operating at the rated power (3 MW) all of the time.

B.1. Base Topology

The base topology, seen in Figure 26, has four cables in a top string (cables 1 to 4) and another four in a bottom string (cables 5 to 8).

B.1.1. ENS Calculation

The ENS is calculated first for the cable failures, then for the disconnector failures and finally for the circuit breakers failures. These failures can be separated into different periods as described before in Chapter 3.4.

For a cable-1 failure, in the first period all the turbines within the top string of the cable are out of service, since they are not connected to the collector system by any path. The second period is when the switching of the remote protection equipment happens, but, since there is no redundancy in the base topology, no alternative path to the collector system can be reached. This means all turbines within the top string will be out of service. The third period is when the manual switching of the disconnectors happens, but, once more, due to the lack of redundancies, no alternative path can be reached. In short, during the repair of the cable all the turbines within the top string out of service, which implies:

$$ENS_{Failure\ cable-1} = (\Delta t_{Period\ 1} + \Delta t_{Period\ 2} + \Delta t_{Period\ 3}) \times ENS_{cable-1\ period\ 1,2,3}$$

$$ENS_{Failure\ cable-1} = 672\ h \times 4 \times 3\ MW = 8064\ MWh$$

For a cable-2 failure, in the first and second periods all the turbines within the top string are out of service, for the same reasons than in a cable-1 failure, as explained in the previous paragraph. However, in the third period, if the cable-2 disconnectors are manually switched off, the first turbine of the top string will be back online. In short, during the first two periods all the turbines within the top string are out of service, but in the third period the first turbine is online, so:

$$ENS_{Failure\ cable-2} = (\Delta t_{Period\ 1} + \Delta t_{Period\ 2}) \times ENS_{cable-2\ period\ 1,2} + \Delta t_{Period\ 3} \times ENS_{cable-2\ period\ 3}$$

$$ENS_{Failure\ cable-2} = 168\ h \times 4 \times 3\ MW + (672\ h - 168\ h) \times 3 \times 3\ MW = 6552\ MWh$$

Applying the same logic to the other cables,

$$ENS_{Failure\ cable-3} = 168\ h \times 4 \times 3\ MW + (672\ h - 168\ h) \times 2 \times 3\ MW = 5040\ MWh$$

$$ENS_{Failure\ cable-4} = 168\ h \times 4 \times 3\ MW + (672\ h - 168\ h) \times 1 \times 3\ MW = 3528\ MWh$$

$$ENS_{Failure\ cable-5} = 672\ h \times 4 \times 3\ MW = 8064\ MWh$$

$$ENS_{Failure\ cable-6} = 168\ h \times 4 \times 3\ MW + (672\ h - 168\ h) \times 3 \times 3\ MW = 6552\ MWh$$

$$ENS_{Failure\ cable-7} = 168\ h \times 4 \times 3\ MW + (672\ h - 168\ h) \times 2 \times 3\ MW = 5040\ MWh$$

$$ENS_{Failure\ cable-8} = 168\ h \times 4 \times 3\ MW + (672\ h - 168\ h) \times 1 \times 3\ MW = 3528\ MWh$$

Every cable failure has a failure rate, so the ENS of all cables for the base topology can be calculated:

$$ENS_{Failure\ cables} = 0.004 \times \sum_{i=1}^{8} ENS_{Failure\ cable-i} = 185.472\ MWh$$

Now, the disconnector failures are analysed. However, instead of having three periods, only the first two occur. This happens because the repair time of these equipments is not greater than the switching time of the disconnectors, which is when the third period starts. If a disconnector failure occurs, in the first period all the turbines within the string of that disconnector are out of service, because there is no available path to the collector system. As explained for the cable failures, the same is true for the second period, because no redundancy is available to remotely create a path to the collector system. This is equal for all disconnectors failures, so:

$$ENS_{Failure\ disconnector-i} = (\Delta t_{Period\ 1} + \Delta t_{Period\ 2}) \times ENS_{disconnector-i\ period\ 1,2}$$

$$ENS_{Failure\ disconnector-i} = 168\ h \times 4 \times 3\ MW = 2016\ MWh$$

Since the topology has a total of fourteen disconnectors and every disconnector failure has a failure rate, the ENS of all disconnectors failures for the base topology is:

$$ENS_{Failure\ disconnectors} = 0.02 \times \sum_{i=1}^{14} ENS_{Failure\ disconnector-i} = 564.480\ MWh$$

It should now be obvious that, for the wind turbine circuit breaker faults, the reasoning behind the calculations of the disconnector faults also applies, so:

$$ENS_{Failure\ circuit\ breaker-i} = (\Delta t_{Period\ 1} + \Delta t_{Period\ 2}) \times ENS_{circuit\ breaker-i\ period\ 1,2}$$

$$ENS_{Failure\ circuit\ breaker-i} = 168\ h \times 4 \times 3\ MW = 2016\ MWh$$

Since the topology has a total of eight wind turbines, eight circuit breaker failures need to be considered. Since each one has a failure rate, the ENS of all circuit breaker failures for this topology is:

$$ENS_{Failure\ circuit\ breakers} = 0.03 \times \sum_{i=1}^{8} ENS_{Failure\ circuit\ breaker-i} = 483.840\ MWh$$

Since the rated power scenario is the only one considered, the final ENS for all failures considered in the reliability analysis for the base topology is:

$$ENS_{3\ MW\ Scenario} = \sum_{k} ENS_{Failure\ k} \times Failure\ Rate_{Failure\ k}$$

$$ENS_{3\ MW\ Scenario} = ENS_{Failure\ cables} + ENS_{Failure\ disconnectors} + ENS_{Failure\ circuit\ breakers}$$

$$ENS_{Base\ Topology} = ENS_{3\ MW\ Scenario} = 1233.792\ MWh$$

B.1.2. Investment Cost

For the base topology, cable-1 must be able to handle the power of a total of four turbines. So, looking at Table 7, a cable rating of 95 mm^2 is needed, with a cost of 100 k€/km (Table 8). Applying the same logic to the others cables, the investment cost is:

$$Investment\ Cost_{Base\ Topology} = 2 \times 100 \frac{k€}{km} \times 1\ km + 6 \times 100 \frac{k€}{km} \times 0.5\ km\ = 500\ k€$$

B.2. Proposed Topology with Rating Upgrades

The proposed topology has a double-sided half ring design, seen in Figure 20, which has four cables in a top string (cables 1 to 4), another four in a bottom string (cables 5 to 8), as well as an additional redundancy cable.

B.2.1. ENS Calculation

For a cable-1 failure, in the first period all the turbines within the top string are out of service, because they are not connected to the collector system, as it can be seen in Figure 21. In the second period, where switching of the remote protection equipment happens, the redundancy can be used. It is now possible to create an alternative path to the collector system for turbines 3 and 4 (see Figure 22). The third period is when the manual switching of the disconnectors happens, if the cable-1 disconnector is switched off, an alternative path to the collector system is created for all turbines, this can be seen in Figure 23. In short, during the first period four turbines are out of service, during the second period two turbines are out of service and during the third period all the turbines are online. This implies:

$$ENS_{Failure\ cable-1} = \Delta t_{Period\ 1} \times ENS_{cable-1\ period\ 1} + \Delta t_{Period\ 2} \times ENS_{cable-1\ period\ 2}$$

$$ENS_{Failure\ cable-1} = \frac{20}{60}\ h \times 4 \times 3\ MW + \left(168\ h - \frac{20}{60}\ h\right) \times 2 \times 3\ MW = 1010\ MWh$$

For a cable-4 failure, in the first period all the turbines within the top string are out of service. In the second period an alternative path to the collector system can be created for turbines 1 and 2 through the redundancy. In the third period, if the cable-4 disconnector is switched of, an alternative path can be reached for turbines 1, 2 and 3. In short, during the first period four turbines are out of service, during the second period two turbines are out of service and in the third period one turbine is out of service:

$$ENS_{Failure\ cable-4} = \Delta t_{Period\ 1} \times ENS_{cable-4\ period\ 1} + \Delta t_{Period\ 2} \times ENS_{cable-4\ period\ 2} + \Delta t_{Period\ 3} \times ENS_{cable-4\ period\ 3}$$

$$ENS_{Failure\ cable-4} = \frac{20}{60}\ h \times 4 \times 3\ MW + \left(168\ h - \frac{20}{60}\ h\right) \times 2 \times 3\ MW + (672\ h - 168\ h) \times 1 \times 3\ MW = 2522\ MWh$$

Applying the same logic to the rest of the other cable faults,

$$ENS_{Failure\ cable-2} = \frac{20}{60}\ h \times 4 \times 3\ MW + \left(168\ h - \frac{20}{60}\ h\right) \times 2 \times 3\ MW = 1010\ MWh$$

$$ENS_{Failure\ cable-3} = \frac{20}{60}\ h \times 4 \times 3\ MW + \left(168\ h - \frac{20}{60}\ h\right) \times 2 \times 3\ MW = 1010\ MWh$$

$$ENS_{Failure\ cable-5} = \frac{20}{60}\ h \times 4 \times 3\ MW + \left(168\ h - \frac{20}{60}\ h\right) \times 2 \times 3\ MW = 1010\ MWh$$

$$ENS_{Failure\ cable-6} = \frac{20}{60}\ h \times 4 \times 3\ MW + \left(168\ h - \frac{20}{60}\ h\right) \times 2 \times 3\ MW = 1010\ MWh$$

$$ENS_{Failure\ cable-7} = \frac{20}{60}\ h \times 4 \times 3\ MW + \left(168\ h - \frac{20}{60}\ h\right) \times 2 \times 3\ MW = 1010\ MWh$$

$$ENS_{Failure\ cable-8} = \frac{20}{60}\ h \times 4 \times 3\ MW + \left(168\ h - \frac{20}{60}\ h\right) \times 2 \times 3\ MW + (672\ h - 168\ h) \times 1 \times 3\ MW = 2522\ MWh$$

Every cable failure has a failure rate, so the total ENS for all cables for this topology is:

$$ENS_{Failure\ cables} = 0.004 \times \sum_{i=1}^{8} ENS_{Failure\ cable-i} = 44.416\ MWh$$

The same reasoning behind the cable failure calculations for the first two periods can be applied to a disconnector failure, which means:

$$ENS_{Failure\ disconnectors\ cable-i} = \Delta t_{Period\ 1} \times ENS_{disconnector\ cable-i\ period\ 1} + \Delta t_{Period\ 2} \times ENS_{disconnector\ cable-i\ period\ 2}$$

$$ENS_{Failure\ disconnectors\ cable-1} = \frac{20}{60}\ h \times 4 \times 3\ MW + \left(168\ h - \frac{20}{60}\ h\right) \times 2 \times 3\ MW = 1010\ MWh$$

$$ENS_{Failure\ disconnectors\ cable-2} = 2 \times \left[\frac{20}{60}\ h \times 4 \times 3\ MW + \left(168\ h - \frac{20}{60}\ h\right) \times 2 \times 3\ MW\right] = 2020\ MWh$$

$$ENS_{Failure\ disconnectors\ cable-3} = \frac{20}{60}\ h \times 4 \times 3\ MW + \left(168\ h - \frac{20}{60}\ h\right) \times 2 \times 3\ MW = 1010\ MWh$$

$$ENS_{Failure\ disconnectors\ cable-4} = 2 \times \left[\frac{20}{60}\ h \times 4 \times 3\ MW + \left(168\ h - \frac{20}{60}\ h\right) \times 2 \times 3\ MW\right] = 2020\ MWh$$

$$ENS_{Failure\ disconnectors\ cable-5} = \frac{20}{60}\ h \times 4 \times 3\ MW + \left(168\ h - \frac{20}{60}\ h\right) \times 2 \times 3\ MW = 1010\ MWh$$

$$ENS_{Failure\ disconnectors\ cable-6} = 2 \times \left[\frac{20}{60}\ h \times 4 \times 3\ MW + \left(168\ h - \frac{20}{60}\ h\right) \times 2 \times 3\ MW\right] = 2020\ MWh$$

$$ENS_{Failure\ disconnectors\ cable-7} = \frac{20}{60}\ h \times 4 \times 3\ MW + \left(168\ h - \frac{20}{60}\ h\right) \times 2 \times 3\ MW = 1010\ MWh$$

$$ENS_{Failure\ disconnectors\ cable-8} = 2 \times \left[\frac{20}{60}\ h \times 4 \times 3\ MW + \left(168\ h - \frac{20}{60}\ h\right) \times 2 \times 3\ MW\right] = 2020\ MWh$$

Since the topology has a total of eight cables and every disconnector failure has a failure rate, the total ENS for all disconnector failures is:

$$ENS_{Failure\ disconnectors} = 0.02 \times \sum_{i=1}^{8} ENS_{Failure\ disconnector\ cable-i} = 242.400\ MWh$$

The same applies to wind turbine circuit breaker faults, with the results being equal for all circuit breaker failures. So:

$$ENS_{Failure\ circuit\ breaker-i} = \Delta t_{Period\ 1} \times ENS_{circuit\ breaker-i\ period\ 1} + \Delta t_{Period\ 2} \times ENS_{circuit\ breaker-i\ period\ 2}$$

$$ENS_{Failure\ circuit\ breaker-i} = \frac{20}{60}\ h \times 4 \times 3\ MW + \left(168\ h - \frac{20}{60}\ h\right) \times 2 \times 3\ MW = 1010\ MWh$$

Since the topology has a total of eight wind turbines and each failure has a failure rate, the total ENS of all circuit breaker failures is:

$$ENS_{Failure\ circuit\ breakers} = 0.03\times \sum_{i=1}^{8} ENS_{Failure\ circuit\ breaker-i} = 242.400\ MWh$$

In this topology load switches also exist, so their failures must be taken into account. For a load switch failure in the top string, in the first period all the turbines of that string are out of service. In the second period the redundancy cannot be used, so all the turbines within the top string remain out of service. In conclusion during the repair of the load switch all the turbines are out of service within the string where the failure occurred, so:

$$ENS_{Failure\ load\ switch-i} = (\Delta t_{Period\ 1} + \Delta t_{Period\ 2})\times ENS_{circuit\ breaker-i\ period\ 1,2}$$

$$ENS_{Failure\ load\ switch-i} = 168\ h\times 4\times 3\ MW = 2016\ MWh$$

In this topology, there are two load switches for which faults need to be considered, each one in each string. Since each failure has a failure rate, the total ENS for all load switches failures is:

$$ENS_{Failure\ load\ switches} = 0.03\times \sum_{i=1}^{2} ENS_{Failure\ load\ switch-i} = 120.960\ MWh$$

Since the rated power scenario is the only one considered, the ENS for all failures considered in the reliability analysis for the proposed topology is:

$$ENS_{TRU} = ENS_{3\ MW\ Scenario} = \sum_{k} ENS_{Failure\ k}\times Failure\ Rate_{Failure\ k}$$

$$ENS_{TRU} = ENS_{Failure\ cables} + ENS_{Failure\ disconnectors} + ENS_{Failure\ circuit\ breakers} + ENS_{Failure\ load\ switches}$$

$$ENS_{TRU} = 650.176\ MWh$$

B.2.2. Investment Cost

Cable-1 must handle the power of a maximum of eight turbines, which happens when a cable fault occurs in cable-5. So, looking at Table 7, the cable rating required is 150 mm^2, with an associated cost of 140 k€/km (Table 8). The redundancy must handle the power of a maximum of four turbines. This happens, for example, when a cable fault occurs in cable one. So, the cable rating needed is 95 mm^2 with an associated cost of 100 k€/km. Since the redundancy is a new additional cable, its vessel and installation costs also need to be considered, as well the load switches introduced. Applying the same logic to the other cables, the investment cost is:

$$Investment\ Cost_{TRU}$$
$$= 2{\times}140\frac{k€}{km}\times 1\ km + 2{\times}110\frac{k€}{km}{\times}0.5\ km + 4{\times}100\frac{k€}{km}{\times}0.5\ km$$
$$+ 1{\times}\left(100\frac{k€}{km} + 200\frac{k€}{km}\right){\times}0.8\ km + 4{\times}10\ k€ = 870\ k€$$

B.2.3. Economic Evaluation

Finally, the increase in reliability is seen by the increase of additional cash flow, which has an associated total cost:

$$CF_y = \left(ENS_{Base\ Topology} - ENS_{TRU}\right){\times}Selling\ Price = 58.36\ k€$$

$$I_0 = Investment\ Cost_{TRU} - Investment\ Cost_{Base\ Topology} = 370\ k€$$

With this result, it is possible to calculate the economic indicators and evaluate if the introduction of the redundancy is profitable or not for the investor:

$$NPV = \sum_{y=1}^{n}\frac{CF_y}{(1+r)^y} - \sum_{y=0}^{n-1}\frac{I_y}{(1+r)^y} = \sum_{y=1}^{20}\frac{58.36\ k€}{(1+0.07)^y} - 370\ k€ = 248.28\ k€$$

$$0 = \sum_{y=1}^{n}\frac{CF_y}{(1+IRR)^y} - \sum_{y=0}^{n-1}\frac{I_y}{(1+IRR)^y} \leftrightarrow IRR = 14.77\ \%$$

B.3. Proposed Topology with Ratings for Regular Conditions

This is the same topology as in the previous calculation, but now the cables can only handle all the scenarios for regular conditions.

B.3.1. ENS Calculation

For a cable-one failure, in the first period all the turbines within the top string are out of service. In the second period the redundancy can be used, creating an alternative path to the collector system for turbines 3 and 4. In the third period, if the disconnector of the faulty cable is manually switched off, it is possible to create an alternative path to the collector system for all the turbines in the top string. However, since the rating of cable-5 only supports 20 MVA, only six turbines can be online (18.75 MVA), as it can be seen in Figure 24. In short, during the first period four turbines are out of service, and during the second and third periods two turbines are out of service.

$$ENS_{Failure\ cable-1} = \Delta t_{Period\ 1}{\times}ENS_{cable-1\ period\ 1} + (\Delta t_{Period\ 2} + \Delta t_{Period\ 3}){\times}ENS_{cable-1\ period\ 2,3}$$

$$ENS_{Failure\ cable-1} = \frac{20}{60}\ h\ {\times}4{\times}3\ MW + \left(672\ h - \frac{20}{60}\ h\right){\times}2{\times}3\ MW = 4034\ MWh$$

For a cable-4 failure, in the first period all the turbines within the top string are out of service. In the second period, the redundancy can be used and it is possible to create an alternative path to the collector system for turbines one and two. In the third period, if the disconnector of the faulty cable is manually switched off, it is possible to create an alternative path to the collector system for turbines 1, 2 and 3, but not for turbine 4. In short, during the first period four turbines are out of service, during the second period two turbines are out of service and in the third period one turbine is out of service.

$$ENS_{Failure\ cable-4} = \Delta t_{Period\ 1} \times ENS_{cable-4\ period\ 1} + (\Delta t_{Period\ 2} + \Delta t_{Period\ 3}) \times ENS_{cable-4\ period\ 2,3}$$

$$ENS_{cable\ 4} = \frac{20}{60}\ h \times 4 \times 3\ MW + \left(168\ h - \frac{20}{60}\ h\right) \times 2 \times 3\ MW + (672\ h - 168\ h) \times 1 \times 3\ MW = 2522\ MWh$$

Applying the same logic to the other cables:

$$ENS_{Failure\ cable-2} = \frac{20}{60}\ h \times 4 \times 3\ MW + \left(168\ h - \frac{20}{60}\ h\right) \times 2 \times 3\ MW + (672\ h - 168\ h) \times 1 \times 3\ MW = 2522\ MWh$$

$$ENS_{Failure\ cable-3} = \frac{20}{60}\ h \times 4 \times 3\ MW + \left(168\ h - \frac{20}{60}\ h\right) \times 2 \times 3\ MW = 1010\ MWh$$

$$ENS_{Failure\ cable-5} = \frac{20}{60}\ h \times 4 \times 3\ MW + \left(672\ h - \frac{20}{60}\ h\right) \times 2 \times 3\ MW = 4034\ MWh$$

$$ENS_{Failure\ cable-6} = \frac{20}{60}\ h \times 4 \times 3\ MW + \left(168\ h - \frac{20}{60}\ h\right) \times 2 \times 3\ MW + (672\ h - 168\ h) \times 1 \times 3\ MW = 2522\ MWh$$

$$ENS_{Failure\ cable-7} = \frac{20}{60}\ h \times 4 \times 3\ MW + \left(168\ h - \frac{20}{60}\ h\right) \times 2 \times 3\ MW = 1010\ MWh$$

$$ENS_{Failure\ cable-8} = \frac{20}{60}\ h \times 4 \times 3\ MW + \left(168\ h - \frac{20}{60}\ h\right) \times 2 \times 3\ MW + (672\ h - 168\ h) \times 1 \times 3\ MW = 2522\ MWh$$

Every cable failure has a failure rate, so the total ENS of all cables is:

$$ENS_{Failure\ cables} = 0.004 \times \sum_{i=1}^{8} ENS_{Failure\ cable-i} = 80.704\ MWh$$

The same logic used for the first two periods of cable failures can be applied to disconnector failures:

$$ENS_{Failure\ disconnectors\ cable-i} = \Delta t_{Period\ 1} \times ENS_{disconnector\ cable-i\ period\ 1} + \Delta t_{Period\ 2} \times ENS_{disconnector\ cable-i\ period\ 2}$$

$$ENS_{Failure\ disconnectors\ cable-1} = \frac{20}{60}\ h \times 4 \times 3\ MW + \left(168\ h - \frac{20}{60}\ h\right) \times 2 \times 3\ MW = 1010\ MWh$$

$$ENS_{Failure\ disconnectors\ cable-2} = 2 \times \left[\frac{20}{60}\ h \times 4 \times 3\ MW + \left(168\ h - \frac{20}{60}\ h\right) \times 2 \times 3\ MW\right] = 2020\ MWh$$

$$ENS_{Failure\ disconnectors\ cable-3} = \frac{20}{60}\ h \times 4 \times 3\ MW + \left(168\ h - \frac{20}{60}\ h\right) \times 2 \times 3\ MW = 1010\ MWh$$

$$ENS_{Failure\ disconnectors\ cable-4} = 2\times\left[\frac{20}{60}\ h\times 4\times 3\ MW + \left(168\ h - \frac{20}{60}\ h\right)\times 2\times 3\ MW\right] = 2020\ MWh$$

$$ENS_{Failure\ disconnectors\ cable-5} = \frac{20}{60}\ h\times 4\times 3\ MW + \left(168\ h - \frac{20}{60}\ h\right)\times 2\times 3\ MW = 1010\ MWh$$

$$ENS_{Failure\ disconnectors\ cable-6} = 2\times\left[\frac{20}{60}\ h\times 4\times 3\ MW + \left(168\ h - \frac{20}{60}\ h\right)\times 2\times 3\ MW\right] = 2020\ MWh$$

$$ENS_{Failure\ disconnectors\ cable-7} = \frac{20}{60}\ h\times 4\times 3\ MW + \left(168\ h - \frac{20}{60}\ h\right)\times 2\times 3\ MW = 1010\ MWh$$

$$ENS_{Failure\ disconnectors\ cable-8} = 2\times\left[\frac{20}{60}\ h\times 4\times 3\ MW + \left(168\ h - \frac{20}{60}\ h\right)\times 2\times 3\ MW\right] = 2020\ MWh$$

Since the topology has a total of eight cables and every disconnector failure has a failure rate, the total ENS of all disconnector failures is:

$$ENS_{Failure\ disconnectors} = 0.02\times\sum_{i=1}^{8} ENS_{Failute\ disconnectors\ cable-i} = 242.400\ MWh$$

The same can be done for wind turbine circuit breaker failures. The results are equal for all circuit breaker failures, so:

$$ENS_{Failure\ circuit\ breaker-i} = \Delta t_{Period\ 1}\times ENS_{circuit\ breaker-i\ period\ 1} + \Delta t_{Period\ 2}\times ENS_{circuit\ breaker-i\ period\ 2}$$

$$ENS_{Failure\ circuit\ breaker-i} = \frac{20}{60}\ h\times 4\times 3\ MW + \left(168\ h - \frac{20}{60}\ h\right)\times 2\times 3\ MW = 1010\ MWh$$

Since the topology has a total of eight wind turbines, eight circuit breaker failures are considered. Since each failure has a failure rate, the total ENS of all circuit breaker failures is:

$$ENS_{Failure\ circuit\ breakers} = 0.03\times\sum_{i=1}^{8} ENS_{Failure\ circuit\ breaker-i} = 242.400\ MWh$$

For the load switch failures, the situation is identical to that of the proposed topology with rating upgrades, already calculated. Again,

$$ENS_{Failure\ load\ switch-i} = (\Delta t_{Period\ 1} + \Delta t_{Period\ 2})\times ENS_{circuit\ breaker-i\ period\ 1,2}$$

$$ENS_{Failure\ load\ switch-i} = 168\ h\times 4\times 3\ MW = 2016\ MWh$$

With a total ENS for all load switches failures of:

$$ENS_{Failure\ load\ switches} = 0.03\times\sum_{i=1}^{2} ENS_{Failure\ load\ switch-i} = 120.960\ MWh$$

Since the rated power scenario is the only one considered, the total ENS for all failures considered in the reliability analysis for the proposed topology with ratings for regular conditions is:

$$ENS_{TRRC} = ENS_{3\ MW\ Scenario} = \sum_{k} ENS_{Failure\ k} \times Failure\ Rate_{Failure\ k}$$

$$ENS_{TRRC} = ENS_{Failure\ cables} + ENS_{Failure\ disconnectors} + ENS_{Failure\ circuit\ breakers} + ENS_{Failure\ load\ switches}$$

$$ENS_{TRRC} = 686.464\ MWh$$

B.3.2. Investment Cost

Since this topology has the same cable ratings as the base topology, the cost associated with all the cables is the addition of the costs to implement the redundancy. This redundancy must handle the power of a maximum of two turbines, which happens, for example, when a cable fault occurs in cable-1. So, looking at Table 7 and Table 8, the cable rating needed is 95 mm^2, with an associated cost of 100 k€/km. The vessel and installation costs of the redundancy, as well as the costs to introduce the load switches also need to be considered. So, the investment cost associated is:

$$Investment\ Cost_{TRRC} = 500\ k€ + 1 \times \left(100 \frac{k€}{km} + 200 \frac{k€}{km}\right) \times 0.8\ km + 4 \times 10\ k€ = 780\ k€$$

B.3.3. Economic Evaluation

Finally, the increase in reliability is seen by the increase of additional cash flow, with its associated cost:

$$CF_y = \left(ENS_{Base\ Topology} - ENS_{TRRC}\right) \times Selling\ Price = 54.73\ k€$$

$$I_0 = Investment\ Cost_{TRRC} - Investment\ Cost_{Base\ Topology} = 280\ k€$$

With these results, it is possible to calculate all the economic indicators and evaluate if the introduction of the redundancy is profitable or not for the investor:

$$NPV = \sum_{y=1}^{n} \frac{CF_y}{(1+r)^y} - \sum_{y=0}^{n-1} \frac{I_y}{(1+r)^y} = \sum_{y=1}^{20} \frac{54.73\ k€}{(1+0.07)^y} - 280\ k€ = 299.84\ k€$$

$$0 = \sum_{y=1}^{n} \frac{CF_y}{(1+IRR)^y} - \sum_{y=0}^{n-1} \frac{I_y}{(1+IRR)^y} \leftrightarrow IRR = 18.94\ \%$$

Appendix C

Software Validation by Third-Party Software

The calculations in this appendix detail the results obtained by a Third-Party Software for the Base and Proposed topologies, their cables and strings, disconnectors, circuit breakers and load switches when a fault occurs. It was considered that the wind turbines were operating at the rated power (3 MW) all of the time. The third-party software does not select cable ratings, it only calculates the reliability analysis for the given topologies. The cables ratings used are the ones already described in Appendix B.

For the Base Topology, all the cables are 95mm^2, so:

$$Investment\ Cost_{Base\ Topology} = 2{\times}100\frac{k€}{km}\times 1\ km + 6{\times}100\frac{k€}{km}{\times}0.5\ km\ = 500\ k€$$

For the Proposed Topology with Rating Upgrades, there are 2 cables of 150mm^2, 2 cables of 120 mm^2, 4 cables of 95mm^2 and the redundancy has 95mm^2, so:

$$\begin{aligned} Investment\ Cost_{TRU} &= 2{\times}140\frac{k€}{km}\times 1\ km + 2{\times}110\frac{k€}{km}{\times}0.5\ km + 4{\times}100\frac{k€}{km}{\times}0.5\ km \\ &+ 1{\times}\left(100\frac{k€}{km} + 200\frac{k€}{km}\right){\times}0.8\ km + 4{\times}10\ k€ = 870\ k€ \end{aligned}$$

For the Proposed Topology with Ratings for Regular Conditions, all the cables are equal to the Base Topology and the redundancy has 95mm^2, so:

$$Investment\ Cost_{TRRC} = 500\ k€ + 1{\times}\left(100\frac{k€}{km} + 200\frac{k€}{km}\right){\times}0.8\ km + 4{\times}10\ k€ = 780\ k€$$

C.1. Base Topology

The base topology, seen in Figure 26, has four cables in a top string and another four in a bottom string.

The reliability analysis gives an ENS for the Base Topology of:

$$ENS_{Base\ Topology} = 1237.662\ MWh$$

C.2. Proposed Topology with Rating Upgrades

The Proposed Topology has a double-sided half ring design, seen in Figure 20, which has four cables in a top string, another four in a bottom string, as well as an additional redundancy cable.

The ENS for all failures considered in the reliability analysis for the Proposed Topology with Rating Upgrades is:

$$ENS_{TRU} = 651.343\ MWh$$

Since the Third-Party software only makes reliability analysis, the calculation of the economic indicators was done through hand calculations as in Appendix B.

Finally, the increase in reliability is seen by the increase of additional cash flow, which has an associated total cost:

$$CF_y = \left(ENS_{Base\ Topology} - ENS_{TRU}\right) \times Selling\ Price = 58.63\ k€$$

$$I_0 = Investment\ Cost_{TRU} - Investment\ Cost_{Base\ Topology} = 370\ k€$$

With these results, it is possible to calculate the economic indicators and evaluate if the introduction of the redundancy is profitable or not for the investor:

$$NPV = \sum_{y=1}^{n} \frac{CF_y}{(1+r)^y} - \sum_{y=0}^{n-1} \frac{I_y}{(1+r)^y} = \sum_{y=1}^{20} \frac{58.63\ k€}{(1+0.07)^y} - 370\ k€ = 251.15\ k€$$

$$0 = \sum_{y=1}^{n} \frac{CF_y}{(1+IRR)^y} - \sum_{y=0}^{n-1} \frac{I_y}{(1+IRR)^y} \leftrightarrow IRR = 14.85\ \%$$

C.3. Proposed Topology with Ratings for Regular Conditions

This is the same topology as in the previous calculation, but now the cables can only handle all the scenarios for regular conditions.

The total ENS for all failures considered in the reliability analysis for the Proposed Topology with Ratings for Regular Conditions is:

$$ENS_{TRRC} = 686.644\ MWh$$

The calculation of the economic indicators was again done through hand calculations, and the increase in reliability, seen by the increase of additional cash flow, and its associated cost are the following:

$$CF_y = \left(ENS_{Base\ Topology} - ENS_{TRRC}\right) \times Selling\ Price = 55.10\ k€$$

$$I_0 = Investment\ Cost_{TRRC} - Investment\ Cost_{Base\ Topology} = 280\ k€$$

The economic indicators are:

$$NPV = \sum_{y=1}^{n} \frac{CF_y}{(1+r)^y} - \sum_{y=0}^{n-1} \frac{I_y}{(1+r)^y} = \sum_{y=1}^{20} \frac{55.10\ k€}{(1+0.07)^y} - 280\ k€ = 303.75\ k€$$

$$0 = \sum_{y=1}^{n} \frac{CF_y}{(1+IRR)^y} - \sum_{y=0}^{n-1} \frac{I_y}{(1+IRR)^y} \leftrightarrow IRR = 19.08\ \%$$